

Ankle Stretch Reflexes during Anticipatory Postural Adjustments

Siddharth Vedula

Department of Biomedical Engineering

McGill University

Montreal, Quebec



January, 2009

A thesis submitted to McGill University in partial fulfillment of the requirements of the degree of Master of Engineering

©Siddharth Vedula, 2008

Abstract

Peripheral muscle stretch reflexes at the calf muscles have been shown to be important in postural control, by opposing forward sway. They are task dependent, and vary based on the conditions at the joint and associated muscle activation levels. Also, dynamic changes in stability, such as those induced by upper body movements, are preceded by anticipatory postural adjustments (APAs) in the rest of the body. To date, nobody has studied how stretch reflexes in the postural muscles change during these APAs.

For forward oriented upper body movements (e.g. arm raise, arm reach), the APA is typically characterized by an inhibition of the calf muscle before the activation of the shoulder muscle, and a recovery of calf muscle activity just before the onset of the arm movement. Biomechanically, this muscle pattern results in anticipatory forward sway, with the body then held at the new position. Hence during this period, one might expect the reflexes in the calf to be initially inhibited (since they oppose forward sway), and then rebound close to movement onset (to assist the slowing down of forward sway).

However, to date, this has not been demonstrated. Therefore, we devised a novel paradigm, where we measured the excitability of the stretch reflex at the calf at different times during the APA associated with unilateral right arm raises in standing humans. Our results showed that in this period, as hypothesized, reflexes followed a general pattern similar to the calf muscle activity. However, the reflex and muscle activity changes showed temporal differences- reflexes were inhibited after the inhibition in muscle activity, and rebounded just before the corresponding rebound in muscle activity. Furthermore, the relative amplitudes of reflex and muscle activity inhibitions were not correlated. We suggest that this is evidence that stretch reflex changes during the APA are mediated by neural mechanisms distinct from those that regulate changes in calf muscle activity.

Résumé

Il a déjà été démontré que les réflexes d'extension périphériques que l'on retrouve dans les muscles du mollet ont un rôle important dans le contrôle de la posture en s'opposant à l'oscillation avant. Ces réflexes dépendent de la tâche accomplie. Ils varient selon la position des articulations et le niveau d'efforts du muscle auquel ils sont associés. D'autre part, les changements dynamiques provoquant un déséquilibre sont causés en partie par les mouvements du torse et sont souvent précédés d'ajustements anticipatoires de la posture (AAP). Les changements causés par les AAP sur les réflexes d'extensions n'ont cependant jamais été étudiés.

Pour les mouvements avant du torse (ex. levé ou extension du bras, se pencher par en avant), les AAP sont habituellement caractérisés par une suppression de l'activité du muscle du mollet avant l'activation du muscle de l'épaule et un rétablissement de l'activité musculaire du mollet à l'amorcement du mouvement du bras. Ceci résulte biomécaniquement par une oscillation anticipatoire avant gardant le corps dans une nouvelle position. Donc, durant cette période, on peut s'attendre à ce que le réflexe d'extension au niveau du mollet soit initialement inhibé (pour opposer l'oscillation avant) et puis réactivé au début du mouvement (afin d'aider le ralentissement de l'oscillation).

Jusqu'à présent, ceci n'a jamais été démontré. Nous avons donc conçu un nouveau paradigme qui nous permet de mesurer la réactivité du réflexe du mollet à différent moment au courant d'un AAP causé par l'action de lever le bras droit en position debout. Nos résultats démontrent comme supposé par l'hypothèse, que durant cette période les réflexes agissent de façon semblable aux mouvements des muscles du mollet. Cependant, les changements observés chez le réflexe et l'activité du muscle ne sont pas synchronisés – le réflexe est inhibé après le muscle et réactivé avant. De plus, l'ampleur relative du réflexe et du mouvement musculaire n'était que faiblement corrélée. Nous croyons que ceci démontre que les réflexes pourraient être modulés par un mécanisme neural, et ce, sans apport direct des muscles impliqués dans le mouvement causant le réflexe.

Acknowledgments

I would like to first express my sincere gratitude to my supervisors Dr. Robert Kearney and Dr. Paul Stapley for providing me with the opportunity to pursue my research. In particular, I would like to thank Dr. Kearney for always keeping his door open to me, and putting up with my undoubtedly infuriating ability to constantly digress. Dr. Stapley has truly been a friend, philosopher, and guide these last few years- and in his own words, an agony-aunt to my constant ‘verbosity’.

I am also extremely grateful to Dr. Ross Wagner for his guidance throughout my research, and being a glutton for my incessant questions. Without his attention to detail and timely input, this project would never have succeeded. On a personal note, my interactions with him made my time here rather interesting.

A special mention to Pina for handling all the administrative details, and always having a cheerful word- definitely a godsend for organizationally challenged graduate students.

I would also like to thank my lab-mates over the past few years: Daniel, Alejandro, Yong, Tanya, and for a brief while, Baher and Heidi. I am particularly indebted to Daniel for all his help and insight throughout my project.

Furthermore, I would like to acknowledge all my friends who have made my time in Montreal thoroughly enjoyable. Thank you Ryan and Alissa for being fantastic roommates, and enduring my culinary experiments. A special thanks to Eve as well for her exemplary (I hope) french translation skills.

Last, but not least, I would like to thank my family for their immeasurable love and support throughout this process. To my elder sister Indu for always looking out for me, and mum and dad for being the most wonderful, supportive parents a child could ever wish for- I am forever grateful.

This work was supported by the Natural Sciences and Engineering Research Council of Canada (NSERC) and the Canadian Institutes of Health Research (CIHR).

Contributions of Authors

The experimental apparatus and paradigm was conceived with feedback from both Dr. Paul Stapley and Dr. Robert Kearney. In the initial stages of the project, Dr. Ross Wagner also assisted me considerably, primarily with the design and construction of the experimental apparatus. This involved acquiring some new skills in machining and electronic design.

I carried out the experiments on my own. After an initial set of pilot experiments to validate the setup, the apparatus and experimental protocol were modified slightly before the final set of experiments were conducted. I also designed a control algorithm and a graphical user interface to conduct the experiments.

I also conducted the data analysis individually. I wrote custom computer scripts to obtain, analyze, and present the results. Preliminary data were presented at the 31st Conference of the Canadian Medical and Biological Engineering Society (Montreal-June, 2008), and the 30th Conference of the IEEE Engineering in Medicine and Biology Society (Vancouver- August, 2008).

I wrote the first draft of the manuscript, and updated it assisted by feedback from both Dr. Kearney and Dr. Stapley. Dr. Stapley largely focused on the introduction, and general organization, while Dr. Kearney provided feedback with respect to the data analysis procedures. The latest version of the manuscript (V5) is presented in Chapter 4.

Table of Contents

ABSTRACT	I
RÉSUMÉ	II
ACKNOWLEDGMENTS	III
CONTRIBUTIONS OF AUTHORS	IV
TABLE OF CONTENTS	V
TABLE OF FIGURES	IX
LIST OF TABLES	XV
LIST OF ABBREVIATIONS	XVI
1. INTRODUCTION	1
1.1 Thesis Outline	3
2. LITERATURE REVIEW	4
2.1 Outline	4
2.2 Structural Anatomy & Physiology	4
2.2.1 Skeletal System	4
2.2.1.1 The Ankle Joint	4
2.2.2 Musculature.....	6
2.2.2.1 Skeletal Muscle Structure.....	6
2.2.2.2 Skeletal Muscle Mechanics	8
2.2.2.2.1 Sliding Filament Theory	8
2.2.2.2.2 Force-length and Force-velocity relationships.....	9
2.2.2.2.3 Frequency of Fiber Contractions & Motor Unit Recruitment.....	10
2.2.2.3 Muscles of the Lower Leg	12
2.2.3 Neural Motor Control.....	13
2.2.3.1 PNS Anatomy	14
2.2.3.1.1 Spinal Cord & Peripheral Neurons	14
2.2.3.1.2 Muscle Sensory Receptors.....	15
2.2.3.1.2.1 Muscle Spindles	15
2.2.3.1.2.2 Golgi Tendon Organs	17
2.2.3.2 Spinal Reflexes.....	17
2.2.3.2.1 Muscle Stretch Reflex.....	18

2.2.3.2.2	Physiological Sources of Stretch Reflex Modulation.....	19
2.2.3.2.3	Reflex Measurement.....	20
2.2.3.2.3.1	Electromyography (EMG)	20
2.2.3.2.3.2	H-Reflexes	21
2.2.3.2.3.3	Reflex Torque	22
2.3	Basic Principles of Balance	22
2.4	Mechanisms of Postural Control.....	25
2.4.1	Passive Influences.....	25
2.4.2	Active CNS Control of Balance	26
2.4.2.1	Feedback CNS Control	27
2.4.2.1.1	Feedback Control of Posture	27
2.4.2.2	Feed-forward CNS Control.....	28
2.4.2.2.1	Predictive Internal Models	29
2.4.2.2.2	Feed-forward Control of Posture.....	31
2.4.2.2.2.1	Anticipatory Postural Adjustments	32
2.4.3	Reflex Contributions- Peripheral Nervous System Control	35
2.4.3.1	Stretch Reflex Characteristics.....	35
2.4.3.2	Modulation and Variability of the Ankle Stretch Reflex	37
2.4.3.2.1	Effect of Joint Position and Muscle Activation Level.....	37
2.4.3.2.2	Task-dependent Modulation of Ankle Stretch Reflexes	39
2.4.3.3	Stretch Reflex Changes During the Preparatory Phase of a Movement	40
2.5	Summary & Thesis Rationale.....	42
3.	METHODS	44
3.1	Outline	44
3.2	General Overview.....	44
3.3	Subjects.....	47
3.4	Paradigm	47
3.5	Apparatus.....	50
3.5.1	Bilateral Electro-Hydraulic Actuator.....	51
3.5.2	Aluminum Frame with Cues and Target Switch	53
3.5.3	Electromyography (EMG).....	56
3.5.4	Wrist Inclinometer.....	58

3.5.5	Real-Time Experimental Control	58
3.5.5.1	Overview	58
3.5.5.2	Real-time Control Model.....	59
3.5.5.2.1	Target Frame Real-Time Controller Subsystem	61
3.5.5.2.2	Perturbation Sequence & Delay Selector Subsystem	65
3.5.5.2.3	Actuator Real-Time Controller Subsystem.....	66
3.5.5.2.4	Sampling Subsystem.....	68
3.5.5.3	Compiling and Executing the Real-Time Control Model	68
3.5.6	Graphical User Interface for Experimental Control (GUI)	69
3.5.7	Data Acquisition System (DAQ)	72
3.5.8	Digital Signal Routing Enclosure.....	73
3.6	Data Pre-Processing.....	73
3.6.1	Event Markers	73
3.6.2	Right Leg Center of Pressure	74
4.	DATA ANALYSIS, RESULTS & DISCUSSION	76
	STRETCH REFLEX CHANGES ASSOCIATED WITH ANTICIPATORY	
	POSTURAL ADJUSTMENTS PRECEDING VOLUNTARY ARM MOVEMENTS IN	
	STANDING HUMANS	77
4.1	Abstract.....	78
4.2	Introduction.....	79
4.3	Methods.....	81
4.3.1	Subjects	81
4.3.2	Overview	82
4.3.3	Experimental Apparatus & Operation.....	82
4.3.4	Experimental Protocol.....	84
	Defining the Operating Point.....	84
	Experimental Paradigm.....	85
4.3.5	Data Analysis	87
4.3.5.1	Trial Selection	87
4.3.5.2	Unperturbed Trials.....	89
4.3.5.3	Perturbed Trials	90
	Time Modulation of Reflexes- Ensemble Changes.....	92

Time Modulation of Reflexes- Onset of Inhibitions and Rebounds.....	92
4.4 Results.....	94
4.4.1 Unperturbed Trials.....	94
4.4.2 Perturbed Trials	96
4.4.2.1 Time Modulation of Reflexes	96
4.4.2.2 EMG Amplitude Modulation of Reflexes.....	99
4.4.2.3 Reflex Torque Changes.....	101
4.5 Discussion	102
4.5.1 Summary.....	102
4.5.2 Possible Neural Mechanisms of Reflex Modulation	103
4.5.3 Analogous Studies	105
4.5.4 Functional Role of Reflex Modulation during the APA.....	107
4.6 Acknowledgments.....	108
5. CONCLUSIONS.....	109
5.1 Summary	109
5.2 Main Findings	109
5.3 Limitations of the Study & Suggestions for Improvement.....	110
5.3.1 Input Perturbations Profile.....	110
5.3.2 Trial Rejection Procedure	111
5.3.3 Determination of Inhibition and Rebound Times.....	113
5.3.4 Measures of Fatigue.....	115
5.3.5 Measurements of Body Sway & Joint Angles	115
5.3.6 Data from the Contralateral Side of the Body	115
5.4 Final Conclusions.....	115
REFERENCES.....	117
APPENDIX.....	128
A. Digital Signal Routing Enclosure.....	128
B. Subject Consent Form.....	130
C. Ethics Approval Form.....	131

Table of Figures

Literature Review (Chapter 2)

Figure 2.1. Ankle joint anatomy. A) Joint capsule showing articulating bones and major ligaments. Adapted from [35]. B) Lateral view showing major tendons. Adapted from [36]. C) Medial view showing major tendons. Adapted from [36].	5
Figure 2.2. The hierarchical organization of skeletal muscle. Labels F-I show cross-sections of the specified regions. Modified from [39].	7
Figure 2.3. Force-length and force-velocity relationships of skeletal muscle contraction. A) During isometric contractions, maximal active force is generated when muscle is contracted from resting length. Adapted from [47]. B) However, the passive force increases as the muscle is contracted from longer resting lengths. Adapted from [51]. C) During isotonic contractions, muscle force varies non-linearly with velocity of lengthening or shortening. Adapted from [51].	10
Figure 2.4. Mycology of the lower leg- superficial dissection. A) Anterior view B) Posterior View. The most prominent muscles are re-annotated on the figures as follows: TA: Tibialis Anterior. GS: Gastrocnemius. Sol: Soleus. MG: Medial Gastrocnemius. LG: Lateral Gastrocnemius. Modified from [59].	12
Figure 2.5. Cross-section of the spinal cord. Modified from [39].	14
Figure 2.6. Schematic of the skeletal muscle spindle. A) Overall structure showing relation of spindle to the extrafusal fibers B) Magnification of the intrafusal fibers. Modified from [39].	15
Figure 2.7. Frequency response of 1a and type II afferent fibers Adapted from [60].	16
Figure 2.8. Stretch Reflex Pathway. The monosynaptic stretch reflex to the homonymous muscle (Path A), reciprocal inhibition (Path B), synergist activation (Path C), and feedback to higher brain centers (Path D) are all shown. Adapted from [47].	19
Figure 2.9. Inverted pendulum model of human stance.	22
Figure 2.10. Inverted pendulum mechanics. A) Oscillations of CoP and CoM in the A/P plane. The CoP oscillations are of larger amplitude and higher frequency. Adapted from [2]. B) A subject maintaining quiet stance at five different times. α : CoM angular acceleration, ω : CoM angular velocity, R: Ground reaction force, W: gravity, g: Downward projection of CoM (moment arm of gravity about the ankle), P: CoP position	

(moment arm of the ground reaction force). Notice that the angular acceleration of the CoM is proportional to the difference between p and g. Adapted from [2].	24
Figure 2.11. General diagram of feedback control. Adapted from [76].	27
Figure 2.12. General schematic of feed-forward control. Adapted from [89].	28
Figure 2.13. Use of forward models in combination with sensory feedback for motor control.	30
Figure 2.14. Combination of feed-forward (inverse model in the cerebellum) and feedback (cortical) CNS control. Adapted from [96].	31
Figure 2.15. EMG activity associated with an upper arm acceleration (A_w). Data is shown for unilateral (left) and bilateral (right) arm raises for ipsilateral (i) and contralateral (c) limbs. Data is aligned with respect to anterior deltoid onset (AD). SOL: Soleus, RF: Rectus Femoris, ST: Semitendinosus, GM: Gluteus Maximus, TFL: Tensor Facia Latae. Note the inhibition in the ipsilateral SOL prior to activation of the deltoid muscle. Adapted from [20].	33

Methods (Chapter 3)

Figure 3.1. A typical subject executing a voluntary arm movement while standing on the actuator. A) Bilateral electro-hydraulic actuator fitted with two foot pedals and torque, position and load transducers. B) Aluminum target frame holding visual and audio cues, torque feedback meter and target switch. C) Surface EMG electrodes on postural and focal muscles. D) Inclinometer used to measure arm position.	44
Figure 3.2. Sample trial from the experiment. A) A small dorsiflexion applied to the right ankle results in a Reflex B) EMG and C) Torque response.	46
Figure 3.3. Chart indicating sequence of temporal events during the experiment for a single trial. RT and MT refer to the approximate average reaction and movement times respectively.	48
Figure 3.4. Schematic of the experimental setup showing components and signal routing: 1) Hydraulically driven rotary pedals with torque sensors, potentiometer, and load cells 2) Frame with visual cue, audio cue, target switch, and visual torque feedback 3) Electromyogram (EMG) to measure muscle activity from the shoulder and lower leg muscles 4) Single-axis inclinometer to measure arm angle 5) Real-time controller which controlled the pedal position and frame components 6) Graphical user interface (GUI)	

which allowed the experimenter to interact with the real-time control model 7) Data acquisition system 8) Digital signal routing enclosure to route signals from controller to the frame.	50
Figure 3.5. Bilateral Electro-hydraulic actuator. A) The right side is shown with components annotated B) Whole system, showing duplication of left and right sides.	51
Figure 3.6. Target Frame. A) Top: Locations of components. B-E) Bottom: Components magnified. From left to right: B) Piezo-electric buzzer (audio “warn” cue). C) Target switch. D) Analog voltmeter for torque feedback. E) “Ready” switch to detect movement onset. The visual “move” cue consisted of a light emitting diode which was enclosed in plastic casing with a clear front face similar to the target switch.	53
Figure 3.7. EMG recording. A) Single differential electrodes used for EMG recording. B) Schematic illustrating the calculation of the voltage differential between the two muscle contacts.	56
Figure 3.8. Inclinometer fixed with a wrist splint, used to measure angular arm position	58
Figure 3.9 Flowchart showing the top-level structure of the real-time controller with four major subsystems. The <i>target-frame real-time controller subsystem</i> monitored pedal torques and inputs from switches to output cues to the target frame. It also triggered the <i>perturbation sequence & delay selector subsystem</i> when a “warn” cue was output. The <i>perturbation sequence & delay selector subsystem</i> was used to select the desired input command to the actuator real-time controller (perturbation trial/control trial/delay of applied perturbation). The <i>actuator real-time controller</i> used this input along with feedback from pedal potentiometers to generate an output command to the pedals using a proportional feedback algorithm. The sampling subsystem operated independently of the other subsystems, and was used for data acquisition. Inputs to the controller are shown on the left, while controller outputs are shown on the right.	60
Figure 3.10. Level 1 of the Target-Frame Controller subsystem. Contents of nested Torquecheck and Running mean Subsystems are also shown.	63
Figure 3.11. Level 2 of the Target-Frame Real-Time Controller Subsystem with the STATEFLOW chart determining the temporal sequence of events.	64
Figure 3.12. Perturbation sequence & delay selector subsystem which was used to specify the delay of perturbed trials with respect to the buzzer and sequence of perturbed/unperturbed trials.	65

Figure 3.13. The Actuator Real-Time Controller incorporating proportional feedback and velocity feed-forward control. Inputs to the right pedal could be switched between a pre-programmed buffer and a triggered pulse input from the perturbation sequence & delay selector subsystem.....	67
Figure 3.14. Sampling subsystem to initiate data collection.....	68
Figure 3.15. The xPC Target Framework, showing the host-target relationship. Adapted from [128].	69
Figure 3.16. Graphical user interface (GUI) to monitor and control experimental parameters in real-time by interacting with SIMULINK block diagrams.	71
Figure 3.17. Event segmentation of data files.....	74
Figure 3.18. Calculation of the CoP. A) Picture of a foot pedal showing the location of the four load cells B) Schematic illustrating the co-ordinate map of the CoP.	74

Data Analysis, Results & Discussion

Figure 4.1. Experimental setup. A) Schematic illustrating the task carried out along with cues and sensors used. B) Chart indicating sequence of temporal events during the experiment.....	83
Figure 4.2. Input perturbation profiles for all subjects. Histograms show number of perturbations applied with respect to the go cue. Estimated RT region is shown by the grey window. Dotted line shows the onset of the “move” cue.....	86
Figure 4.3. Cumulative distribution functions of the distance to the A) mode RT and B) mode MT for all trials and all subjects. Cutoff threshold values for trial rejection: mode RT \pm 100 ms, and mode MT \pm 60 ms.....	87
Figure 4.4. Reaction Time (top) and Movement Time (bottom) histograms for all subjects. The chosen trials are shaded in black overlaying all trials (grey).	88
Figure 4.5. Perturbation profile with respect to movement onset after trial selection for perturbed trials. Dotted line signifies movement onset.	89
Figure 4.6. Calculation of the Reflex EMG and Reflex Torque. A) Foot pedal position. Dorsiflexing pulse of magnitude 0.025 radians causes a delayed reflex response shown in B) Soleus EMG. The EMG peaks at a lag of 50-60 ms from the pulse onset. The reflex EMG has a mechanical torque response which has to be separated from C) the	

overall torque response with D) intrinsic, reflex, and voluntary components, so as to compute the E) reflex torque.91

Figure 4.7. Ensemble average of unperturbed trials for a typical subject. A) Arm position. B) Anterior Deltoid, C) TA D) and SOL EMG's. E) Ankle Torque. Signals were aligned on movement onset (black line). Arrows indicate approximate start of change in each signal. Arm position 0° is defined as perpendicular, and 90° as parallel to the floor. Dorsiflexing torques are taken as positive. Postural muscle changes preceded focal (deltoid) muscle activity.95

Figure 4.8. Reflex modulation in time. A) Reflex EMG modulation. Data was binned into 20 ms bins and pulses within each bin were aligned, at times indicated by vertical dashes. Every alternate bin is shown. EMG peaks show a biphasic pattern with an initial decrease followed by an increase closer to movement onset. B) Reflex Torque Component modulation. Torques profiles were aligned similarly in 20 ms bins. It follows a pattern similar to the EMG with an initial decrease followed by an increase. .96

Figure 4.9. Box-Whisker Plot Analysis. Data was segmented into 20 ms bins. Box boundaries are at the lower and upper quartile, encompassing the median (red). The dashed 'whisker' lines represent 1.5 times the inter-quartile range and outliers are shown by crosses. A) Reflex B) SOL muscle activity. Downward arrows highlight periods of inhibition and rebound in each parameter. Reflex inhibition occurs after muscle activity inhibition while reflex rebound occurs at the same time as muscle activity rebound.97

Figure 4.10. Modulation of reflex activity with respect to muscle activity across subjects. Data are quantized into 20 ms bins. A) Reflex and muscle activity inhibition and rebound times for the SOL. B) I. Onset of reflex inhibition with respect to muscle activity inhibition. All histogram bars are located at positive lags, indicating that reflex inhibitions followed muscle activity inhibitions. II. Onset of reflex rebound with respect to muscle activity rebound. Most subjects had reflex rebound times that were equal or less than muscle activity rebound times. Subject flagged with (+) behaved differently. 98

Figure 4.11. Percent SOL reflex inhibition versus percent inhibition in SOL muscle activity for all subjects, with respect to resting levels. The dotted line represents a linear relationship with unity gain. The results indicate that no direct linear relationship (R=0.35) exists between the reflex inhibition and muscle activity inhibition. 100

Figure 4.12. Relationship between reflex EMG and rectified reflex torques. Data from all subjects is shown, along with respective correlation coefficients. 101

Appendix

Figure A.1. Circuit diagram of the PCB used to interface frame components to the real-time controller and data acquisition system. 129

List of Tables

Methods (Chapter 3)

Table 3.1. Subject information	47
Table 3.2. Muscle EMG's recorded, describing electrode placement and orientation.	57
Table 3.3. Data of interest. Variables, transducers and relevant channels on the DAQ are indicated.....	72

Data Analysis, Results & Discussion (Chapter 4)

Table 4.1. Trial selection data. The total number of trials, along with the % rejected for each subject is indicated. The color legend corresponds to the curves in Figure 4.3.....	88
Table 4.2. Reflex and muscle activity inhibitions for the SOL. Data are normalized with respect to baseline levels.....	99

List of Abbreviations

Abbreviations used often are underlined.

A/D: Analog to Digital Converter

AAP: Ajustements Anticipatoires de la Posture

ANOVA: Analysis of Variance

APA: Anticipatory Postural Adjustments

APR: Automatic Postural Responses

ATP: Adenosine Tri-phosphate

BF: Biceps Femoris

BNC: Bayonet Neill Concelman (RF connector for coaxial cable)

BoS: Base of Support

BVML: Balance and Voluntary Movement Laboratory, Dept. of Kinesiology, McGill

CIHR: Canadian Institutes of Health Research

CNS: Central Nervous System

CoM: Center of Mass

CoP: Center of Pressure

D/A: Digital to Analog Converter

DAQ: Data Acquisition System

D I/O: Digital Input Output

DSP: Digital Signal Processing

EMG: Electromyogram/ electromyography

GABA: Gamma-aminobutyric acid

GRF: Ground Reaction Force

GS: Gastrocnemius

GUI: Graphical User Interface

IC: Integrated Circuit

LED: Light Emitting Diode

LG: Lateral Gastrocnemius

M1, M2, M3: Short, medium and long-latency components of the muscle stretch reflex

MG: Medial Gastrocnemius

MT: Movement Time

MUAP: Motor Unit Action Potential

NSERC: Natural Sciences and Engineering Research Council of Canada

PCB: Printed Circuit Board

PNS: Peripheral Nervous System

PRBS: Pseudo-random Binary Sequence

RAM: Random Access Memory

REKLAB: Neuromuscular Research Lab, Dept. of Biomedical Engineering, McGill

RT: Reaction Time

SOL: Soleus

TS: Triceps-surae Muscle Group

TTL: Transistor-transistor Logic

1. Introduction

In humans, the position of the back is entirely upright both during quiet stance and locomotion. In fact, typically, relaxed (quiet) stance is modeled biomechanically as an inverted pendulum pivoting about the ankle joint [1]. This upright position is fundamentally unstable as the center of mass (CoM) of the body is located in the trunk region over a small support base at the feet. During quiet stance, there is constant sway about a set-point in both the medial/lateral and anterior/posterior planes [2].

Studies of quiet stance have shown that the center of vertical pressure (CoP) at the feet is constantly displaced so that the vertical projection of the CoM is maintained slightly anterior (5mm) to the ankle joint [3]. In this position, gravity acting at the CoM exerts a rotational torque about the ankle causing the body to fall forwards. It is currently thought that this is prevented by active contraction of the calf muscles (referred to as the triceps-surae muscle group (TS) composed of the soleus (SOL), and gastrocnemius (GS)), mediated by a combination of active control from the central nervous system (CNS) incorporating vestibular, visual and proprioceptive information [4-6], and muscle stretch reflex mechanisms at the peripheral nervous system (PNS) [7, 8]. The passive resistance provided by the visco-elastic properties of the ankle muscles, tendons and ligaments also plays a role [1].

Stretch reflexes in the TS can contribute to postural control by opposing forward sway. When a muscle is stretched, muscle spindles in the muscle belly initiate a spinal reflex arc via 1a afferents and α -motorneurons. This causes the muscle to contract and return to its resting length. Typically, stretch reflex dynamics in the GS were associated with two components: a short latency reflex at a delay of 40 ms and a longer latency reflex at delays varying between 100-120 ms [9]. A number of early studies suggested that the stretch reflex dynamics were stereotyped throughout the body, and identified the long latency component as critical for postural stability [9-11]. Studies investigating joint stiffness (i.e. resistance of ankle to sway) have also shown that the reflexes contribute a significant component to the overall joint stiffness [7, 8, 12].

However, reflex properties have been shown to be highly variable. Muscle activation level and joint position significantly influence reflex sensitivity [8, 13]. Studies

have shown that ankle stretch reflexes are modulated during natural tasks such as walking and cycling [14]. Other studies have also suggested that reflexes can be modulated voluntarily if subjects are given appropriate feedback [15-17]. However, it is not known if this occurs during natural conditions. In summary, while it is agreed that the TS stretch reflex plays an important role in the control of sway by counteracting forward lean, there is no consensus about the underlying neural mechanisms regulating it, and its relative functional contribution to postural stabilization.

Voluntary movements result in internally generated destabilizations of the body. This is because the body is a multi-segmented structure, and the movement of one segment (e.g. reaching forward, raising one's hand, lifting a leg) will have a direct mechanical effect on others [18]. In such situations, it is widely accepted that a feed-forward mode of postural control, mediated by descending commands from the CNS, is adopted. Indeed, it has been shown that for a range of voluntary arm, trunk or leg movements, that there are anticipatory postural adjustments (APAs) in other body segments, whereby postural muscle activity precedes that of the focal muscles required for the movement [19-22]. A common task used in postural control studies is the unilateral arm raise, during which the TS shows a characteristic APA [20]. It is characterized by an inhibition of the SOL muscle approximately 60ms before the activation of the deltoid (focal) muscle. The antagonist flexor muscles (e.g. the tibialis anterior (TA), tensor faciae latae) do not typically show anticipatory activity, but are strongly activated at about the same time as the focal muscle. Just before movement onset, there is a recovery of TS activity[19]. The biomechanical effect of this APA pattern is to cause a backward shift in the CoP, and a forward motion of the CoM which is then held at the new forward position. Functionally, the APA was traditionally interpreted as being used to counteract the inertial reactive forces associated with the movement, which would throw the body segment backwards [23-26] (although more recent interpretations suggested that the APA role might not strictly be for CoM stabilization and instead used to for focal movement initiation [21, 27, 28]).

Active stretch reflexes at the TS would counter the forward sway initiated by the APA. Hence, one might hypothesize that the TS stretch reflex should be inhibited during

the APA. To our knowledge, no one has demonstrated this. However, there have been a few analogous studies which have shown that the SOL H-reflex is inhibited during the APA phase of voluntary movements, such as arm raises, ballistic head movements, and stepping movements [29-31]. H-reflexes are caused by direct external electrical stimulation of the 1a afferent fibers innervating the muscle spindle, and assess the excitability of the α -motorneurons. Since the methodology of H-reflex assessment bypasses the muscle spindles, their influence on the changes observed cannot be accounted for. Accordingly, it has also been shown that changes in the H-reflex do not exactly correspond to changes in the stretch reflex [32, 33].

Hence, using a paradigm where subjects executed a voluntary raise of the right arm, we aimed to systematically document stretch reflexes changes in the TS by applying a small dorsiflexing pulse perturbation to the right ankle at different times during the APA phase. Using EMG techniques, we studied both the time and amplitude modulation of the reflex and associated background muscle activity. Mechanical reflex torque responses were also quantified.

1.1 Thesis Outline

The thesis is structured as follows, with five chapters. Chapter 2 is a literature review with two major components. The first component focuses on physiological principles of the skeletal, muscular, and neural systems with respect to the voluntary control of the musculoskeletal system. The second component provides a review of previous studies that have explored the neural mechanisms involved in postural control.

Chapter 3 is an extended methods chapter that describes the experimental setup and construction in detail.

Chapter 4 is presented in manuscript format, to be submitted to Experimental Brain Research. It describes the experimental protocol, data analysis techniques, presents the results, and finishes with a discussion of our findings.

Chapter 5 summarizes the findings, and discusses the limitations of the experiment along with recommendations to be implemented for further work.

2. Literature Review

2.1 Outline

This chapter is a review of the fundamental physiological, biomechanical, and neural control principles involved in the control of human posture. Section 2.2 describes the anatomy and physiology of the structures involved. The general musculature, skeletal system, and neural circuits pertaining to motor control are described, with the focus on lower-leg musculature and peripheral stretch reflexes. Section 2.3 explains the general biomechanical principles of balance. Section 2.4 provides a review of studies which have explored the neural mechanisms involved in postural control, focusing on studies of APAs and stretch reflexes. Lastly, Section 2.5 provides a rationale for the thesis and introduces the work to be presented in chapters 3 and 4.

2.2 Structural Anatomy & Physiology

2.2.1 Skeletal System

Broadly defined, the skeletal system consists of bones, cartilage, ligaments, and tendons. It provides the physical framework for the body. The skeleton can be divided into two categories: the central axial skeleton consisting of the skull, hyoid bone, vertebral column and the rib cage, and the appendicular skeleton consisting of the limbs. With regards to postural stability, the control of the lower limbs and the ankle joint is of particular importance [34].

2.2.1.1 The Ankle Joint

The ankle, or talocrural, joint is a hinge joint between the tibia, fibula, and talus bones. Specifically, the medial malleolus of the tibia and the lateral malleolus of the fibula form a cavity into which the medial and lateral facets of the upper talus fit.

The major ligaments that hold the bones together are:

1. Capsular
2. Internal lateral (or deltoid)
3. Anterior talofibular
4. Posterior talofibular
5. Calcaneofibular [35].

The joint also has a number of tendons from the surrounding muscles associated with it including: 1. Tibialis anterior 2. Extensor hallucis proprius 3. Extensor digitorum longus 4. Peroneus tertius 5. Tibialis posterior 6. Flexor digitorum longus 7. Flexor hallucis longus 8. Peroneus longus 9. Peroneus brevis. The major bones and ligaments, and most prominent tendons are illustrated in Figures 2.1a through 2.1c [35].

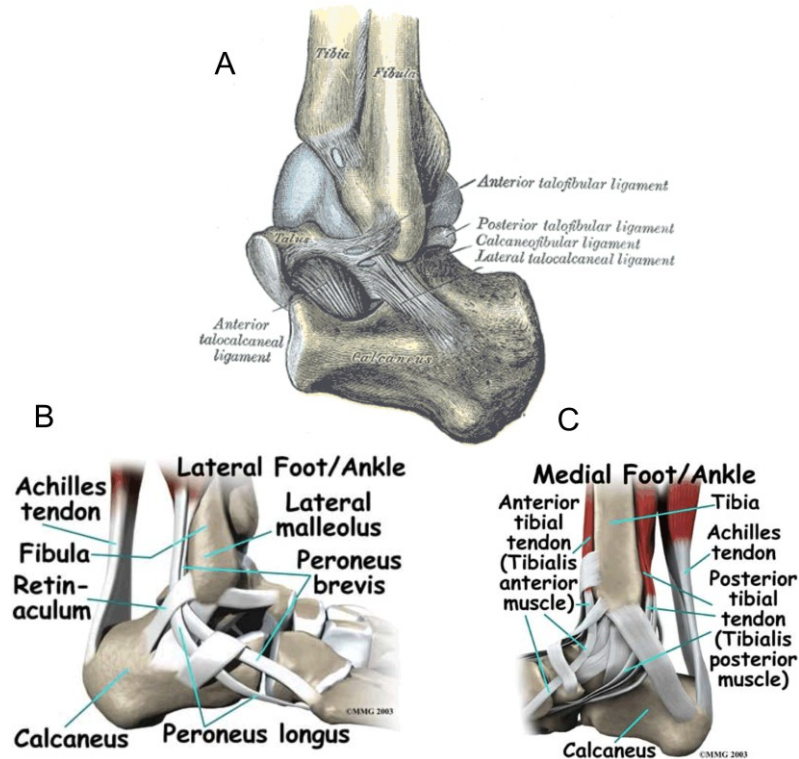


Figure 2.1. Ankle joint anatomy. A) Joint capsule showing articulating bones and major ligaments. Adapted from [35]. B) Lateral view showing major tendons. Adapted from [36]. C) Medial view showing major tendons. Adapted from [36].

Major nerve innervations are derived from the deep peroneal and tibial branches, while blood flow is provided by the anterior tibial and peroneal arteries [35].

The talocrural joint allows the foot to be either plantarflexed or dorsiflexed (i.e. rotate the foot downwards or upwards respectively). The range of motion varies from 50° to 90° depending on the individual. It should be noted that about 35° degree of inversion and 15° of eversion (rotation of the ankle so that the plantar surface of the foot faces medially or laterally) is also possible. This range of motion is primarily attributed to the transverse tarsal joint between the talus and calcaneus (heel bone), which is located underneath the talocrural joint [35, 37].

2.2.2 Musculature

Muscles are the major contractile tissues of the body whose primary function is to generate active forces and cause motion. Muscle tissue is typically grouped by both structure and function. Striated muscles have visible bands (striations) as opposed to non-striated muscles. Voluntary muscles are under conscious control as opposed to involuntary muscles. Based on this dual classification, three distinct muscle tissue types can be identified in the human body: skeletal (striated voluntary), smooth (striated involuntary), and cardiac (non-striated involuntary). While cardiac muscle is the unique myogenic muscle of the heart, smooth muscles are located in the walls of hollow organs, blood vessels, eyes and glands and are responsible for movements in the digestive, urinary and reproductive systems. However, it is skeletal muscle with its associated connective tissue which is responsible for locomotion, posture, and the coordination of voluntary movement of the skeletal system under the control of the nervous system [38].

2.2.2.1 Skeletal Muscle Structure

The organization of skeletal muscle from the gross to the molecular level is shown in Figure 2.2. The basic units of skeletal muscles are the skeletal muscle fibers arranged end to end. Each muscle fiber is a cylindrical multinucleated cell which develops from pre-cursor multinucleated cells known as myoblasts. Fibers range in length from 1mm to 4 cm, and are about 10-100 μm in diameter. [34].

Fibers are organized in a set of nested layers. The plasma membrane of each fiber, the sarcolemma, is surrounded by a loose network of connective tissue known as the endomysium. A bundle of fibers with the interspersed endomysium is in turn covered by a stronger connective tissue layer called the perimysium, all together known as a muscle fasciculus. A muscle is made up of numerous fasciculi (Figure 2.2b) grouped together and covered by a final layer of connective tissue known as the epimysium or fascia. The axons of motor neurons which innervate the fibers branch repeatedly at the level of the perimysium, such that every fiber receives a branch of an axon. Hence, each motor neuron innervates more than one muscle fiber [38].

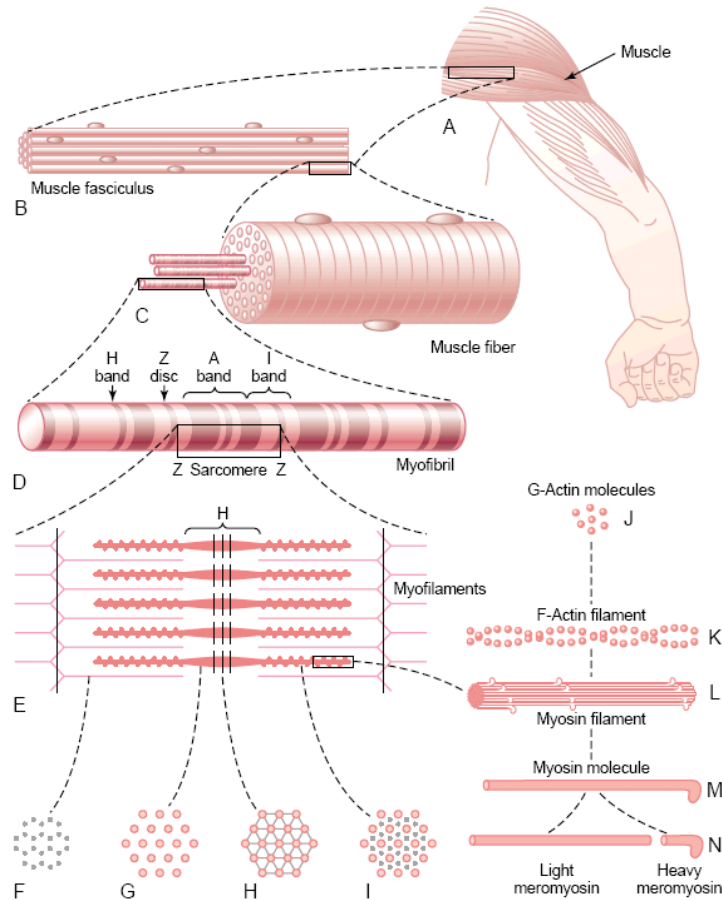


Figure 2.2. The hierarchical organization of skeletal muscle. Labels F-I show cross-sections of the specified regions. Modified from [39].

As shown in Figure 2.2d, muscle fibers are made up of a large number of myofibrils, threadlike structures 1-3 μm in diameter. These consist of highly ordered units known as sarcomeres (Figure 2.2e) arranged end to end, which are the basic contractile units of the fibers. Sarcomeres contain two kinds of protein myofilaments arranged in parallel. Thin actin filaments (8 nm diameter, 1000 nm long), shown in Figures 2.2j-k, are made up two strands of fibrous actin (F and G actin), and a series of tropomyosin and troponin molecules. Thicker (2nm diameter, 1800 nm long) myosin filaments, shown in Figures 2.2l-2.2n, consist of a rod section made up of two intertwined helices, and a head portion extending orthogonally which is made up of four smaller myosin molecules. Boundaries of sarcomeres are defined by a thin filamentous network of protein known as a Z disk, to which one end of the actin myofilaments attach. Myosin

myofilaments lie in the middle of the sarcomere, in an area known as the A band. The region where the two filaments do not overlap is known as the H zone, and the area where actin myofilaments are exclusively located is known as the I band. This classification is shown in Figure 2.2d [40, 41].

2.2.2.2 Skeletal Muscle Mechanics

2.2.2.2.1 Sliding Filament Theory

Skeletal muscle contracts via a mechanism known as the sliding filament theory, first described in 1954 by Huxley through X-ray diffraction studies [42, 43].

Ca^{+2} ions are stored in highly specialized compartments adjacent to the sarcomeres known as the sarcoplasmic reticulum. The sarcolemma also has a network of tubules (T tubules) wrapping around the sarcomeres near the A band. Muscle contraction is initiated when action potentials, initiated by the nervous system, are propagated along the T tubules. These rapidly depolarize the cell and cause voltage gated Ca^{+2} ion channels in the sarcoplasmic reticulum to open, thereby flooding the sarcomeres with Ca^{+2} .

1. Ca^{+2} binds to the troponin molecules on the actin myofilaments, shifting the tropomyosin molecules and exposing active binding sites on the actin to which the myosin heads bind forming cross-bridges.
2. Using energy stored in the myosin heads, the actin filaments are pulled towards the center of the sarcomere (power stroke). This shortens the sarcomere, with the Z disks brought closer, but the lengths of the filaments themselves do not change.
3. An ATP molecule attaches to the myosin head detaching it from the actin strand. Hydrolysis of the ATP molecule to ADP and phosphate causes the myosin head to return to its original position (recovery stroke), after which the process can be repeated (cross-bridge cycling).

During muscle relaxation, active transport of Ca^{+2} back into the sarcoplasmic reticulum restores the troponin-tropomyosin complex on the actin myofilament and blocks the binding sites for myosin. It should also be noted that, within the sarcomere, there are smaller proteins such as titin and nebulin which hold the actin and myosin molecules in place. The titin attaches to the Z disks, extending to the middle of the H

zone (M line). The region of the titin strand in the I band works like a spring giving the muscle both extensibility and elasticity in response to a passive stretch [43-46].

2.2.2.2.2 Force-length and Force-velocity relationships

Experiments in isolated muscle preparations have shown that in addition to the basic contractile mechanism summarized above, the amount of active force generated is a function of the length of the muscle and the velocity at which it is shortened or lengthened. Although muscle mechanics are not identical in-vivo (e.g. due to different kinds of inhibitory or excitatory neuromuscular control and limb inertia, among other factors) these basic principles are still useful to understand.

The force-length relationship is critical during isometric contractions (e.g. pushing against a wall with the elbow joint at a fixed angle- forearm muscles do not change length). As shown in Figure 2.3a, if the muscle is shortened to less than 60% of its resting length before the contraction is initiated, the actin filaments at either end of the sarcomere overlap and interfere with the formation of cross-bridges with the myosin. Alternately, when the muscle is stretched to more than 70% times its resting length, the filaments do not overlap at all and hence cross-bridges cannot be formed. Maximal tension is generated when contractions are elicited from the resting length of the muscle, corresponding to a sarcomere length of approximately 2 μm . However, it should be noted that if the muscle is stretched greatly, there will be a large passive elastic force generated, independent of the sliding filament contraction mechanics, and the net force generated will actually be larger than that due to the active force alone, as shown in Figure 2.3b. The force-velocity relationship is important during isotonic contractions where the muscle length actively changes to generate a constant force (e.g. a bicep curl). It is illustrated in Figure 2.3c. During concentric isotonic contractions, the active force generated decreases sigmoidally as the velocity with which the muscle shortens is increased. This occurs due to the fact the heads of the myosin molecules get detached from the actin filaments. However during eccentric isotonic contractions, the muscle is able to generate more force as it is stretched beyond resting length to a certain point, after which the force output plateaus [47-51].

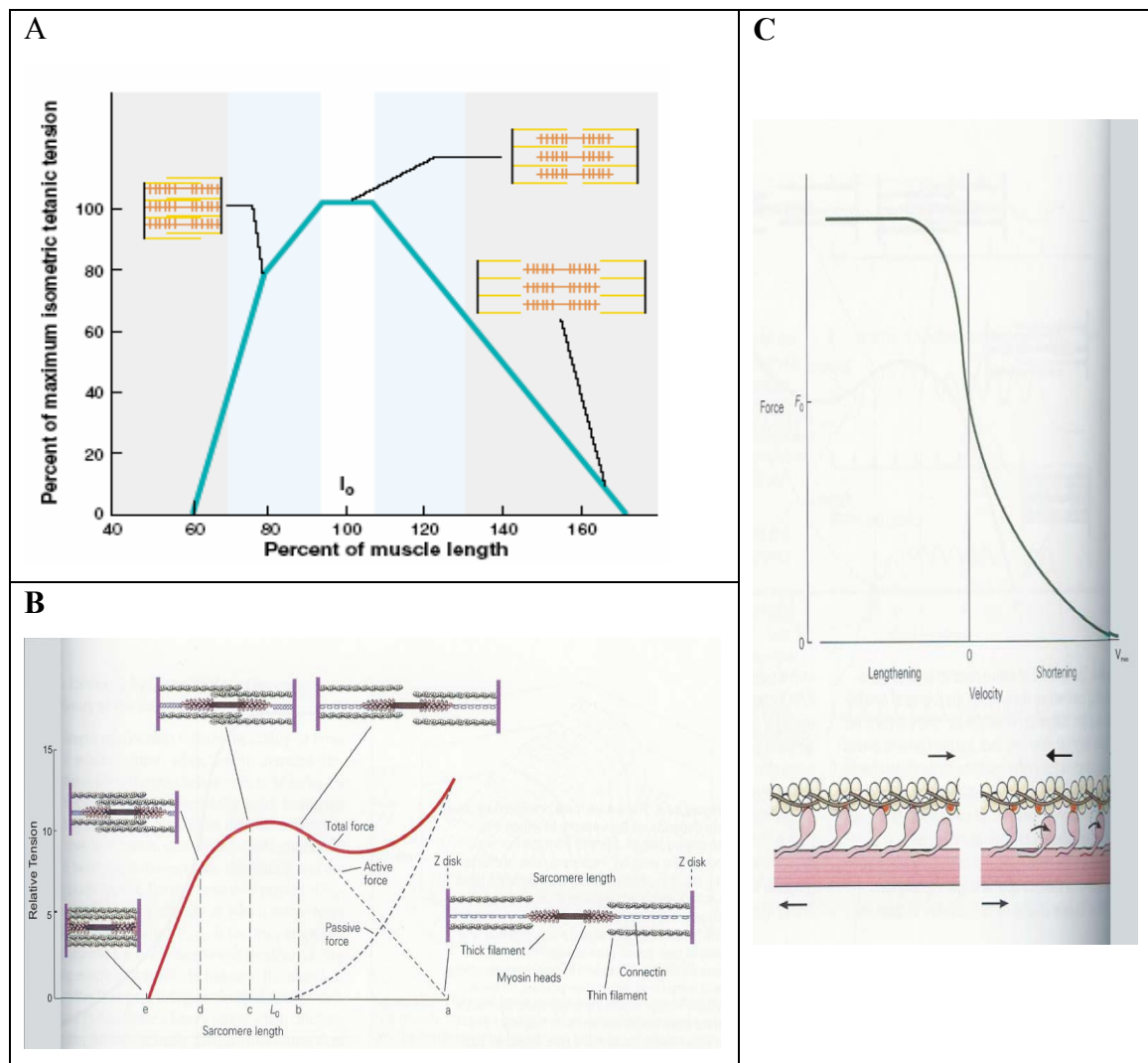


Figure 2.3. Force-length and force-velocity relationships of skeletal muscle contraction. A) During isometric contractions, maximal active force is generated when muscle is contracted from resting length. Adapted from [47]. B) However, the passive force increases as the muscle is contracted from longer resting lengths. Adapted from [51]. C) During isotonic contractions, muscle force varies non-linearly with velocity of lengthening or shortening. Adapted from [51].

2.2.2.2.3 Frequency of Fiber Contractions & Motor Unit Recruitment

The force generated by the muscle is also influenced by two neural control mechanisms: 1) The rates at which individual fibers are excited (rate coding). 2) The total number of fibers recruited (recruitment) [52].

The mechanical response of a single muscle fiber to an action potential is known as a twitch and can last for up to 100ms. However, if a second action potential arrives

before the end of the twitch a second contraction of the fiber can be initiated. In such an event, the Ca^{+2} ions will not have had enough time to be actively transported back to the sarcoplasmic reticulum. This causes a phenomenon known as tetanus, where the force of contraction will be greater, due to a summation of the two twitches. In the limit, if enough action potentials occur often enough, a state of complete (or fused) tetanus contraction with force output up to 5 times greater than from a single twitch can be achieved. The active force generated can also be influenced by the number of muscle fibers recruited at a given time. A motor unit is defined as a single motor neuron along with all the fibers that it innervates within a single skeletal muscle. It should be noted that every motor unit has a different number of fibers, and the fibers themselves have different response characteristics (fast or slow twitch). The response characteristic of individual fibers typically depends on their cross-sectional area, and the myofilament makeup [51].

In a traditional view known as the size principle, the units are thought to be recruited in an organized fashion depending on the size of the innervating motor neuron (smaller motor units depolarize at a lower threshold and are hence recruited first). If a greater muscle output force is required for the task at hand, progressively larger units are recruited. However, more recent studies have shown that alternate strategies might be implemented, where motor units can be functionally grouped for different tasks. For instance, during repetitive or cyclical movements (e.g. walking), activation-deactivation kinetics require that the motor unit recruitment patterns must conform to the mechanics of the task. Renshaw cells, located in the peripheral nervous system, which inhibit α -motor neuron activity, are thought to be involved in the process by selective modulation of motor units. For example, motor units that are prone more easily to fatigue are thought to be less inhibited, depending on the level of force required and the size of the muscle, rate coding and recruitment are used to different degrees [53].

Rate coding has been shown to be typically used at lower force levels (<10% maximal voluntary contraction). However, the length of the muscle can also affect the relative contribution effects of the two factors. For instance, the discharge rate and the number of fibers recruited are increased at shorter muscle lengths during isometric

contractions. Also, during isotonic shortening contractions the discharge rate is increased, but not for increases in muscle length [54-58].

2.2.2.3 Muscles of the Lower Leg

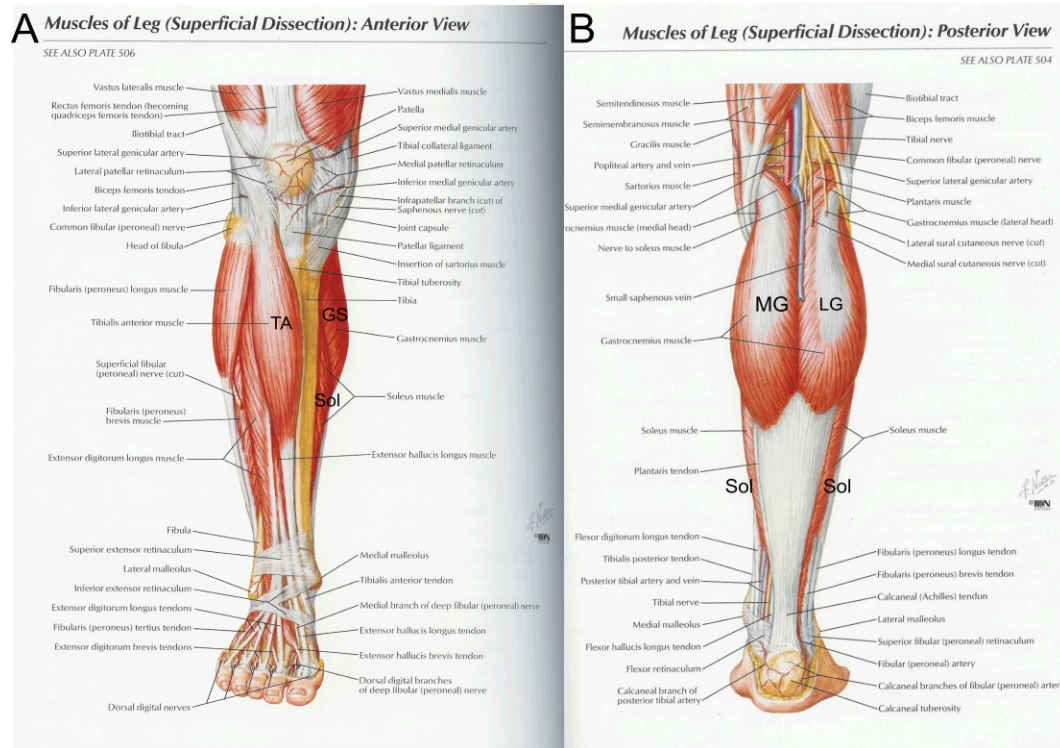


Figure 2.4. Mycology of the lower leg- superficial dissection. A) Anterior view B) Posterior View. The most prominent muscles are re-annotated on the figures as follows: TA: Tibialis Anterior. GS: Gastrocnemius. Sol: Soleus. MG: Medial Gastrocnemius. LG: Lateral Gastrocnemius. Modified from [59].

As shown in Figure 2.4, in terms of postural control, the major muscles of the lower leg that interact with the ankle joint complex are the GS, SOL and TA. The GS is the most prominent calf muscle. It originates from the posterior surface of the femur where it bifurcates into a medial (MG) and lateral (LG) head and attaches to the calcaneus via the Achilles tendon. The SOL lies underneath the GS and originates from the posterior head of the fibula and the middle of the tibia. It is similarly connected to the calcaneus. Both muscle groups plantarflex the foot. Due to their similar action and anatomical proximity, they are often classified together as the TS muscle group. The TA, the antagonist muscle to the TS, is located on the front of the lower leg. It originates

from the upper half of the lateral tibia and inserts into the medial cuneiform and first metatarsal bones of the foot. Its primary action is to dorsiflex the foot [34].

2.2.3 Neural Motor Control

The nervous system is the processing and control center of the body. Functionally, the nervous system can be classified into the somatic (voluntary) or autonomic (involuntary) branch. It is the voluntary branch that receives external information and interacts with the musculoskeletal muscle system, and is therefore responsible for coordinating the body's movements under conscious control. Structurally, the nervous system is typically divided into the central and peripheral branches. The central nervous system (CNS) encompasses the brain and the spinal cord with all structures enclosed in cavities protected by bone. Cortical and associated brain stem structures integrate sensory information, whether it is visual, somatosensory or vestibular, and produce neural commands. Associated structures such as the cerebellum and the basal ganglia play a crucial role in fine-tuning these descending commands to produce smooth, coordinated movements. These commands descend to the spinal cord, where they influence the circuitry of the peripheral nervous system (PNS). The PNS consists of the efferent (output) nerves from the spinal cord that innervate the muscles, and the afferent (input) nerves that return information to the CNS from the sensory receptors. Together, the afferents and efferent connections form important spinal reflex pathways [38].

Since the work presented in this thesis concerns peripheral muscle stretch reflexes, the rest of Section 2.2.3 focuses on the PNS.

2.2.3.1 PNS Anatomy

2.2.3.1.1 Spinal Cord & Peripheral Neurons

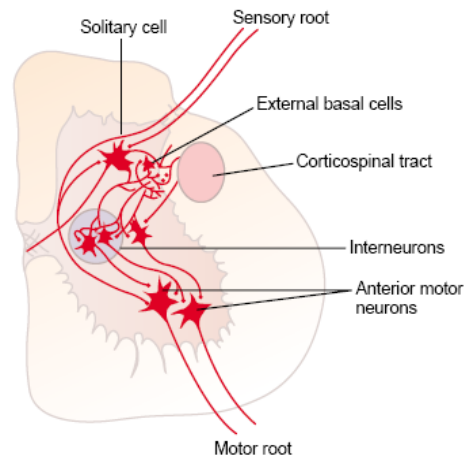


Figure 2.5. Cross-section of the spinal cord. Modified from [39].

As shown in Figure 2.5, sensory neurons from the peripheral receptors enter the grey matter of the spinal cord through the dorsal root. These neurons synapse with interneurons, which in turn synapse directly with efferent motor neurons innervating the muscles. Interneurons are the main relay and integration centers of the spinal cord. They are small, and highly excitable (often firing at a rate of 1.5 KHz), and up to 30 times as numerous as the motor neurons. They are highly interconnected and receive a large portion of the descending command from the upper CNS. Sensory neurons also synapse directly with efferent motor neurons innervating muscles. Lastly, a second branch of the sensory neurons relays information back up to higher levels structures in the CNS. The motor neurons exit the spinal cord from the anterior root. The major motor neurons are the α -motor neurons and γ -motor neurons. The large α -motor neurons average approximately 14 micrometers in diameter, and are the fundamental source of skeletal muscle innervation via the motor units. The smaller, and less numerous γ -motor neurons, about 5 micrometers in diameter, innervate special skeletal muscle fibers known as intrafusal fibers in an area of the muscle known as the muscle spindle. There are also a large number of ascending and descending propriospinal fibers which link different segments of the spinal cord, and the CNS to the PNS [38].

2.2.3.1.2 Muscle Sensory Receptors

2.2.3.1.2.1 Muscle Spindles

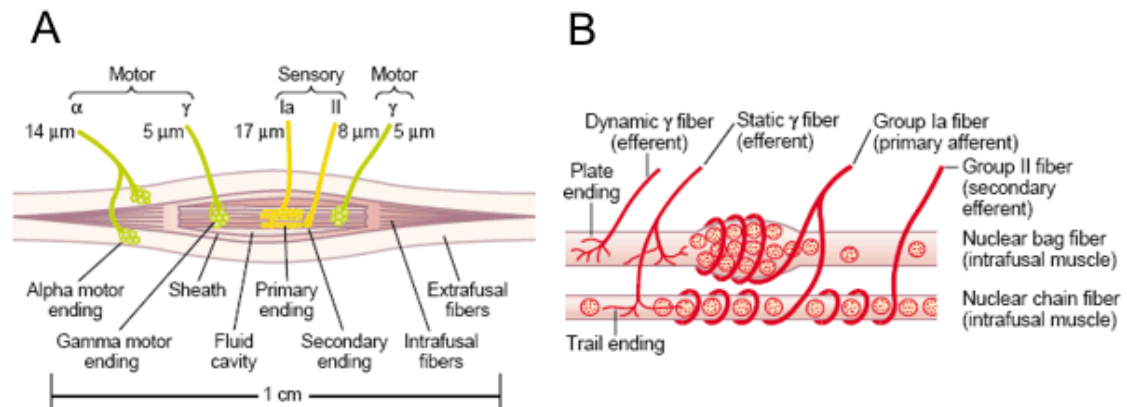


Figure 2.6. Schematic of the skeletal muscle spindle. A) Overall structure showing relation of spindle to the extrafusal fibers B) Magnification of the intrafusal fibers. Modified from [39].

The muscle spindles, as shown in Figure 2.6a, are sensory organs located in the belly of striated muscles. Each spindle is 3 to 12 millimeters long and built around small intrafusal muscle fibers, whose ends are attached to the surrounding large extrafusal muscle fibers. The region in the middle of the intrafusal fibers, which has the spindle receptors, is conspicuous by its absence of actin and myosin filaments and hence cannot actively contract. Two types of sensory receptor endings are found the middle region of the spindle: these are the primary and secondary endings. The primary endings are type Ia afferents and are about 17 micrometers in diameter on average. They wrap tightly around the center of the spindle. The secondary endings are much smaller type II fibers, only about 8 micrometers in diameter. These are called ‘trail’ or ‘flower-spray’ endings due to the way they spread out on one or both sides of the primary endings. Furthermore, as shown in Figure 2.6b, there are two classes of intrafusal fibers known as nuclear bags and nuclear chains respectively. The nuclear bag fibers have a large concentration of nuclei accumulated in the central region of the spindle, while the nuclear chains have their nuclei spread out more evenly. While both nuclear bags and chains are innervated by the type Ia afferents, the nuclear chains are almost solely innervated by the smaller type II sensory afferents [47, 51].

The spindle receptors are concentrated in the middle of the spindle and therefore are excited in two situations- either when the whole muscle is lengthened thereby stretching the spindle as a whole, or when the ends of the intrafusal fibers contract with no changes in muscle length. Due to the segregation of intrafusal fibers and innervating sensory neurons, the spindle is able to respond to changes in length of the muscle, rates of changes in length (velocity), and acceleration. As shown in Figure 2.7, in terms of their frequency response, both 1a afferents and type II afferents have high-pass characteristics with a break frequency of about 1 Hz. However the gain of the type II afferent is of an order of magnitude lower than the 1a afferent. Below 1 Hz, both sets of afferents respond to static changes in muscle length. Above this frequency, they become sensitive to the velocities of muscle contractions. However, the 1a afferents have a smaller linear range and become acceleration sensitive beyond approximately 20 Hz [60].

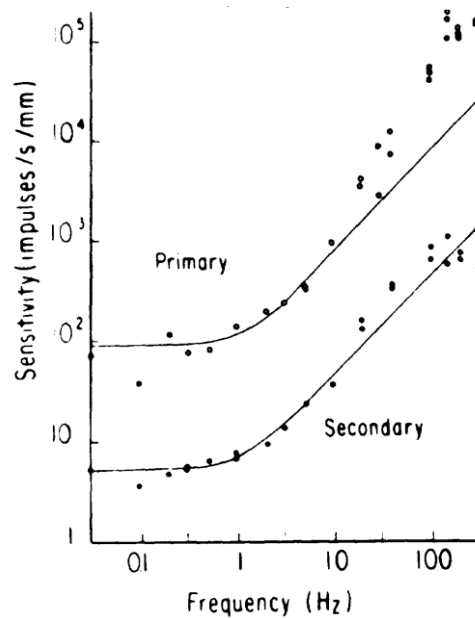


Figure 2.7. Frequency response of 1a and type II afferent fibers Adapted from [60].

The firing rates of these afferents, and hence the sensitivity of the spindle, are regulated by the γ -motor neurons projecting to the intrafusal fibers. These neurons can be subdivided into γ -d (for γ -dynamic) and γ -s (for γ -static) which innervate the nuclear bags and chains respectively. γ -d activity enhances the 1a velocity response, while the γ -s

activity increases the tonic discharge of both 1a and type II afferents. The precise anatomical origins of this γ -drive are still contentious, although central commands are known to be involved. It should be noted that during voluntary contractions of the surrounding extrafusal fibers mediated by the α -motor neurons, the γ -nerves are also co-activated in a phenomenon known as α - γ -co-activation. This shortens the ends of the intrafusal fibers and stretches the central receptor region of the spindle even if the muscle as a whole is contracted. This ensures that the spindle receptor region is at the optimal length to detect the stretch, and does not oppose the muscle contraction [38, 61, 62].

2.2.3.1.2.2 Golgi Tendon Organs

The Golgi tendon organs are sensory receptors about 1mm long and 0.1mm in diameter. They are located in the boundary between the muscles and their connecting tendons. Each organ is connected in series with 10 to 15 muscle fibers, and is stimulated by changes in tension over these fibers. Golgi tendon organs are more sensitive to active tensile forces, as opposed to passive changes in tension induced by stretching of the muscle. They are primarily made of a network of branched collagen fibers, within which sensory receptors are entwined, and are innervated by 1b afferent nerves approximately 16 micrometers in diameter. Active tension in the muscle stretches the tendon, distorts the collagen fiber organization, and hence activates the 1b receptor endings [47].

2.2.3.2 Spinal Reflexes

As shown in Figure 2.5, the peripheral afferents synapsing with motor neurons (either directly or through interneurons) result in a number of peripheral spinal reflex circuits which provide involuntary, almost instantaneous, motor responses not initiated by the CNS. A commonly known reflex is the flexion-withdrawal muscle reflex initiated by the stimulation of pain receptors in the skin (e.g. stepping on a piece of glass results in flexion of the leg and withdrawal of the foot). Another example is the Golgi-tendon reflex, which inhibits muscles when there is a build-up of tension sensed by the Golgi tendon receptors.

2.2.3.2.1 Muscle Stretch Reflex

The focus of this experimental work is the muscle stretch reflex initiated by the muscle spindles. It is primarily monosynaptic with a direct connection between the spindle afferents and the α -motorneurons innervating the homonymous muscles. Its actions at the ankle are believed to contribute to postural stabilization, by providing a resistive stiffness component to the ankle joint [8].

Figure 2.8 shows the pathways involved in the knee-jerk stretch reflex, typically used by physicians to study the peripheral nervous system, invoked by a tap of the patellar tendon. Stretch reflexes at the ankle muscles follow the same neural principles. Tapping the tendon stretches it and the associated quadriceps muscle. This is sensed by the spindles of the quadriceps and results in the activation of the primary (1a) and secondary (type II) afferent fibers.

As shown by pathway A, which is the monosynaptic reflex arc, the afferent (mostly 1a) synapses with the α -motorneuron, and results in a contraction of the quadriceps (i.e. the homonymous muscle). Furthermore, as shown in pathway C, efferents projecting to synergistic muscles that aid the homonymous muscle are also activated by the afferent fibers. This is shown in pathway C. At the same time, as shown in pathway B, branches of the afferent synapse with inhibitory interneurons that in turn pre-synaptically inhibit the efferents innervating the antagonist muscle. This is called reciprocal inhibition, and ensures that the antagonist action does not oppose the reflex action in the homonymous muscle or trigger a stretch reflex in the antagonist muscle. Lastly, as shown in pathway D, ascending pathways carry the sensory information to higher structures in the CNS. Since the neural signals have to travel from the spindles to the spinal cord and back to the efferent, there is a delay associated with the reflex action. In the TS, the monosynaptic stretch reflex delay (with respect to muscle stretch onset) is typically 40-50 ms (known as the M1 response) [47].

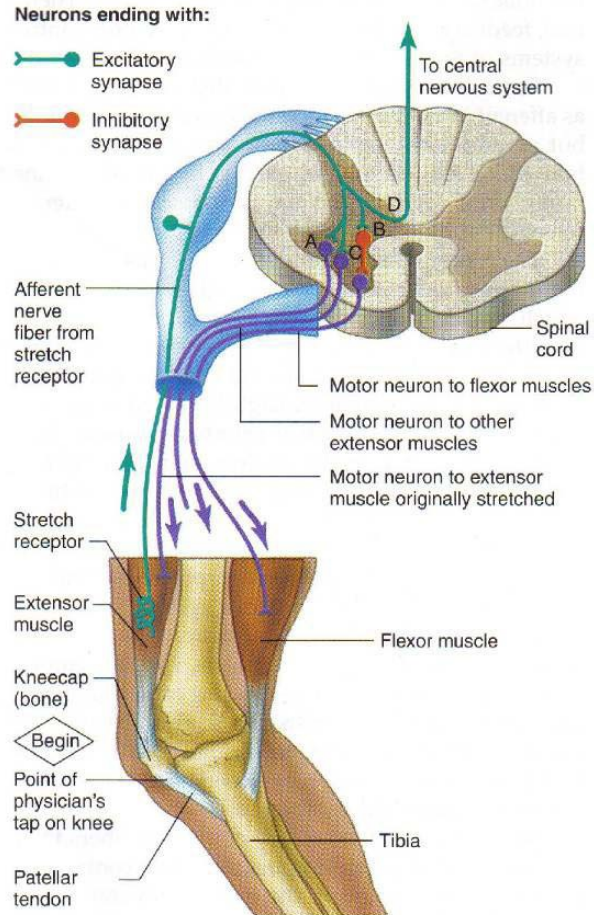


Figure 2.8. Stretch Reflex Pathway. The monosynaptic stretch reflex to the homonymous muscle (Path A), reciprocal inhibition (Path B), synergist activation (Path C), and feedback to higher brain centers (Path D) are all shown. Adapted from [47].

2.2.3.2.2 Physiological Sources of Stretch Reflex Modulation

Research has shown that stretch reflexes are not static, but modulated under a variety of conditions. These studies will be discussed in Section 2.4.3.2. The possible neural mechanisms which facilitate this modulation are briefly summarized here. Most of these mechanisms have already been alluded to before in the discussion of spinal circuitry and spindle properties.

The activity of the α -motorneuron is directly influenced by monosynaptic connections from descending corticospinal neurons originating in the cortex and cerebellum. This efferent modulation therefore also has a direct effect on the sensitivity of the reflex pathway. In addition, the numerous polysynaptic reflex cord pathways, utilizing an intermediary interneuron between the sensory and motor neurons, also

receive higher order inputs from the CNS which can then in turn influence the efferent neuron output [13, 63].

γ -motorneuron drive is an important mechanism via which the sensitivity of the spindles is regulated. The γ -neurons are thought to be influenced by descending commands from higher order brain centers either directly, or via interneurons synapsing from the corticospinal tract [62].

Lastly, at the level of the spinal cord, pre-synaptic and post-synaptic inhibitions regularly occur. Ia inhibitory interneurons and Renshaw cells, which receive a copy of the α -motorneuron command and then inhibit them post-synaptically to regulate the amount of efferent drive, are thought to be involved [29, 30, 57, 64].

2.2.3.2.3 Reflex Measurement

2.2.3.2.3.1 Electromyography (EMG)

Reflexes are typically quantified using EMG. Electromyography (EMG) is a technique of measuring the neural activity of muscles. Muscle fibers are activated by the spread of action potentials and the depolarization of the fiber membrane, which can be detected by electrodes. The summation of all the recruited fibers of a motor unit is referred to as a motor unit action potential (MUAP). It is difficult to isolate a single MUAP since many motor units are activated during skeletal muscle contractions, often asynchronously. Moreover, the shape of each MUAP will be influenced by the number and composition of the recruited fibers [51].

Regardless, the EMG provides a spatial and temporally filtered estimate of neural drive to the muscles. Both surface and needle electrodes can be used. Needle electrodes allow a small number of muscle fibers to be isolated, allow for a high signal to noise ratio, and can be potentially used to study single MUAPs. However, the procedure is invasive and requires a trained medical professional to physically insert the electrodes through the skin into the muscle tissue. A more general picture of muscle activation, noisier but less invasive, can be obtained by using surface electrodes placed accurately on the skin above the muscle of interest [65].

2.2.3.2.3.2 H-Reflexes

As opposed to mechanically inducing a stretch, the 1a afferents innervating the spindles can also be directly electrically stimulated by the experimenter. This is the basis for the Hoffman reflex (H-reflex), a test that is typically used to assess α -motor neuron excitability with EMG measurements.

At low levels of stimulation, an H-wave is seen at a lag of 40 ms similar to the M1 peak described previously. However, as the stimulation amplitude increases, a response known as the M-wave is also seen at a shorter lag of 10 ms. This is due to the direct activation of the α -motorneuron efferent fibers, which have a higher activation threshold than the 1a afferents. If the stimulation amplitude is increased even more, the H-wave decreases in amplitude to zero. This is due to antidromic conduction, where the generated action potential travels in the opposite direction along the afferent nerve and cancels out the H-wave reflex activity [51].

It should also be noted that even with low levels of stimulation, H-reflex changes do not necessarily directly translate to stretch reflex changes. Andersen et al. [33] investigated the two reflex mechanisms during walking, and found significant differences during the late phase of stance which is associated with the unloading of the muscle spindles. Morita et al.[32] investigated differences between the effects of pre-synaptic inhibition on H-reflexes and stretch reflexes, and found that H-reflexes were more sensitive to pre-synaptic inhibitory mechanisms. Since the effects of the spindle are ignored in the H-reflexes, they suggested that mechanical and electrical stimuli might cause differences in the composition and/or temporal dispersion of the 1a afferent signals. During an H-reflex the 1a afferents are all activated almost simultaneously. This leads to a motor volley that is highly synchronized. However, during a mechanically elicited stretch-reflex the 1a afferents are not activated synchronously; some afferents may also discharge multiple times. Therefore during a stretch reflex, the α -motor neuron discharge patterns are a factor of the size, velocity, and acceleration of the muscle spindle receptor stretch (Figure 2.7) [32].

2.2.3.2.3.3 Reflex Torque

During pulse perturbations used to elicit a reflex, the mechanical effects of reflex changes can also be assessed by studying torque changes at the ankle. The torque measured at the ankle will typically have two components:

- An intrinsic component determined by the passive visco-elastic properties of the ankle joint, tendons, ligaments and musculature, and the inertia of the limb.
- A reflex component as contributed by the muscle stretch reflex.

The intrinsic torque principally occurs while the perturbation is in effect (due to the motion of the ankle). However, the reflex torque does not typically occur till 80-100 ms after the reflex EMG peak (i.e. 120-160 ms after stretch onset), and after the ankle has stopped moving. Hence the two components can be distinguished temporally [66].

These torques are typically used to calculate the intrinsic and reflex stiffness respectively, and hence the total joint stiffness which is defined as the dynamic relationship between the position of the joint and the torque acting about it [67]. For the experimental work described in this thesis, only the reflex torque was measured.

2.3 Basic Principles of Balance

Studies investigating postural sway in the anterior/posterior plane have generally modeled the human body during quiet stance as a rigid inverted pendulum pivoted about the ankle joint [1, 68], although this is understandably a working oversimplification of the system [69, 70]. The inverted pendulum model is illustrated in Figure 2.9.

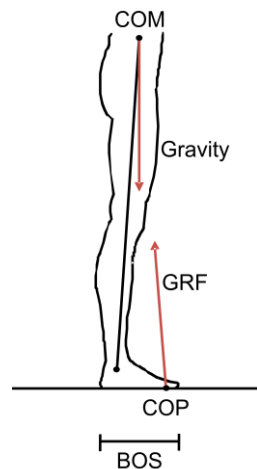


Figure 2.9. Inverted pendulum model of human stance.

It illustrates the interplay between the four fundamental concepts described below:

- **The Center of Mass (CoM)** refers to the average spatial location of the mass of a given object. For the purposes of studying the object's reaction to a uniform external force, it can be used as a representative point. With respect to the human body, it is calculated by a weighted summation of the locations of the CoMs of the individual body segments. Hence, its position in 3-D space is directly dependent on the body's postural configuration [71]. Research has shown that, during quiet stance, the position of the CoM actually lies slightly anterior to the ankle [3]. As per Newton's 2nd law, in the absence of any other external forces acting on the rigid body pendulum, the downward gravitational force will exert a clockwise rotational moment about the ankle joint and cause the pendulum to fall forward. A condition of stability therefore necessitates the existence of an upward external force that can produce a counter-clockwise torque about the ankle joint.
- **Center of Pressure (CoP) and Ground Reaction Force (GRF):** As indicated previously (Section 2.2.2.3), the activity of the muscles of the lower leg- primarily the TS and the antagonist TA flexor muscle- produces ankle torques that plantarflex and dorsiflex the foot respectively. The center of pressure (CoP) is the point at which the resultant downward force (comprised of gravity, active muscular forces, inertia) acts. It is also the point at which the equal and opposite (Newton's 3rd law) upward ground reaction force (GRF) acts. Since the foot is not actually lifted off the ground during quiet stance, the active contraction of the muscles effectively shifts the center of pressure (CoP) within the foot surface. Therefore, by constantly regulating the ankle torque, and thereby moving the CoP (i.e. changing the point of action and hence the moment arm of the GRF about the ankle joint), the size of the stabilizing counter-clockwise torque about the ankle can be manipulated [2].
- **Base of Support (BoS):** The Base of Support (BoS) is defined as the area outlined by the feet on the ground. For instance, by adopting a wide stance the BoS becomes larger. The BoS provides the physical limits within which the position of the CoP can be actively manipulated [71].

It should also be noted here it has been shown that the position of the CoM is also influenced by internal perturbations (e.g. breathing, movement of the abdomen) [72, 73].

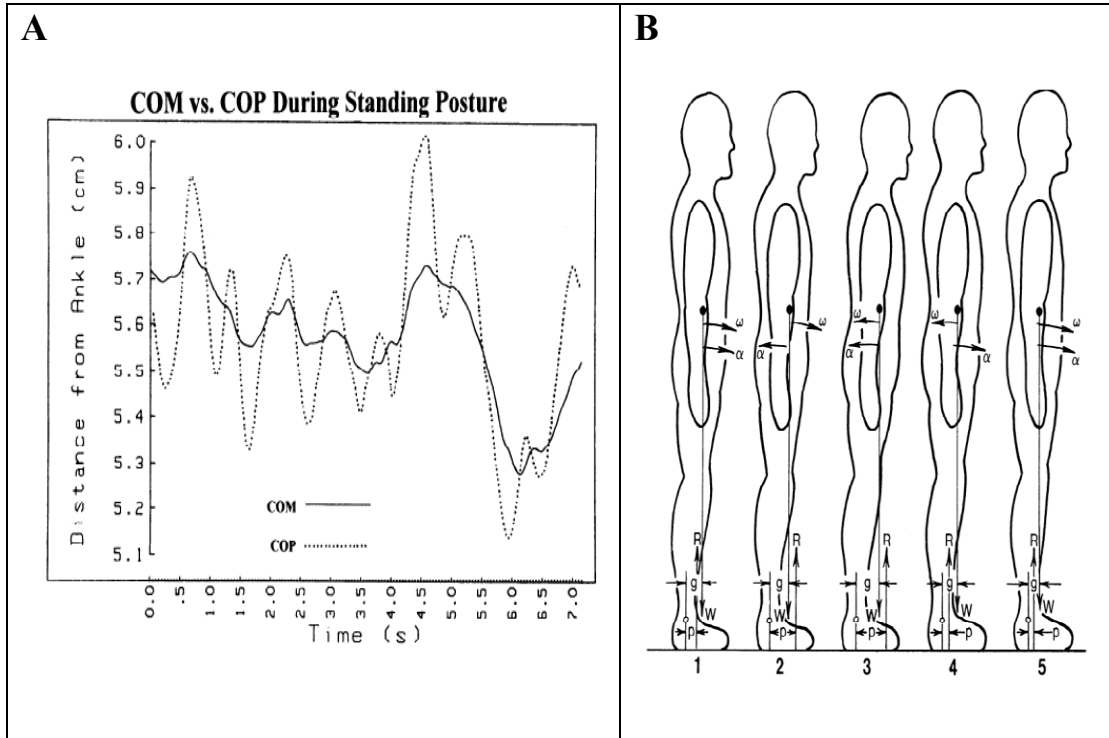


Figure 2.10. Inverted pendulum mechanics. A) Oscillations of CoP and CoM in the A/P plane. The CoP oscillations are of larger amplitude and higher frequency. Adapted from [2]. B) A subject maintaining quiet stance at five different times. α : CoM angular acceleration, ω : CoM angular velocity, R: Ground reaction force, W: gravity, g: Downward projection of CoM (moment arm of gravity about the ankle), P: CoP position (moment arm of the ground reaction force). Notice that the angular acceleration of the CoM is proportional to the difference between p and g. Adapted from [2].

The control system does not lead to perfect stabilization of the body. As shown in Figure 2.10a, the body behaves like an under-damped oscillator with the CoP (and hence the CoM) constantly oscillating about a set-point. Furthermore, as illustrated in Figure 2.10b, the position of the CoP and the location of the downward projection of the CoM with respect to the ankle joint determine the length of the moment arm for the torques created by the GRF and gravity about the ankle joint respectively. Since during quiet stance, the $GFR \approx W$, the respective lengths of the moment arms (p and g) determines which torque dominates the other. Therefore, the polarity and

magnitude of the acceleration (α) of the CoM will be directly proportional to the difference between the CoP and the downward projection of the CoM on the ground [2].

2.4 Mechanisms of Postural Control

While useful as a model to understand the fundamental physical necessities to maintain balance, the inverted pendulum model makes no predictions about the nature of the underlying control (i.e. the mechanisms leading to the detected changes in CoP and CoM).

The main suggestions in this lieu have included:

- *Passive influences* due to the mechanical visco-elastic and inertial properties of the ankle joint, muscles, tendons and ligaments.
- *Active control* from the CNS incorporating vestibular, visual and proprioceptive information. These sensory inputs are incorporated into:
 - Feedback (reactive) control mechanisms
 - **Feed-forward (predictive) control mechanisms.**
- ***Active control through stretch reflex mechanisms*** in the PNS.

The experimental work presented in this thesis (Chapters 3 and 4) investigates the stretch reflex mechanisms associated with feed-forward active control from the CNS, in the time period just preceding self-destabilizing voluntary arm movements (hence highlighted in bold above). Therefore, previous studies that explored passive control, and active feedback CNS mechanisms, are not directly relevant to this study. Regardless, they are briefly summarized for the sake of completeness in Section 2.4.1 and Section 2.4.2.1. The rest of the chapter provides a more comprehensive review of the feed-forward and stretch reflex literature.

2.4.1 Passive Influences

Winter et al.[1] put forward a simplified stiffness control model which suggested that the inverted pendulum could be balanced entirely passively, without any major active inputs from the CNS except to set the initial muscle tone in the postural muscles. In terms of physics, stiffness is typically defined as the resistance of an elastic body to the deformation applied by an external force. With respect to the inverted pendulum model,

the ankle joint along with its ligaments and tendons can be thought to provide an intrinsic stiffness to the pendulum with inertial, viscous and elastic components. The postural muscles then essentially act as damped rotational springs about the joint.

Their conclusions were based on results which showed that the CoP and CoM oscillate in phase during quiet stance, with the CoM lagging the CoP by 4-6ms. Based on this information, the authors ruled on any form of any active reactive CNS feedback control which would theoretically introduce CoM-CoP lags of 150-200ms due to neural conduction delays. They also found that sway did not significantly change if eyes were kept open or closed, and that head accelerations and limb velocities of their subjects were below previously found thresholds for detection by the otoliths. Hence, they concluded that no complex sensory integration incorporating vision and/or vestibular information was necessary to minimize sway [1].

In my view, it is misleading to suggest that this theory truly represents passive, mechanical control. After all, the muscles cannot contract spontaneously and require CNS inputs. However, perhaps the key point to realize with such a control schema is that the CNS does not need to play an active role in monitoring and regulating the sway; it just sets up the initial resistance in the system, after which the passive mechanics take over.

2.4.2 Active CNS Control of Balance

Several subsequent studies showed that the intrinsic ankle stiffness alone, as modeled by Winter et al. [1], would be below the threshold (critical value of stiffness) required to oppose the gravitational destabilizing torque [68, 74, 75]. They also suggested that Winter et al.'s [1] estimates of the ankle stiffness were flawed as his methods did not take into account irregularities in the modulation of neural activity. Furthermore, Morasso and Schieppatti [74] disagreed with Winter's interpretation of the CoM/CoP phase lock and small delay. As illustrated in Figure 2.10b and explained in Section 2.3, the biomechanics of the inverted pendulum dictate that the acceleration of the CoM will be directly proportional to the difference between the CoP and the downward projection of the CoM on the ground. Given that it is a physical necessity of such an inverted

pendulum model, they refuted the claim that this could be used as evidence to substantiate any particular control theory. In general, these studies suggested that the CNS had to play a more active role in postural regulation [74].

2.4.2.1 Feedback CNS Control

Figure 2.11 shows a general schematic of feedback control. The controller aims to minimize the error between the output and the reference input signal by constantly monitoring information about the output state. An example relevant to motor control would be a situation where a person is required to maintain his/her arm at a particular position while holding a load but is perturbed by a sudden external disturbance (e.g. an increase in the load).

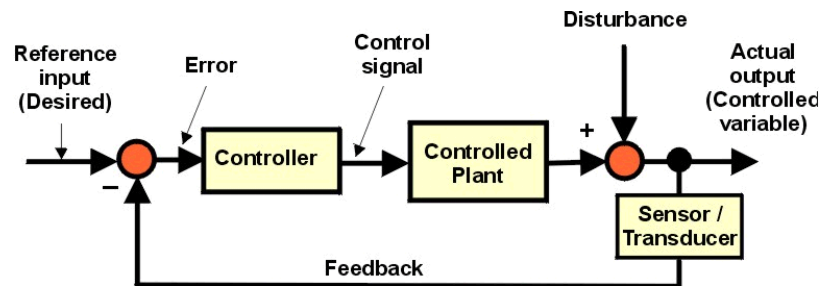


Figure 2.11. General diagram of feedback control. Adapted from [76].

2.4.2.1.1 Feedback Control of Posture

Studies exploring feedback postural control have typically done so through the use of perturbed support surfaces. The subject maintains quiet stance on a stable support base usually embedded with force sensors, which is then unexpectedly translated in the horizontal plane. Electromyography (EMG) and force sensor readings are then used to draw conclusions about postural strategies adopted. Typically within about 70-100 ms of the perturbation, a pattern of muscle responses in the supporting limbs is detected which restores the position of the CoM within the BoS. The latencies of these responses are much less than voluntary movements (e.g. reacting to a visual or audio cue) which are in the order of approximately 200ms. They are also much larger than those typical of a simple monosynaptic stretch reflex (approximately 40-50 ms) [77, 78].

The sudden change in postural orientation and CoM in the direction of platform acceleration is sensed by the major sensory modalities of the body (i.e. vestibular, visual,

and somatosensory). It is thought that the cortex then uses this feedback information to trigger the appropriate postural muscle responses known as Automatic Postural Responses (APR's). The vestibular system, as a detector of linear and angular accelerations of the head, is thought to counter large unexpected postural changes by modulating the spatial patterns of postural muscle contractions through the actions of the vestibular nucleus[79-81]. Visual information, which one might expect to be too slow to be useful for such stabilization, has also been shown to affect the APR's and attenuate sway [82, 83]. Somatosensory information from joint receptors, muscle spindles, and Golgi tendon organs is relayed to higher brain centers through ascending corticospinal neurons, with some authors suggesting that they might be the most crucial of the three modalities [84-86]. In situations where one modality is disrupted, either due to external conditions (e.g. darkness and hence no vision) or internal conditions (e.g. physiological lesions in the vestibular system) the other channels are up-regulated to compensate accordingly- a theory known as sensory re-weighting [5, 87, 88].

It should also be noted that this theory of automatic reactive feedback control as a truly cortical process is debatable. For example, the latencies of these APR's are very similar to 'functional stretch reflexes' described in earlier work by Nashner [9], using similar paradigms. Although he suggested that these reflexes were cortically modulated, there are others who suggest that they could be attributed to type II afferent reflexes or other non spindle related afferents. This will be discussed further in Section 2.4.3.1.

2.4.2.2 Feed-forward CNS Control

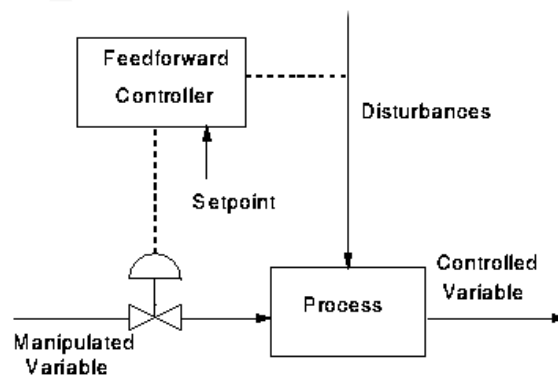


Figure 2.12. General schematic of feed-forward control. Adapted from [89].

Figure 2.12 shows a general schematic of feed-forward control. As opposed to feedback control, the nature of the disturbance to the system is assumed to be known a-priori (or by measurement as it enters the system). The controller then combines this information along with the required change in the manipulated variable using a pre-existing internal model, so that it is able to keep the controlled variable at the desired set-point. This allows the control system to predict changes as opposed to reacting to them. Theoretically it is more robust than a feedback system, as disturbances should not destabilize the system and delays associated with state information update become a non-issue. However, feed-forward control is limited by the fact that the controller must be designed uniquely to deal with a specific application. Also, in a feed-forward system the controlled variable is not monitored, and hence errors cannot be fixed.

2.4.2.2.1 Predictive Internal Models

Therefore it is unlikely that only a feed-forward neural controller is used in neural control, given the potential for instability and the high degree of computational complexity associated with any given task. Furthermore, in situations which involve unpredictable external disturbances, the CNS must rely on sensory feedback to adopt compensatory actions. However, given the inherent delays in the sensorimotor system, it is has long been believed that the CNS does use internal models of motor control that are able to act in an anticipatory fashion in situations that involve predictable, self-generated disturbances (e.g. due to voluntary movements). Both forward and inverse predictive models have been postulated.

Forward models are built upon the theory of efference copy, first proposed by von Holst and Mittlestaedt studying the vestibular-ocular reflex in fruit flies[90]. These models have been extended to explain a number of motor control situations involving self-generated motions such as the modulation of grip force, the maintenance of postural equilibrium, and the identification of active versus passive head movements [91-95] .

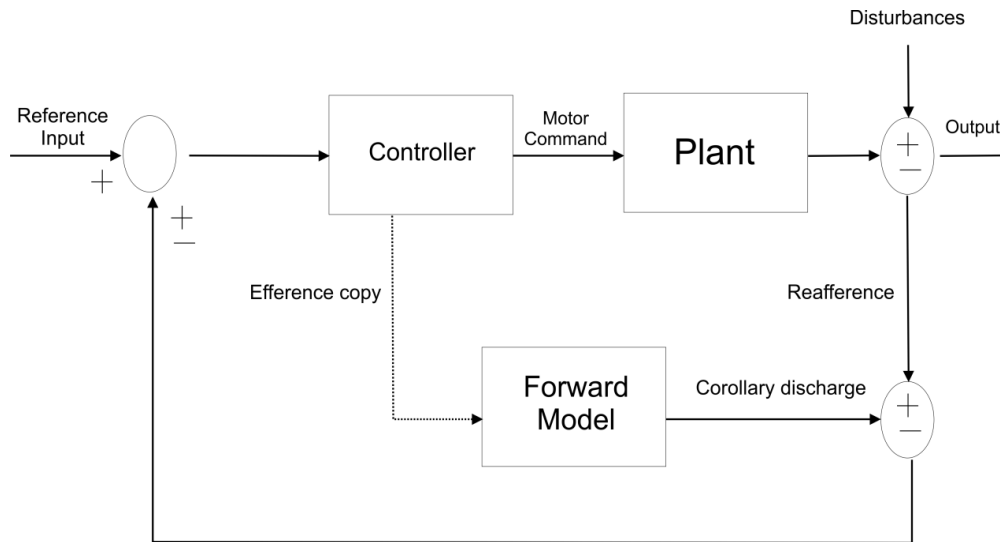


Figure 2.13. Use of forward models in combination with sensory feedback for motor control.

As shown in Figure 2.13, it is believed that when an efferent signal is generated by the CNS controller, a copy of the signal known as an efference copy is produced. Using a forward model, this efference copy signal is then used to estimate the sensory feedback due to the output motor command, a term defined as corollary discharge. The corollary discharge is thought to be an inhibitory command sent out at the same time as the motor command. In the event that the action is self-generated, the corollary discharge should match the sensory feedback (reafferece), hence negating the feedback loop. The system therefore behaves as a feed-forward controller anticipating the disturbances prior to their actual occurrence. Furthermore, in a situation where this is not the case, the body is able to detect that the changes are indeed due to external disturbances, and modify the subsequent motor commands [95].

A complementary theory suggests that the controller itself adopts a predictive inverse dynamics model whereby the desired sensory feedback is directly translated into an estimate of the required motor command. As shown in Figure 2.14, it is postulated that the cerebellum might contain such models, which allow it to execute novel actions where no feedback is initially available. Furthermore, the output from the inverse model could also potentially be used as an input to the forward models [96-98]. It should be noted that both the forward and inverse models need to be updated through learning in order to

remain useful in generating anticipatory commands. This is thought to be done through feedback learning (i.e. by trial and error) to adjust the model parameters [97].

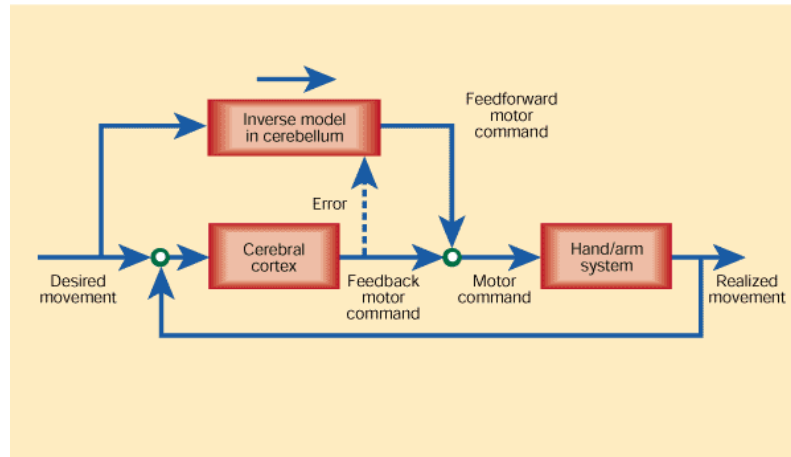


Figure 2.14. Combination of feed-forward (inverse model in the cerebellum) and feedback (cortical) CNS control. Adapted from [96].

2.4.2.2.2 Feed-forward Control of Posture

A number of authors have attempted to investigate whether predictive feed-forward mechanisms are used in postural control.

For the APR's (Section 2.4.2.1.1), response latencies (with respect to the perturbation) were in the range of 70-100 ms. These latencies are longer those for a simple monosynaptic stretch reflex but much shorter than responses due to purely voluntary movements. However, in these experiments, the authors also found that the APR latency times typically decreased as a function of the number of perturbation trials experienced by the subject. Therefore, even though the primary neural control model is a feedback one reacting based on sensory changes, the authors suggested that a feed-forward learning/adaptive component might also be involved [78]. The CNS was postulated to use knowledge from prior perturbations, and incorporate them into pre-programmed motor actions to facilitate future responses, thereby reducing the demand on strictly feedback processes. A similar rationale, based on the incompatibility of feedback conduction delays, was proposed by Morasso and Schieppati [74] in their analysis of Winter's [1] passive control hypothesis.

Gatev et al. [99] investigated if the CNS used body sway in a predictive fashion by analyzing EMG, kinetic, and kinematic data from subjects maintaining quiet stance. Narrow and wide stance positions, with eyes open and closed conditions were tested. They detected a strong positive correlation between EMG activity in the lateral GS and the anterior/posterior changes in CoP, with time lags of 200-350 ms. This was interpreted as evidence for a feed-forward modulation of lower leg muscle activity, with the CNS actively anticipating the body position and regulating the body sway in advance by contracting the postural muscles.

However, Masani et al. [100] interpreted these same results differently, and showed through simulations that a PD controller, optimized to a high gain for ankle joint velocity information (feedback system with memory of the rate of change of error) can produce the same ‘anticipatory’ control without necessarily requiring a feed-forward controller. They verified their model through experimental recordings of body kinematics and EMG activity.

In general, it is difficult to draw conclusions about the underlying controller with quiet stance studies. As discussed above, in theory, both a reactive feedback velocity controller and an anticipatory feed-forward position controller can produce the same observable output. Unless the current state of a system (i.e. the effect of the initial condition) is defined, it is impossible to clearly determine cause and effect. This can be achieved by perturbing the system with an input at a specific set-point.

2.4.2.2.2.1 Anticipatory Postural Adjustments

More conclusive evidence for the existence of feed-forward mechanisms in postural control has come from studies exploring the destabilizing effects of voluntary movements on posture, where the movement functions as perturbation to the system at a point in time. The execution of voluntary movements in a multi-segmented body brings forth a set of challenges for maintaining postural stability. In addition to the obvious static differences caused by a body movement (i.e. different relative limb segment orientation, alteration of the CoM before and after movement), the initiation of the

movement results in the production of dynamic destabilizing internal reactive forces and torques at the various linked body joints [21, 101].

As first shown by Belenkii et al. [24], stereotyped activation of the leg musculature occurs 50-100 ms prior to the onset of the focal (deltoid) muscle during a simple arm raising task. This proximal-to distal sequence of postural muscle activity, which is typically characterized by an inhibition of SOL muscle activity followed by an activation of the TA muscle, were termed as Anticipatory Postural Adjustments (APAs) [20, 23, 24]. The direct biomechanical effect is a backward shift in the CoP, and forward acceleration of the CoM. Figure 2.15 shows an EMG recording of the APA (data is aligned to the onset of the deltoid muscle activity- vertical line in each panel).

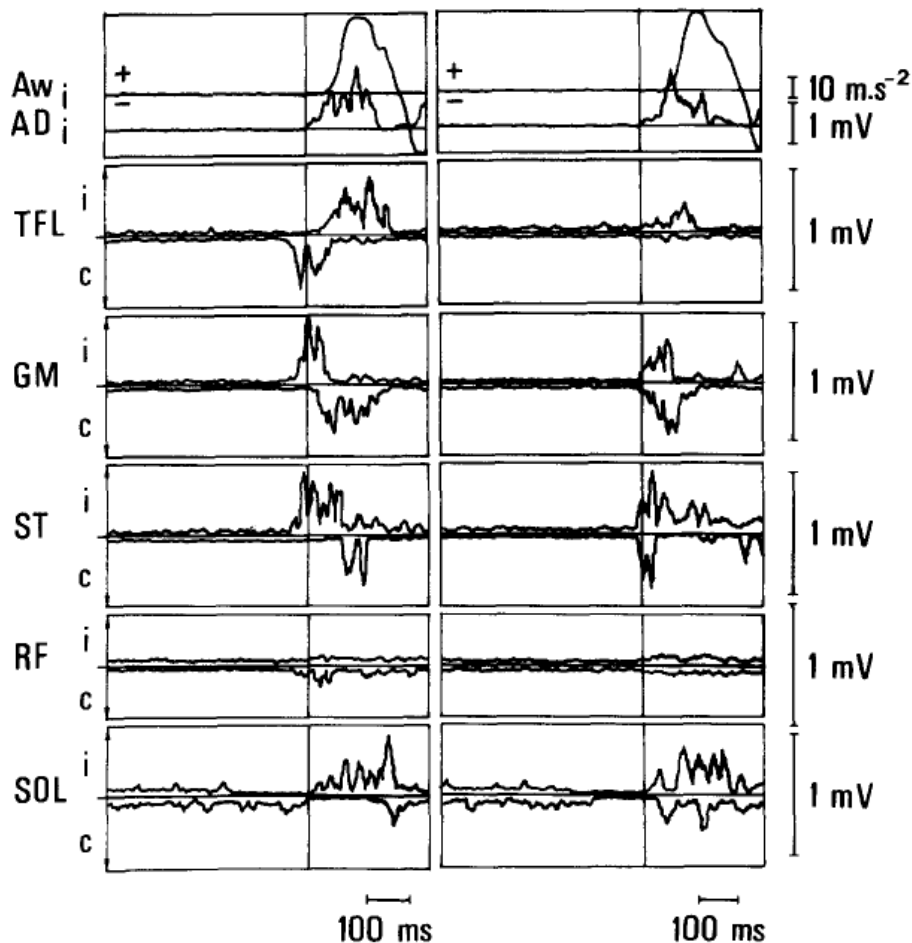


Figure 2.15. EMG activity associated with an upper arm acceleration (A_w). Data is shown for unilateral (left) and bilateral (right) arm raises for ipsilateral (i) and contralateral (c) limbs. Data is aligned with respect to anterior deltoid onset (AD). SOL: Soleus, RF: Rectus Femoris, ST: Semitendinosus, GM: Gluteus Maximus, TFL: Tensor Facia Latae. Note the inhibition in the ipsilateral SOL prior to activation of the deltoid muscle. Adapted from [20].

The arm raise however induces a downward and backward reactive force on the lower body which should accelerate the CoM backwards. Similarly, in experiments where subjects were asked to make backward arm raises, thereby causing the opposite biomechanical effect (an initial forward acceleration of the CoM due to the reactive force), the frontal postural muscles were activated as opposed to the dorsal postural muscles [25, 102]. Hence, the APA was traditionally interpreted as a source of CoM stabilization, opposing and minimizing the disturbances caused by the reactive forces on the body due to the voluntary movements [20, 103, 104].

However, an alternate interpretation of the role of the APA is that it might actually be used to facilitate the execution of the desired task by creating the dynamic conditions needed to execute the task, and not solely for CoM stabilization. Crenna and Frigo [19] showed that for a set of forward oriented movements including forward bending, rising on tip toes, whole body reaching, and gait initiation, the same characteristic APA pattern defined by an inhibition of the SOL followed by an activation of the TA occurred. The key point here is that, whereas some of these tasks would require a postural stabilization strategy similar to an arm raise whereby the CoM should be maintained within the BOS, others (e.g. gait initiation) would necessarily call for a destabilization of equilibrium moving the CoM forward. The global occurrence of the APA therefore casts its role as a CoM stabilizer into doubt. Lee et al. (1990), using a lever-pulling task, suggested that the APA might be used to facilitate the movement, as they showed that the amplitude of the APA was directly correlated to the size of the load and speed of the movement [105]. Amplitudes of the APA during gait initiation have also been correlated with the velocity of the forward movement [19, 106]. A set of arm reaching, and forward bend-and-reach experiments showed that the size of the APA was directly correlated to the size and distance of the target, as long as it was beyond arm's length [107, 108]. These effects were directly reflected in the changes in the CoP, with greater backward shifts for tasks that required greater CoM destabilization [107, 108].

Lastly, two more recent studies re-analyzing the arm raising task have both suggested that the role of the APA might be to control the various joint moments at the body segments as opposed to stabilizing the CoM [21, 28]. Patla et al. [28] compared

the changes in CoM during a movement with a simulated inverted pendulum model with only passive control. They found that initial control, up to 200 ms after movement onset, was entirely passive as the experimental and simulated profiles did not differ in this period, and instead suggested that the APA activity would be more useful for joint stabilization. Pozzo et al. [21] also discounted the idea of the APA as a CoM stabilizer during arm raises. They constructed a four joint model of the human-body (shoulder, hip, knee, and ankle). By segmenting the body as such, they showed that the effects of the arm movement were mostly at the hip and trunk, and that the overall CoM disturbances were minimal for the arm raise action (1.5 mm anterior displacement, which is still well within the BOS), and hence did not necessarily warrant any active compensation. They also indicated that the deceleration of the arm at the end of the movement would change the polarity of the initially de-stabilizing reaction forces on the body and lead to self-stabilization.

In summary, while the muscle patterns and biomechanical changes associated with the APA are well understood, its functional role is still debatable.

2.4.3 Reflex Contributions- Peripheral Nervous System Control

2.4.3.1 Stretch Reflex Characteristics

A third modality of postural control that has been extensively investigated has been the potential use of the muscle stretch reflex at the ankle. As mentioned previously, the vertical projection of the CoM during quiet stance lies about 5-6mm anterior to the ankle joint [3]. Biomechanically, this means that the body has a tendency to fall forwards due to the clockwise gravitational torque. This will stretch the TS, and should be therefore opposed by a stretch reflex at the TS. Intuitively, we could also expect any sway in the anterior and posterior directions to be countered by a dynamic stretch reflex in the TS and TA group respectively. Unfortunately, there has been little consensus to date on the relative importance of the reflex (with respect to the other control mechanisms discussed) and the specific conditions where it might be used.

Nashner [9] observed two kinds of stretch reflex responses at the ankle, a short latency response (M1) at a delay of 45-50 ms after the perturbation, and a long latency

response at lag of 100-120 ms relative to the perturbation. The longer latency response was thought to be cortically modulated and termed the functional stretch response (FSR) as it was functionally modulated depending on the specifics of the postural perturbation. This is described further in Section 2.4.3.2.2 [9, 109, 110].

However, the characterization and origin of the long latency component is still not well understood. For one, some studies have reported the occurrence of both medium (M2) and long latency (M3) components in the range of 60-100 ms, and their distinction is not always clear [111]. Peterson et al. [112] attributed the M3 component to cortical influences. However, one alternate hypothesis is that the M2 is caused by group II afferents, which have slower conduction times (and hence will result in a longer latency) [113]. Alternately, it has also been suggested that the M2 component is not due to spindle stretch at all but rather due to the activation of afferent terminals in the skin/subcutaneous tissues [114]. For example, there are numerous small afferent fibers with unmyelinated axons that terminate in free endings outside the spindles or Golgi-tendon organs. With respect to the TS, it has been shown that when the Achilles tendon is prodded (which activates only stretch receptors), as opposed to prodding the sole of the foot (which activates both skin and muscle receptors), the M2 response does not occur [114]. This is consistent with results from our lab, using both a supine and a standing foot actuator, where the foot is mechanically dorsiflexed, and only an M1 response is obtained.

Furthermore, reflex characteristics vary from muscle to muscle. Kearney and Chan [115] showed that the reflex characteristics differ considerably between the GS and the agonist TA muscle group. While only a short latency (M1) component (35-40 ms) after perturbation was found in the GS, foot plantarflexion produced two responses in the TA at latencies of 40 and 75 ms respectively, but of comparatively smaller magnitude than the GS responses. Grey et al. [116] also found responses with similar latencies (36 ms) when they applied a rapid dorsiflexion to the ankle during the step cycle. Sinkjaer et al. [117] found short, medium, and longer latency reflex responses in the GS and SOL at latencies during walking.

In summary, while the short latency component is consistently detected and well understood, the occurrence, characterization and neural mechanisms underlying the longer latency components are not clear.

2.4.3.2 Modulation and Variability of the Ankle Stretch Reflex

Moreover, the sensitivity of the stretch reflex has been found to be highly dependent on the conditions at the joint, especially the joint position and the activation level of the homonymous muscle. This is of direct relevance to this study, as the activity of the TS is inhibited during the APA period of a voluntary arm movement.

2.4.3.2.1 Effect of Joint Position and Muscle Activation Level

The position of the joint influences the reflex sensitivity. For instance, Weiss et al. [118] found that the magnitude of the TS reflex was proportional to the degree of ankle dorsiflexion, while the TA reflex was independent of joint position. Similar results were found by Stein & Kearney [13] who showed that reflex EMG and torque responses were greater when the ankle was perturbed with dorsiflexing pulses while in a flexed initial position as opposed to a relaxed initial position. In addition to the position of the ankle, the amplitudes of the reflex response also depended on the amplitude, duration and direction of the pulse (flexion pulse vs. extension pulse). The responses were highly non-linear as the pulse perturbations needed to be of a minimum amplitude and velocity threshold to elicit a response, with flexion pulses having a lower threshold. The responses also saturated as the input pulse amplitude and velocity increased.

Second, a number of studies have shown that reflex levels were directly influenced by levels of associated muscle activation. Some studies have suggested that reflexes scale directly with background activity levels (automatic gain principle) [119, 120].

However, other studies have shown that the relationship between reflex EMG and background activation levels is non-linear. Gottlieb and Agarwal [121] showed that, with isotonic contractions, the stretch reflex gain (Reflex EMG/Rate of muscle stretch) in the SOL was proportional to the level of tonic activation of the homonymous muscle. During

shortening (concentric) contractions, the reflex gain increased. However at very high rates of concentric contraction, the reflex gain decreased. Similarly during eccentric contractions (i.e. muscle lengthening, or contraction of the antagonist muscle), the reflex gain decreased. They found similar results in the TA as well.

Toft et al. [122] studied both the mechanical and EMG responses to stretches in the SOL muscle. With background torques (i.e. activation levels) ranging from 0 to 70 Nm, the ankle was dorsiflexed over a range of 5°. Similar to the results found by Gottlieb and Agarwal [121], they found that the reflex EMG did initially increase when the background activation level increased up to 30Nm, but beyond that there was no strict dependence of the reflex EMG on background levels. This was found to be the case for both the short latency (M1) and long latency (M2) components.

Stein & Kearney [13] showed that both the reflex EMG and the reflex torque in the GS extensor muscle increased non-linearly with activation of the extensors (homonymous muscle), and decreased with activation of the flexors (antagonists). The response saturated when background extensor torques greater than 20Nm were in effect. Furthermore, pulses that extended the ankle consistently produced larger reflex EMGs and torques than pulses that flexed the ankle at the same level of background torque.

This non-linear behavior of the SOL stretch reflex has also been demonstrated in decerebrate cats by Hoffer and Andreassen [123]. Since the SOL muscle is tonically activated during quiet stance, it has been suggested that this behavior might be explained by a saturation of the efferent motor neuron pool- the reflex EMG peaks are similar in magnitude to maximal voluntary contractions (MVC) in this muscle [122].

It should also be noted that EMG changes do not translate directly to mechanical torque and stiffness changes at the ankle. As indicated by Toft et al. [122], the monosynaptic reflex EMG measured is due to a highly synchronized activation of the different motor units. However the torque responses depend on the response characteristics of the individual muscle fibers themselves, and are hence not strictly equivalent to the reflex EMG. Sinkjaer et al. [7] investigated the reflex (and intrinsic) stiffness contributions at different levels of muscle activation. They showed that the reflex stiffness was maximal (0.5-1.5 Nm/deg) at 30-50% MVC, beyond which it

decreased. Mirbagheri et al. [8] conducted similar experiments to investigate the effects of different muscle activation levels (0 to -24Nm, more negative signifies a larger voluntary activation) on ankle stiffness. They found that both the reflex EMG and reflex stiffness increased when background activation levels were incremented from 0 to -3Nm. However beyond this level (-3 to -24Nm) the reflex EMG was constant, while the reflex stiffness gain decreased. Toft et al. [122] had similar results showing that the reflex stiffness contributed more than 50% to the overall stiffness at low background torque levels (~-10Nm), after which its contribution steadily decreased, culminating at less than 10% at high background torque levels (~60 Nm).

2.4.3.2.2 Task-dependent Modulation of Ankle Stretch Reflexes

A number of other studies have investigated how stretch reflexes at the ankle vary during different natural tasks, to understand if they are modulated in a functional, task-dependent manner.

Nashner [9] conducted a set of experiments where subjects stood on a platform that was either translated backwards, and hence induced forward sway, or directly rotated upwards at the ankles (which would not induce any direct forward sway). In both cases, the calf muscles are stretched and a stretch reflex is elicited. However, in the first situation a stretch reflex would be functionally beneficial to minimize the forward sway, while in the second situation it would not be useful, as it would induce sway. It was found that subjects rapidly inhibited the long latency reflex (over 3-5 trials) in the second postural set, as would be functionally appropriate. However, no such functional changes were found in the short latency reflex.

Sinkjaer et al. [124] investigated the modulation of the monosynaptic stretch reflex (M1) in the SOL during walking and compared it with standing. The reflex was maximal in the stance phase (comparable to normal standing), decreased to zero during the early swing phase, and recovered to about 45% of the stance phase levels in the late swing phase. They also found that the latency of the stretch reflex was invariant, suggesting that the spindles were kept sensitized during the different stages of the step-cycle (e.g. through α - γ co-activation). Lastly, they found that the maximal reflex EMG

amplitude constantly preceded the maximal background EMG. They concluded that the reflexes were used in the late phase of the stance cycle to strongly activate the homonymous muscles during heel contact and early stance, when the inertial torque on the body is greatest.

Grey et al. [14] investigated a number of different common tasks such as walking, cycling and sitting. Using dorsiflexions of the ankle generated with a portable device, they found that the short latency component of the stretch reflex did not change significantly across the three conditions, whereas the medium latency reflex was increased in the walking task, as opposed to the sitting and cycling task. They suggested that this was due to the fact that during the seated tasks (sitting or cycling) the body was well supported, while during walking the body had to account for the additional instability (and hence augment the reflex).

Kearney et al. [125] conducted analogous experiments, where they superimposed perturbations on simulated walking movements imposed by a hydraulic actuator on supine subjects. They also measured the mechanical torque responses. They found that the SOL reflex EMG was typically inhibited relative to steady-state conditions, and that it was modulated throughout the walking cycle (low at heel contact, maximum when ankle was dorsiflexed). As with earlier studies recording both reflex EMG and reflex torque measures, it was found that reflex torque changes did not strictly correlate with the EMG changes. The reflex torque was minimal during the late stance and swing phase, whereas the reflex EMG was maximal at this time.

2.4.3.3 Stretch Reflex Changes During the Preparatory Phase of a Movement

Therefore, while there have been numerous studies that have explored reflex modulation over a range of tasks, there have not been any studies that have documented the stretch reflex changes in the postural muscles during the APA phase of voluntary movements.

Woollacott et al.[126] showed that the overall sensitivities of the SOL short and long latency reflex pathways were voluntarily conditioned in preparation for an arm movement if subjects were given advance information on the nature of the arm movement (push vs. pull movement of the right arm). The excitability of the pathways

was determined at three fixed times: 100,300 and 500 ms prior to the onset of the visual cue which instructed the subject to execute the arm movement. They found that both the short and long latency components exhibited a generalized inhibition, and that the long latency component was inhibited more for push as opposed to pull trials. However, these measures do not correspond to the period of the APA as described in Section 2.4.2.2.2.1. Furthermore they are static measures of reflex sensitivities as opposed to an estimate of reflex variability over time.

Ramos and Stark [101] used simulations to predict reflex changes during the APA. With a two joint model of the body during a voluntary arm raise, they assessed the importance of anticipatory extensor, flexor, and reflex activity for postural stabilization by selectively removing these components and simulating the mechanical consequences. They suggested that anticipatory silencing of the postural extensor followed by a brief period of extensor activation and synchronous reflex activity was the optimal control strategy. However, while their models were tested with EMG data of the APA (from Bouisset [20]), they only validated the muscle activity changes (but not the reflexes).

However, there have been a few analogous studies which have investigated the SOL H-reflex during the APA phase of voluntary movements, such as arm raises, ballistic head movements, and stepping movements [29-31]. With respect to arm raise movements, they found that the SOL H-reflex inhibited approximately 60-80 ms before the activation of the focal deltoid muscle and rebounded approximately 60 ms after. The changes in the SOL H-reflex were also found to follow the same temporal pattern as the changes in the homonymous SOL muscle activity. The H-reflex inhibition was divided into two phases; prior to deltoid activation and after deltoid activation.

In the first inhibition phase, Kasai and Komiyama [30] found that the H-reflex inhibition occurred in both normal and counterbalanced stance, but that it was larger in the normal stance condition. While using low-intensity conditioning stimuli on the common peroneal nerve, they found no changes with a control condition, suggesting that local pre-synaptic inhibition was not responsible for the initial inhibition. Instead, they showed that the H-reflex changes prior to deltoid muscle activation were closely linked to

the anticipatory excitation of the biceps femoris (BF) muscle (hamstring), and the inhibition of the SOL muscle as mentioned above.

Kawanishi et al. [29] followed up on these experiments by conducting a set of experiments where the BF tendon was vibrated at 30 Hz at various times during the APA. This technique artificially induces pre-synaptic inhibition of the 1a afferents of the SOL by the 1a afferents of the BF and can be detected by a reduction in the SOL H-reflex. However, if large pre-synaptic inhibitory mechanisms between these two afferents are naturally in effect, then the vibration will have no additional influence as the GABA mediated inhibitory pathway will be saturated. Between vibration and non-vibration cases, they only found significant differences in the reflex in the time period prior to focal deltoid muscle activation. They suggested that this was evidence that only the inhibition phase post deltoid muscle activation was naturally mediated by local pre-synaptic inhibition.

The conclusion from these experiments was that the H-reflex inhibition was mediated by descending central commands altering α -motorneuron activity during the inhibition phase prior to deltoid muscle activation, and local pre-synaptic inhibition mechanisms in the inhibition phase post deltoid muscle activation.

2.5 Summary & Thesis Rationale

A number of theories have been proposed to better understand the neural mechanisms underlying postural control. While there is still much disagreement on a number of aspects, postural control can be thought to be mediated by an unknown combination of passive, reflex and active CNS inputs incorporating visual, vestibular and somatosensory information. Furthermore, the CNS commands have been incorporated into both feed-forward and feedback neural control mechanisms to explain how the body might counter various situations of postural instability [1, 4-8].

Of specific interest to us was a specific condition of postural instability (self-induced destabilizations of posture arising from voluntary movements of the limb). In such situations, feed-forward postural muscle activity (APAs) precedes the activation of the focal muscle involved in the movement. For forward oriented voluntary movements

(e.g. an arm raise, forward bend) this is characterized by an inhibition of the SOL muscle followed by an activation of the TA. This results in anticipatory forward sway, although it is still debatable whether the functional role of this sway is for CoM stabilization or movement initiation [19-22, 27, 28].

Our research group has traditionally investigated the role of ankle stretch reflexes in postural stabilization. These experiments were typically conducted on a supine apparatus (subject lies on his/her back with ankle fixed to an actuator), so that joint properties could be investigated. Past results from our laboratory, and other groups, have shown that the stretch reflexes do contribute significantly to the stiffness of the ankle joint and are therefore important postural stabilizers [8, 113, 118].

However, to our knowledge, no one has investigated how the stretch reflexes behave during the APA period. We aimed to address this question. We hypothesized that active stretch reflexes at the TS would theoretically counter the forward sway initiated by the APA, and hence we expected them to be inhibited during the APA period. Moreover, as discussed in Section 2.2.3.2.2, these reflex inhibitions could occur either simply due to the decreased activity in the TS (and hence a local decrease in α -motorneuron activity) or due to other centrals and peripheral mechanisms [13, 29-30, 57, 62-64].

Hence, using a voluntary arm raise paradigm, we systematically documented stretch reflexes changes in the TS by applying a small dorsiflexing pulse perturbation to the right ankle at different times during the APA phase. We studied both the time and amplitude modulation of the reflex using EMG techniques. These EMG changes were compared to the changes in background muscle activity EMG to shed light on the possible underlying neural mechanisms. Mechanical reflex torque changes at the ankle were also quantified to see if the changes in the reflex EMG corresponded to significant mechanical effects (i.e. in terms of a reflex torque response).

3. Methods

3.1 Outline

This chapter is structured as follows: Section 3.2 provides a general overview of the experiment. Section 3.3 provides details about the subjects used in the study. Section 3.4 summarizes the experimental paradigm. Section 3.5 provides a detailed description of the major components of the experimental setup, describing the apparatus, real-time control and data acquisition system. Lastly, Section 3.6 describes the pre-processing that was carried out on the collected data. Details about the data analysis and subsequent results are presented in Chapter 4, as part of a manuscript submission.

3.2 General Overview



Figure 3.1. A typical subject executing a voluntary arm movement while standing on the actuator. A) Bilateral electro-hydraulic actuator fitted with two foot pedals and torque, position and load transducers. B) Aluminum target frame holding visual and audio cues, torque feedback meter and target switch. C) Surface EMG electrodes on postural and focal muscles. D) Inclinometer used to measure arm position.

The goal of the experiment was to quantify the stretch reflex in the TS during the APA phase of a voluntary movement. To this end, subjects stood upright and repeatedly executed a unilateral right arm raise to a target anterior to the subject, positioned at arm's-length and shoulder height. At different times before and after the arm movement a small position perturbation was applied to the right ankle of the subject to elicit a stretch reflex. Over a number of repetitions of the task the reflex response, quantified using electromyography (EMG- Figure 3.1c) and mechanical torque responses at the ankle, was determined as a function of time with respect to the onset of the movement.

The experimental apparatus is now briefly summarized to facilitate an understanding of the experimental paradigm, to be described in Section 3.4. A more detailed description of the apparatus is provided in Section 3.5.

Figure 3.1a shows the subject standing on two rotary foot pedals, spaced 36 cm apart, of a bilateral electro-hydraulic actuator, a device that was previously designed in our laboratory [127]. The pedals were fitted with load cells, potentiometers, torque sensors and controlled by identical hydraulic actuators. This apparatus was used to apply a small position perturbation to the right ankle joint of the subject, eliciting a stretch reflex in the right leg.

Also, Figure 3.1b shows a custom-built aluminum frame fixed to the floor 55 cm in front of the actuator. It housed an audio “warn” cue (piezoelectric buzzer), a visual “move” cue (light emitting diode-(LED)), an adjustable target for the arm raise (push button switch), and two analog voltmeters to provide the subject with visual feedback of the torque at each ankle (and hence sway). A second, portable, “ready” switch was strapped to the subject's right thigh, to measure the start of the movement. The subject wore a custom-fit thermoplast cast around the elbow to prevent flexion. A single-axis inclinometer (Figure 3.1d) was attached to a wrist splint and oriented orthogonally to the radial bone to measure angular arm position.

Both the actuator and the components on the frame were controlled by a real-time controller that was responsible for coordinating the sequence of experimental events. A custom-built graphical user interface (GUI) allowed the experimenter to modify

experimental parameters and monitor the experiment. A second workstation was used for data acquisition and storage purposes.

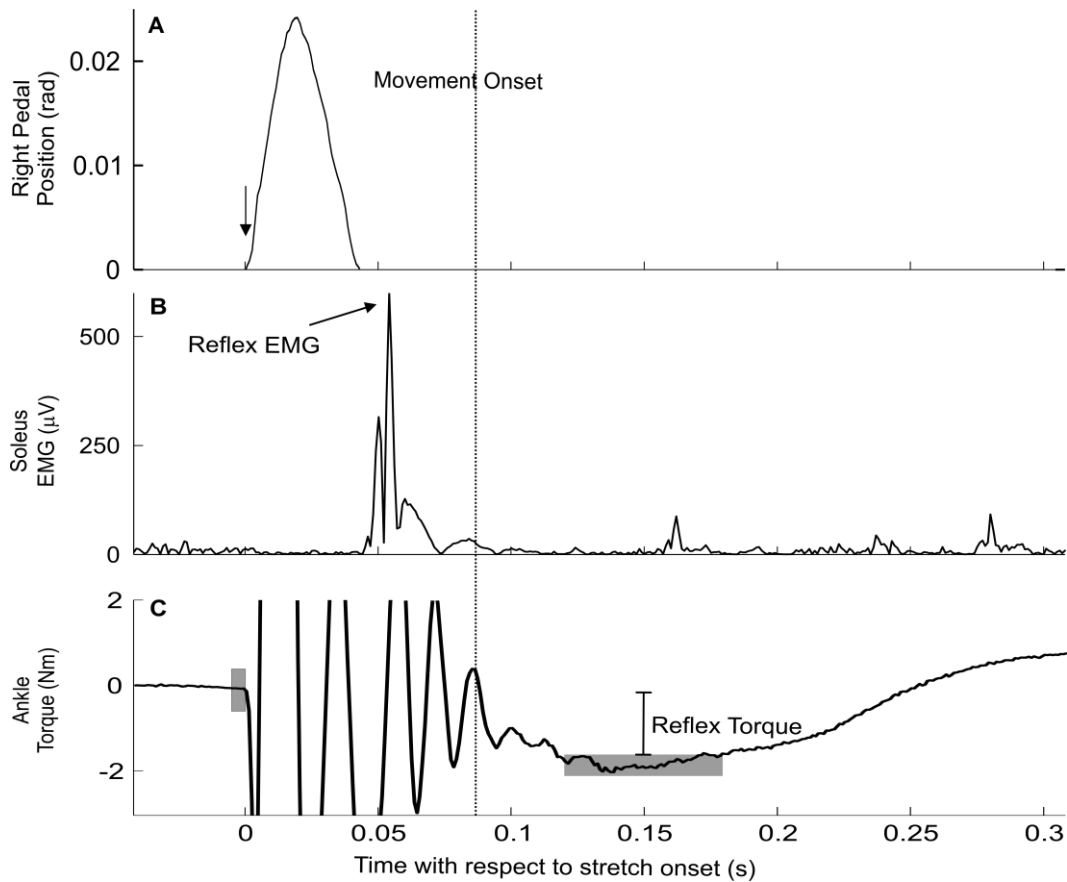


Figure 3.2. Sample trial from the experiment. A) A small dorsiflexion applied to the right ankle results in a Reflex B) EMG and C) Torque response.

Figure 3.2 shows a sample pulse perturbation trial from the experiment. Note that for every trial, the pulse was applied at a different time with respect to the onset of movement. The time of stretch onset is shown by the downward arrow in Figure 3.2a. This resulted in a reflex EMG response (Figure 3.2b) with a lag of approximately 50-60 ms, and a subsequent mechanical reflex torque response (Figure 3.2c) 120-180 ms after stretch onset, observed as a trough in the torque profile. The torque profile in Figure 3.2c is truncated at ± 2 Nm to magnify this trough. More details about the data analysis and results are presented in Chapter 4.

3.3 Subjects

Four male, and four female volunteers were tested for this study. All subjects were right-handed, and ranged from 21-26 years in age. They were provided with a detailed written and verbal description of the experiment. Subjects were required to sign a consent form, which had previously been approved by the McGill University Research Ethics Board. Consent and ethics approval forms are attached in Appendices B and C. Table 3.1 summarizes details about the subjects.

Table 3.1. Subject information

Subject initials	Age (years)	Gender (M/F)	Height (cm)	Weight (kg)
B R	22	F	175	57.8
E S	21	M	188	86.8
J D	23	M	167	75.0
J W	21	F	178	65.0
M O	21	F	165	65.5
R K	23	F	155	49.1
R O	26	M	185	75.0
W L S	24	M	172	74.6

3.4 Paradigm

Prior to the start of the experiment subjects were instructed to stand on the two foot pedals, and maintain a relaxed stance (with constant torque at both ankles) using the real-time feedback from the analog voltmeters for a period of 20 seconds. The average torque value over this period was used as a baseline, along with a modifiable tolerance limit, by the real-time controller.

The experimental paradigm was defined by a sequence of temporal events involving actions from the subject, activation of the cues on the target frame by the real-time controller, and a perturbation of the right pedal in 75% of the trials. This sequence of events is illustrated in Figure 3.3 and summarized below.

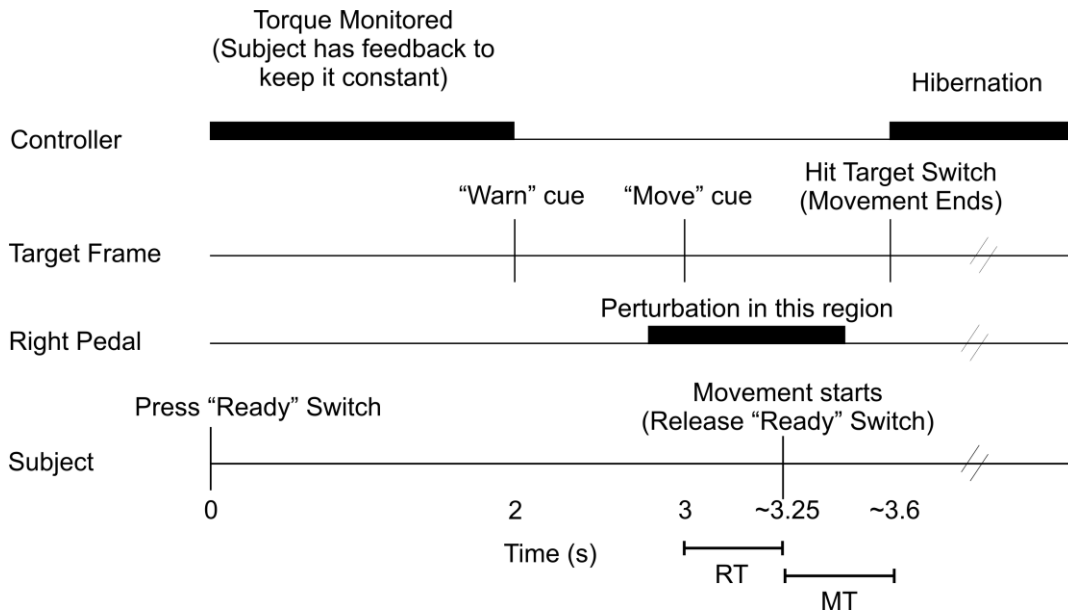


Figure 3.3. Chart indicating sequence of temporal events during the experiment for a single trial. RT and MT refer to the approximate average reaction and movement times respectively.

As indicated in Figure 3.3, subjects pressed the “ready” switch with their inner palm to initiate a trial. The torques at both ankles were monitored. Subjects were required to maintain torque levels within the defined baseline operating point and tolerance limit for a period of 2 seconds. Once this requirement was met, the controller issued an audio “warn” cue (10ms beep from the piezoelectric buzzer). One second later, the “move” cue LED (light) on the target frame was illuminated. Subjects were instructed to react by quickly raising their right arm raise to depress the target “end” switch with their right fist. This action caused the LED “move” cue to turn off immediately, signaling the end of the trial. After a mandatory 2 second rest period, during which the controller hibernated, subjects depressed the “ready” switch to repeat the task.

In an initial practice period, subjects executed trials until a consistent, repeatable movement was achieved. To this end, reaction times (RT- delay between “move” cue onset and release of “ready” switch) and movement times (MT- delay between release of “ready” switch and depression of target “end” switch) were monitored using the GUI. Once the subject had achieved a desirable movement pattern, with reaction times of 0.2-0.3s and movement times of 0.3-0.4s, usually after 25-30 trials, data collection was initiated. Subjects were able to execute the task comfortably with no perceptible fatigue.

In approximately 25% of the trials, no perturbations were applied to the right pedal. The data from these trials were used as controls to estimate changes in EMG and torques associated with the movement. In the remainder, a small dorsiflexing pulse displacement (0.025 radians, 40 ms wide) was applied to the right ankle at a random delay (800ms-1400ms) from the “warn” cue, as indicated by Figure 3.3. The pulse amplitude and width were chosen based on previous experiments in our laboratory [17, 127].

Perturbed and unperturbed trials were interspersed randomly. Each subject executed approximately 350-450 trials during one experiment. A mandatory 2 minute rest period was provided every 5 minutes to minimize the effects of fatigue.

It should be noted that the desirable range of RT and MT indicated above was found during a set of pilot experiments, and based on studies done in the BVML laboratory at the Department of Kinesiology, McGill studying muscle force constraints during the APA phase of arm reach movements (data not published yet). It should also be noted that we did not specifically monitor fatigue during the experiments (with EMG for instance).

3.5 Apparatus

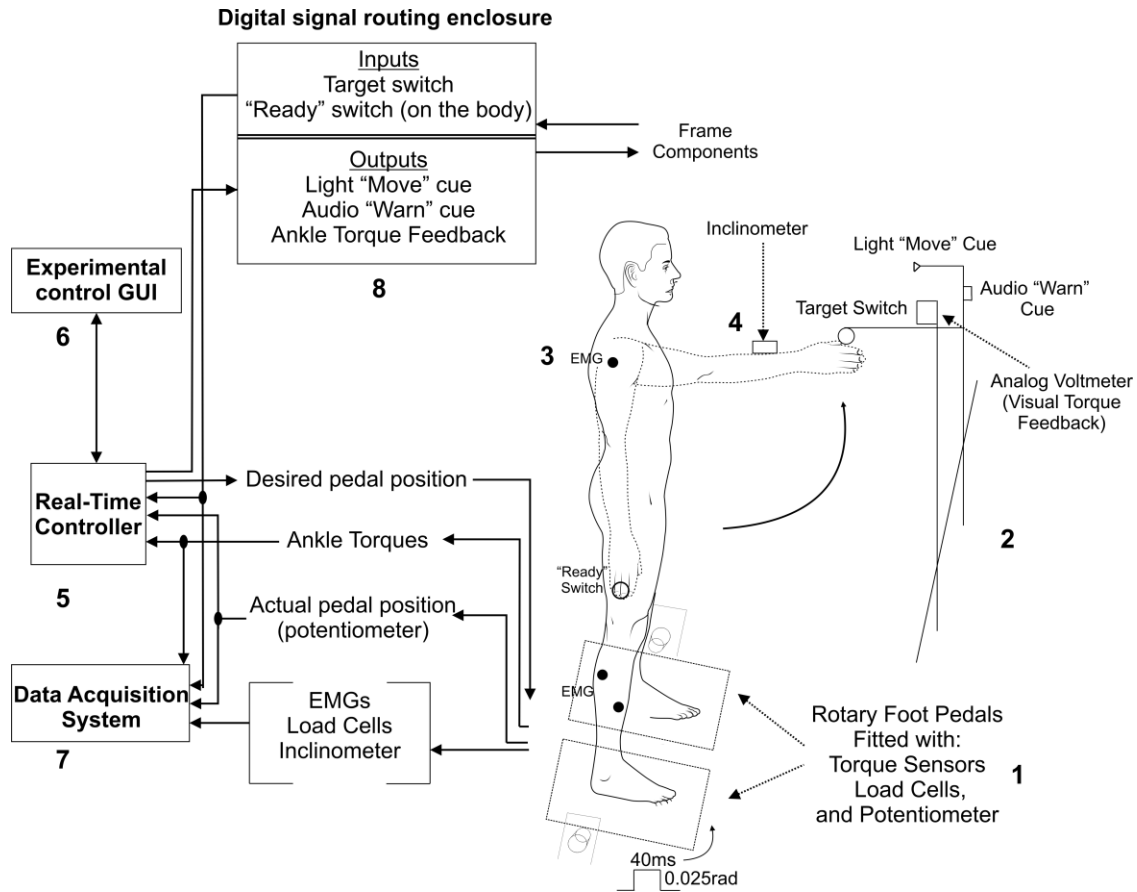


Figure 3.4. Schematic of the experimental setup showing components and signal routing: 1) Hydraulically driven rotary pedals with torque sensors, potentiometer, and load cells 2) Frame with visual cue, audio cue, target switch, and visual torque feedback 3) Electromyogram (EMG) to measure muscle activity from the shoulder and lower leg muscles 4) Single-axis inclinometer to measure arm angle 5) Real-time controller which controlled the pedal position and frame components 6) Graphical user interface (GUI) which allowed the experimenter to interact with the real-time control model 7) Data acquisition system 8) Digital signal routing enclosure to route signals from controller to the frame.

Figure 3.4 shows a schematic of the experimental setup. The major features are numbered 1 through 8 on the figure, with sensors (1 through 4), followed by the control apparatus and data acquisition systems. These are elaborated in the subsections below (Sections 3.5.1 to 3.5.8), enumerated as per Figure 3.4.

3.5.1 Bilateral Electro-Hydraulic Actuator

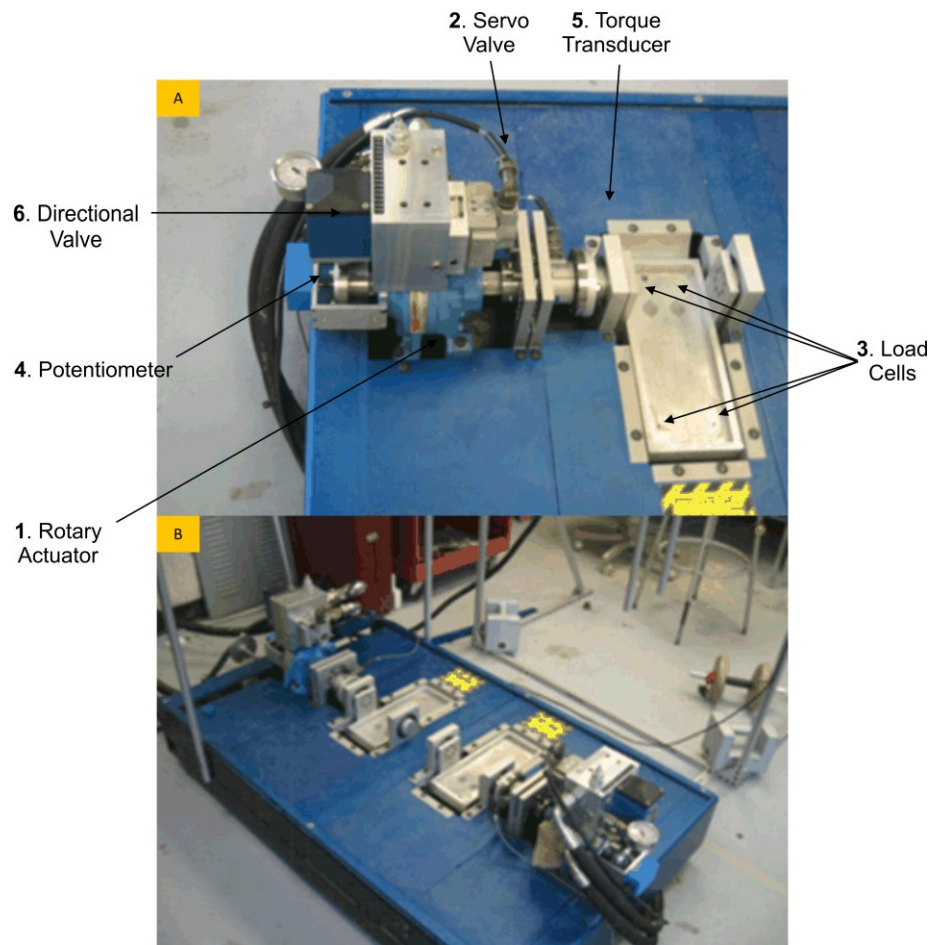


Figure 3.5. Bilateral Electro-hydraulic actuator. A) The right side is shown with components annotated B) Whole system, showing duplication of left and right sides.

Figure 3.5 shows the bilateral electro-hydraulic actuator used to control the aluminum rotary foot pedals. The major components on the right side of the apparatus are annotated on Figure 3.5a and described below. As can be seen in Figure 3.5b, the setup was duplicated for the left side. Detailed technical drawings, sensor calibration curves, and purchasing information can be found at the *REKLAB* manual website [128].

1. A high pressure rotary actuator (*Rotac 26R-2 1V*) was used to drive the foot pedal. It was run at a pressure of 2000 PSI. It had a maximum torque capability of 583.1 Nm.
2. A two-stage servovalve (*Moog D671-3001*) with mechanical feedback pilot stage was used to control the flow to the actuator. The speed of the actuator rotation was directly related to the aperture of the servo spool. The valve responded to input

current supplied through a four-pin electrical box connector (MS3106F14S2S). A voltage to current converter module was used to interface the servo valve to the analog output on the real-time computer controller. The module had a 10-90% rise-time of 0.5 ms, and low-pass characteristics with a cut-off frequency of $\sim 800\text{Hz}$, and roll-off of -2.5dB/KHz .

3. Four stainless steel compression load cells (*Omega* LC302-100, 0.75" diameter), each with a 446 N capacity, were embedded in the pedal, one at each corner. These were used to measure the downward force exerted on the pedal. The load cells were interfaced to a strain-gage conditioner module and calibrated using a 23 kg, class F, Type II *Troemner* Weight [127] to read 45.1 N/V. They had a resolution of $\pm 0.1\text{N}$.
4. A conductive plastic 5k rotary potentiometer (*Maurey Instruments* 112-P19) was attached to the shaft of the actuator to measure the angular position of the pedal. The potentiometer had a linearity of $\pm 0.5\%$ over a range of $340 \pm 5^\circ$. The signals from the potentiometer were conditioned using a custom built electronic module which allowed the gain and offset to be adjusted. The module was calibrated to have an output sensitivity of 0.1rad/V . It had a resolution of $\pm 0.0087\text{ rad}$.
5. A torque transducer (*Lebow* 2110-5k) was used to measure the torque exerted on the pedal. It had a capacity of 565Nm and a torsional stiffness of 103941Nm/rad . The torque output was processed via a conditioner module. The calibration was set to produce 20Nm/V where positive torque values corresponded to dorsiflexions and negative values to plantarflexions. It had a resolution of $\pm 0.04\text{ Nm}$.
6. A directional valve (*Mannesman Rexroth*) was used as a safety mechanism to limit the range of motion of the actuator. Its operating element was a roller/plunger actuated by a cam, which in turn was attached to the actuator's shaft. The cam limited the foot pedal's range between -12° (plantarflexion) and 5° (dorsiflexion), by raising the plunger and redirecting the hydraulic fluid flow away from the actuator if it reached the specified limit of rotation.

3.5.2 Aluminum Frame with Cues and Target Switch

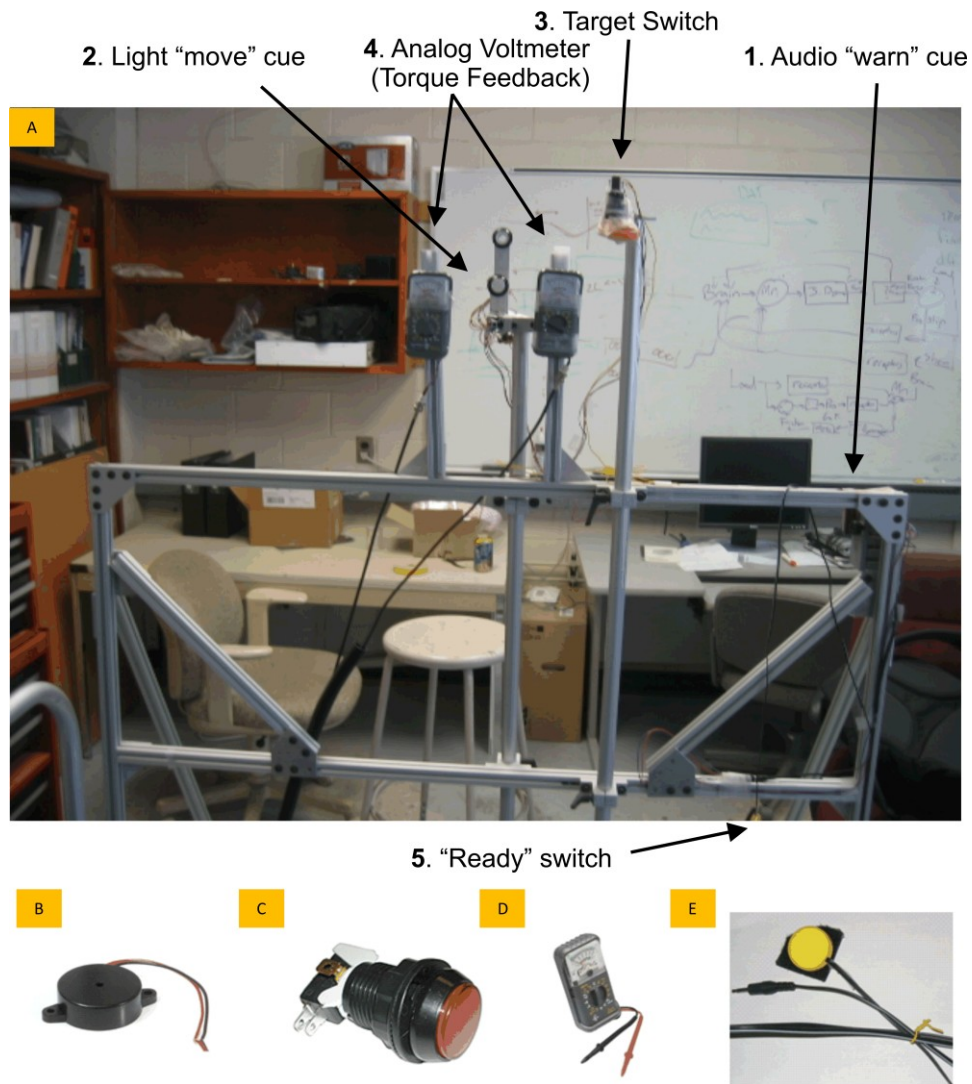


Figure 3.6. Target Frame. A)Top: Locations of components. B-E) Bottom: Components magnified. From left to right: B) Piezo-electric buzzer (audio “warn” cue). C) Target switch. D) Analog voltmeter for torque feedback. E) “Ready” switch to detect movement onset. The visual “move” cue consisted of a light emitting diode which was enclosed in plastic casing with a clear front face similar to the target switch.

Figure 3.6 shows the custom built target frame (beams and fixtures purchased from *McMaster Carr*). The frame had a rectangular front face (127 cm X 140 cm) supported by base legs and diagonal cross beams. The front and back ends of the frame were bolted to the floor and also weighted down with two 23 kg weights, making it resistant to translational forces applied by the subject. The locations of the major components are indicated on Figure 3.6a. The components are magnified in Figures 3.6b-

3.6e and described below. All components were interfaced to a common screw-terminal post at the side of the frame, which received ground and 5V signals from a power supply. This provided a consolidated access point to relay signals between the frame and the workstation housing the real-time controller and digital input/output cards.

1. A “warn” cue was used to provide the subject with a 10ms warning tone 1 second prior to the movement cue. For this purpose, a piezoelectric buzzer (*www.thesource.ca* catalog # 2730059), 3-20 V DC, 2700Hz tone, was mounted onto the inside of the frame. It was driven by TTL logic and was activated when a logic high signal was output from the digital output card of the real-time controller.
2. A “target” switch was mounted onto the frame. The single-pole, double-throw, push-button gaming switch (*RP Electronics*, model 459512) was enclosed in a corrugated plastic casing (hole diameter: 24mm, length: 63mm) with a clear front face. It was mounted facing the ground, and padded with foam to cushion the subject’s hand from the impact at contact. The horizontal and vertical position of this switch could be adjusted by two clamps to accommodate the subject’s height and arm length. When depressed, a 0-5V circuit was closed, and a 5V step input was sent to the digital input card of the real-time controller.
3. A visual signal was provided to act as a cue for the movement. For this purpose, a super-bright red light emitting diode (*Active Electronics*, 5mm super bright red led, model # 55-557-5) was enclosed in corrugated plastic casing (similar to the switch) and mounted directly in front of the subject, at a distance of 105 cm, just below eye level so that it could be easily seen. The LED was activated by a combination of two logic low outputs from two channels on the real-time controller digital output card, which were relayed through a 3-8 line decoder (Appendix A). When the target switch was pressed, the real-time controller turned the light off.
4. The subject had direct feedback of his/her postural sway prior to the start of each trial and was instructed to minimize it. Visual feedback of the torque at each foot pedal was provided to the subject using two pocket-sized analog multimeters (*Nexxtech*, *www.thesource.ca* catalog # 2218200) that were fitted to the frame on either side of

the visual light cue. The multimeter measurement leads were un-soldered and replaced with BNC connectors, and the torque signals from the pedals were sent to the voltmeters through a signal routing panel. The meters had a cut-off frequency of approximately 1Hz (typical body sway is about 0.2 Hz). They were set to the 0-2.5V DC scale (corresponding to 0-50Nm of torque), and were accurate within $\pm 5\%$ of the indicated value. During quiet stance, subjects typically maintained the torque at both feet to within ± 1.5 Nm of the baseline torque values.

5. A trigger switch was attached to the subject's thigh so that he/she could initiate the trial while maintaining a relaxed stance with arms to the side. This was a circular push-button switch (*Enabling Devices Inc. - Toys for Special Children*, Item # 745, Compact Switch- 3 pack), 3.5 cm in diameter, with a single phono (3.5 mm) male lead. It had a yellow, flat front face and a Velcro attachment on the back. The female end of a phono jack was connected to a set of leads across a 0-5V circuit. It was secured to the frame, so that it could mate with the trigger switch lead. Pressing the switch closed the circuit and sent a rising-edge to the real-time controller digital input card. The phono jack connection at the frame could be disconnected easily and re-connected. This allowed the subject to move from the immediate proximity of the setup during the 2 minute rest periods.

Signals were routed to and from the frame via a digital signal routing enclosure, described in Appendix A. A copy of the input signals (from the frame components to the real-time controller) was also sent to the data acquisition system, as indicated in Figure 3.4.

3.5.3 Electromyography (EMG)

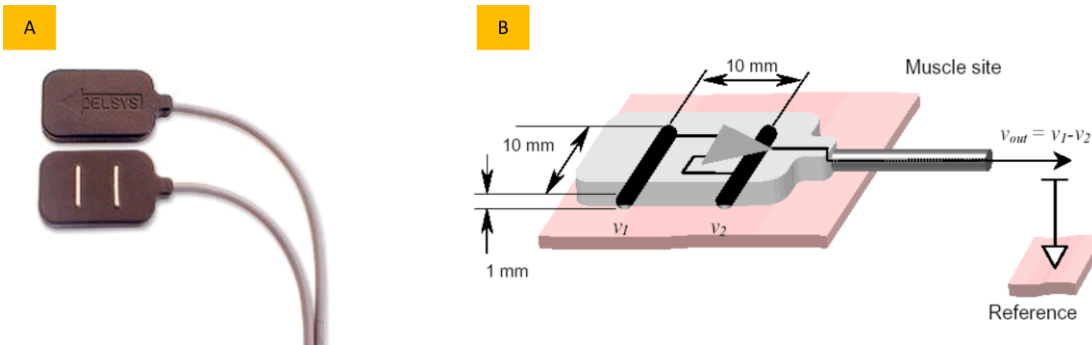


Figure 3.7. EMG recording. A) Single differential electrodes used for EMG recording. B) Schematic illustrating the calculation of the voltage differential between the two muscle contacts.

The DELSYS *Bagnoli* 8 channel desktop system was used to measure EMG. Figure 3.7a shows the surface electrodes (*D.E 2.1*). These were single differential sensors with two 1mm muscle contacts, separated by 10 mm. An additional disposable, adhesive Ag/AgCl reference electrode was placed on either the left or right knee cap (3M Red Dot) as a reference. Both the measurement and reference electrodes were connected to a portable belt-mounted interface unit.

As shown in Figure 3.7b, the EMG measured was the potential difference between the two contacts ($v_{out}=v_2-v_1$), with respect to the common ground reference electrode measure. It was pre-amplified by a gain of 10, and then sent to a main amplifier unit through a network cable. The main amplifier unit had three pre-set selectable amplification settings of 10, 100 or 1000. The gain setting of 100 was used, and therefore the system had an overall gain of 1000. Signals were then forwarded to the data acquisition system.

The EMG system had a bandwidth of 20-2000Hz, a root mean square noise floor of 1.2 μ V, input impedance that exceeded $10^{15}/0.2$ (ohm//pF), and a common mode rejection ratio that exceeded 80dB at 60 Hz. The unit was powered with a medical grade isolated power supply with safety isolated to 3750 V_{RMS} and leakage currents lower than 10 μ A. It conformed to UL2601, CSA601, and IEC 60601-1 safety standards.

The skin was prepared by shaving the skin above the muscle of interest using a disposable razor, and rubbing down the surface with an alcohol swab. Proper preparation of the skin surface, via removal of any oils or dry dermis which could attenuate or distort the EMG signal, was crucial.

EMG activity was recorded from the right anterior deltoid, which has been typically identified as the prime focal muscle for the upward arm raising movement [25]. The activity from the TA, LG and SOL of both legs was also recorded. The remaining EMG channel was used to record activity from the MG of the right leg. The electrodes were placed in accordance with the guidelines specified by the Surface Electromyography for the Non-Invasive Assessment of Muscles [65]. Electrode placement and orientation is summarized below in Table 3.2.

Table 3.2. Muscle EMG's recorded, describing electrode placement and orientation.

EMG Channel	Muscle	Electrode Placement	Orientation
3	Anterior Deltoid (Right Arm)	One finger width distal and anterior to the acromion.	In the direction of the line between the acromion and the thumb.
1,5	TA (Both legs)	One third the distance between the tip of the fibula and the tip of the medial malleolus.	In the direction of the line between the tip of the fibula and the tip of the medial malleolus.
2,6	LG(Both Legs)	On the prominent belly of the lateral head of the muscle-highlighted by a plantarflexion.	Along the axis of the leg.
7	MG (Right Leg)	On the prominent belly of the medial head of the muscle-highlighted by a plantarflexion.	Along the axis of the leg.
8	SOL (Both Legs)	Two thirds of the way between the medial condylis of the femur to the medial malleolus.	Along the line between the medial condylis to the medial malleolus.

The electrode orientation method indicated in Table 3.2 attempted to ensure that the electrodes were oriented parallel to the underlying muscle fibers. This ensured that the recording bars were in turn orthogonal to the fibers, and a differential measure of the MUAP (motor unit action potential) which propagates along the fibers could be detected.

3.5.4 Wrist Inclinometer



Figure 3.8. Inclinometer fixed with a wrist splint, used to measure angular arm position

Figure 3.8 shows the inclinometer (*Microstrain FAS-G*) used to measure the angular arm position as the subject lifted his/her arm. It was secured to the subject's wrist with a splint, such that its axis of rotation was oriented orthogonally to the radial bone. The device combined an angular rate gyro with two orthogonal DC accelerometers. Its output was an analog voltage (0-4.096V) linearly proportional to inclination about its axis of rotation in both dynamic and static environments, for the 360° range of motion (87.9°/V). It had a resolution of 0.1°, an accuracy of $\pm 1^\circ$, and a cut-off frequency of 30Hz.

3.5.5 Real-Time Experimental Control

3.5.5.1 Overview

Real-time experimental control was achieved in three major steps.

First, a graphical model was designed on a workstation (referred to henceforth as the host workstation (AMD Athlon, 2.2 GHz, 2 GB RAM)) using the MATLAB SIMULINK tool. This is a graphical block diagramming tool with a set of pre-programmed block libraries that can be used to model, simulate and implement control systems. Each block represents specialized pieces of code that can carry out specific digital signal processing operations. The model was designed to control the position of the pedals of the actuator, specify the timing of the perturbations applied to the ankle, and send/receive signals from the components on the frame.

Second, this model was compiled and sent to a second workstation (referred to henceforth as the target workstation (AMD Athlon, 1.6 GHz, 256 MB RAM)) using an Ethernet connection. The target workstation was dedicated to real-time control of the experimental apparatus. It was equipped with digital I/O boards, digital to analog (D/A) and analog to digital (A/D) converters.

Third, the experimenter was able to interact with the real-time controller using a Graphical User Interface (GUI), which ran on the host workstation. The real-time controller running on the target workstation was polled at 50Hz during the experiment, and the GUI was updated with information such as the number of trials completed, and the movement and reaction times of individual trials. The experimenter was also able to change the parameters of the real-time control model through this GUI.

These three steps are described in Sections 3.5.5.2 through 3.5.5.4 respectively.

3.5.5.2 Real-time Control Model

The real-time controller block diagram was hierarchically structured with a set of four major linked subsystems, each with further nested subsystems. The signal flow between the different subsystems is shown by the top-level flowchart in Figure 3.9, and can be summarized as follows:

1. The *target frame real-time controller subsystem* monitored the subject's baseline torque at the start of the experiment and also sent/received signals from the components on the frame. When a trigger input (from the "ready" switch) was received from the digital input card, this subsystem generated the audio ("warn") and visual ("move") cues. It also sent a trigger to activate the *perturbation sequence & delay selector subsystem* at the same time as the "warn" cue.
2. The *perturbation sequence & pulse delay selector subsystem* was used to specify the desired input to the *actuator real-time controller subsystem*. The input to the left pedal was always specified to be zero. However, for the right pedal, this subsystem specified the delay relative to the "warn" cue at which perturbations were applied to the ankle, or alternately set the input to be zero, thereby selecting the sequence of perturbed and unperturbed trials during the experiment.

3. The *actuator real-time controller subsystem* used the command signal from the *perturbation sequence & pulse delay selector subsystem*, along with feedback signals from potentiometers on the pedals, to control the position of the actuator pedals with a proportional feedback control algorithm.
4. The *sampling subsystem* initiated data collection by triggering the Data Acquisition Cards. It operated independently of the other subsystems.

Each of the subsystems is elaborated in Sections 3.5.5.2.1 through 3.5.5.2.4.

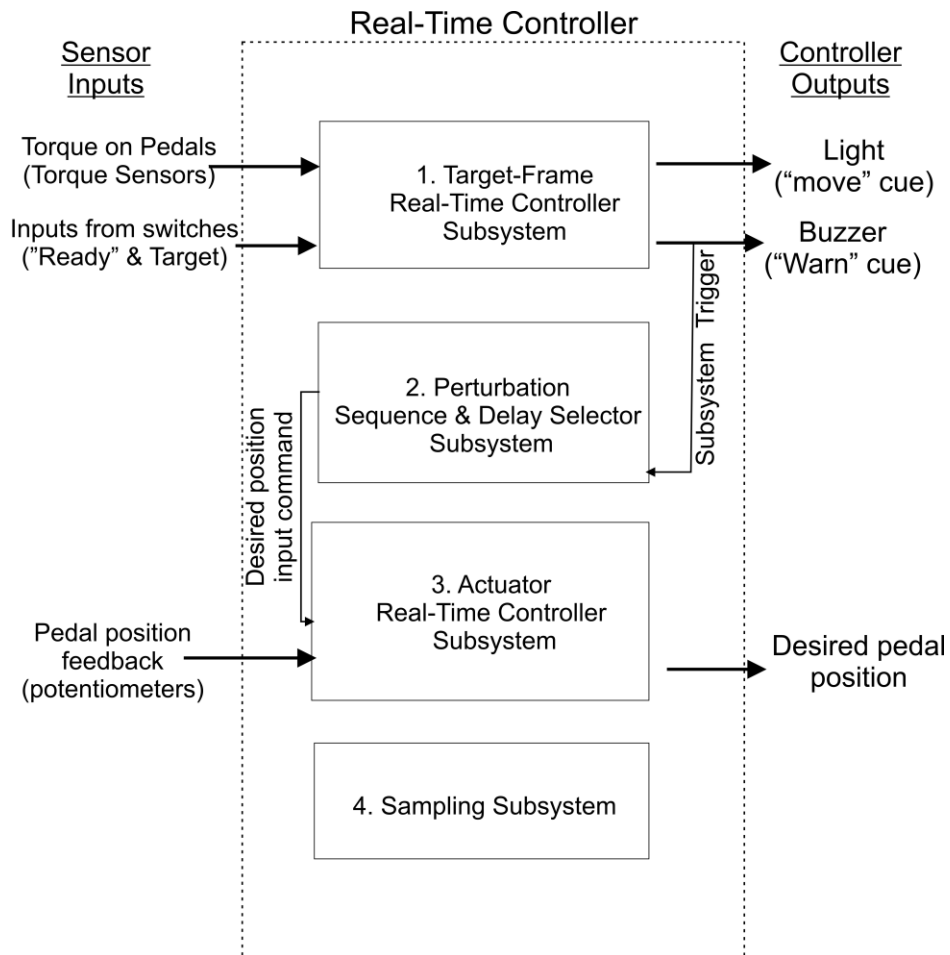


Figure 3.9 Flowchart showing the top-level structure of the real-time controller with four major subsystems. The *target-frame real-time controller subsystem* monitored pedal torques and inputs from switches to output cues to the target frame. It also triggered the *perturbation sequence & delay selector subsystem* when a “warn” cue was output. The *perturbation sequence & delay selector subsystem* was used to select the desired input command to the actuator real-time controller (perturbation trial/control trial/delay of applied perturbation). The *actuator real-time controller* used this input along with feedback from pedal potentiometers to generate an output command to the pedals using a proportional feedback algorithm. The sampling subsystem operated independently of the other subsystems, and was used for data acquisition.

Inputs to the controller are shown on the left, while controller outputs are shown on the right.

3.5.5.2.1 Target Frame Real-Time Controller Subsystem

Figures 3.10 and 3.11 show the target frame real-time controller subsystem, which was subdivided into two levels. Level 1 monitored the subject's baseline torque at the start of the experiment. Level 2 sent/received signals from the components on the frame.

Level 1

In level 1, shown in Figure 3.10, a high level TTL input from the “ready” switch activated the *Torquecheck* subsystem and *Runningmean* subsystems. The *Runningmean* subsystem continually monitored the torque input from the pedals and calculated running mean values using a single *SIMULINK* block already designed for such a purpose.

The *Torquecheck* subsystem continually compared the input torque values to a user-defined baseline (obtained using the *Runningmean* subsystem prior to the start of the experiment with the subject standing still for 20 seconds). If the torque at both feet was maintained within acceptable limits for 2 seconds (by checking if a triggered counter reached the appropriate count number), the *Torquecheck* subsystem output a “Torque ok” command. This allowed the model to progress to level 2.

Level 2

In level 2, shown in Figure 3.11, different sets of blocks were used to control the “move” cue (LED), “warn” cue (buzzer), and generate a perturbation to be sent to the actuator. Timer blocks measured the reaction and movement times of each trial. Specifically:

1. A set of logic blocks controlled the digital output signals to either turn on or turn off the light target. Triggered counter blocks were used to count the number of times this occurred and hence keep track of the number of trials executed.
2. Triggered ‘n-sample enable blocks’ which output an n-number of logic high values, were used to send pulses of length 10 ms (10 samples at 1 KHz) to the buzzer, and 40ms(40 samples) to the actuator.
3. Free-running timer blocks, appropriately triggered/stopped by rising edge inputs from body and target switches, calculated the reaction and movement times (MT and RT as defined previously). Light, buzzer, and actuator signals were sent back to level 1

(Figure 3.10) and subsequently to the top-level to be output to the hardware (Figure 3.9).

Stateflow Chart

An embedded *STATEFLOW* logic chart, enlarged in Figure 3.11 (in the lower-left hand corner) was used to control the temporal activation of the set of blocks in level 2. *STATEFLOW* is an interactive design tool for event driven and embedded systems. Within the chart, which incorporated a timer, two state variables were used with binary values. The chart had the following sequence of temporal events:

1. When the chart was initiated (after receiving the “Torque OK” command from the *Torquecheck* subsystem in level 1), the “optbuzz” variable was set to 1 which activated the ‘n-sample enable blocks’.
2. After a delay of 1 second, the “light” variable was set to 1 to activate the logic blocks.
3. When an input from the target switch was received as a trigger to the *STATEFLOW* chart, both state variables were zeroed. This reset the chart and also turned off the signal to the logic blocks.
4. The *STATEFLOW* chart then entered a state of hibernation for 2 seconds during which inputs to the chart were ignored. This ensured that the subject rested between trials.

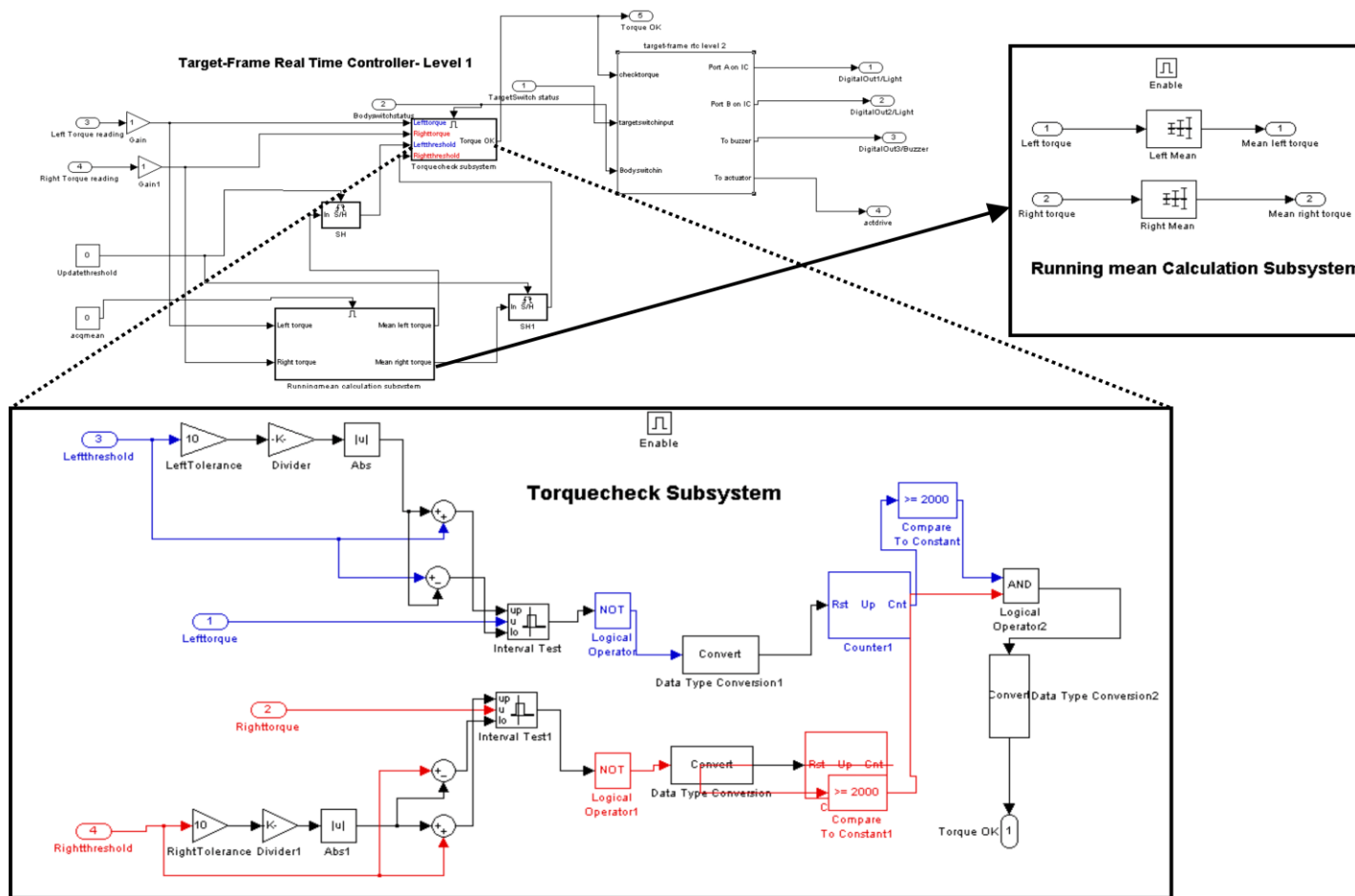


Figure 3.10. Level 1 of the Target-Frame Controller subsystem. Contents of nested Torquecheck and Running mean Subsystems are also shown.

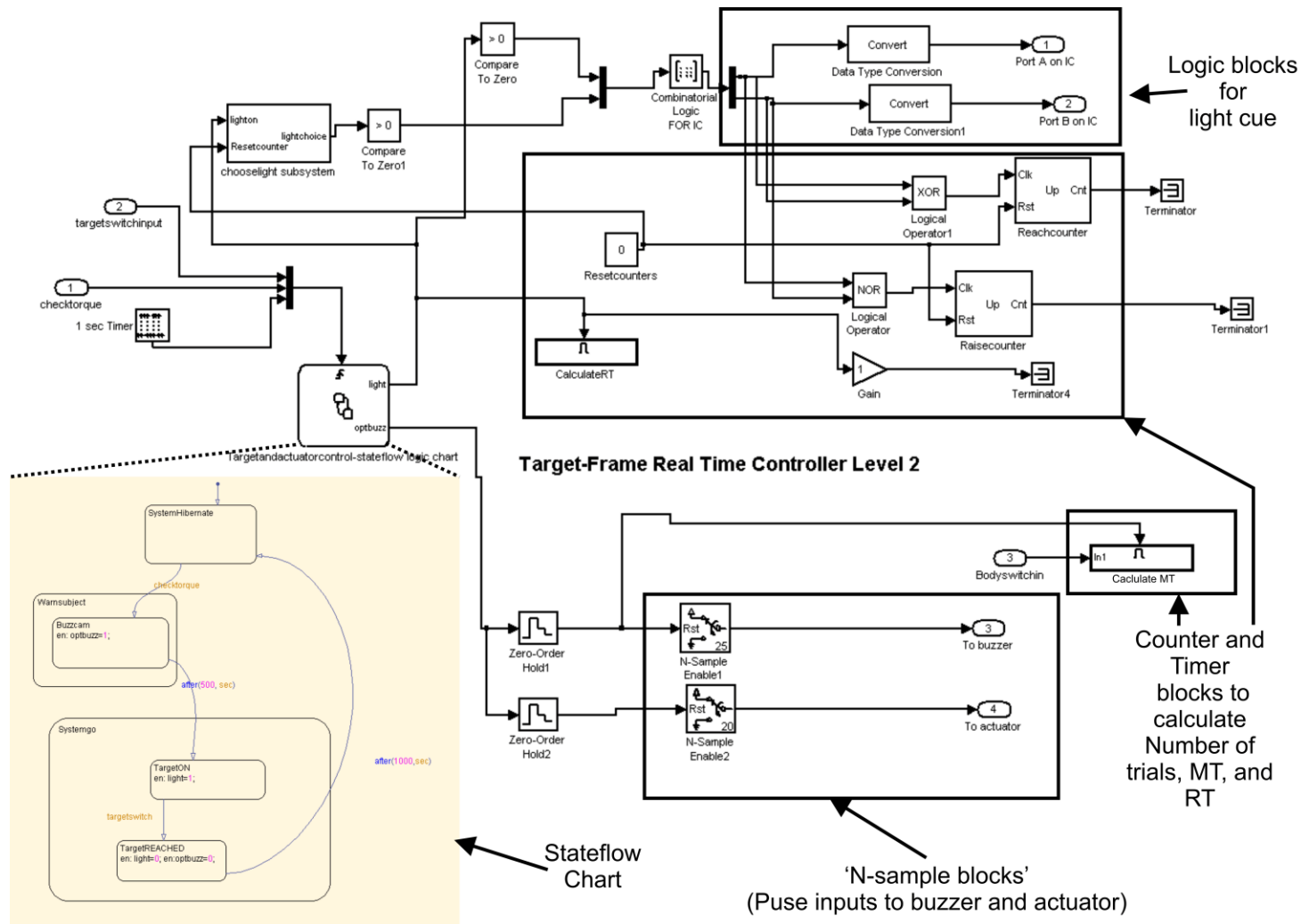


Figure 3.11. Level 2 of the Target-Frame Real-Time Controller Subsystem with the STATEFLOW chart determining the temporal sequence of events.

3.5.5.2.2 Perturbation Sequence & Delay Selector Subsystem

As indicated in Section 3.5.5.2.1, the output signals from Target-Frame real-time controller Level 1 were sent to the base (top-level) model (Figure 3.9). At this point, the frame-bound signals (signals to “warn” cue and “move” cue) were sent directly to the digital output blocks and the interfacing hardware. However, the actuator bound signals were first routed via the pulse-sequence selector subsystem, shown in Figure 3.12.

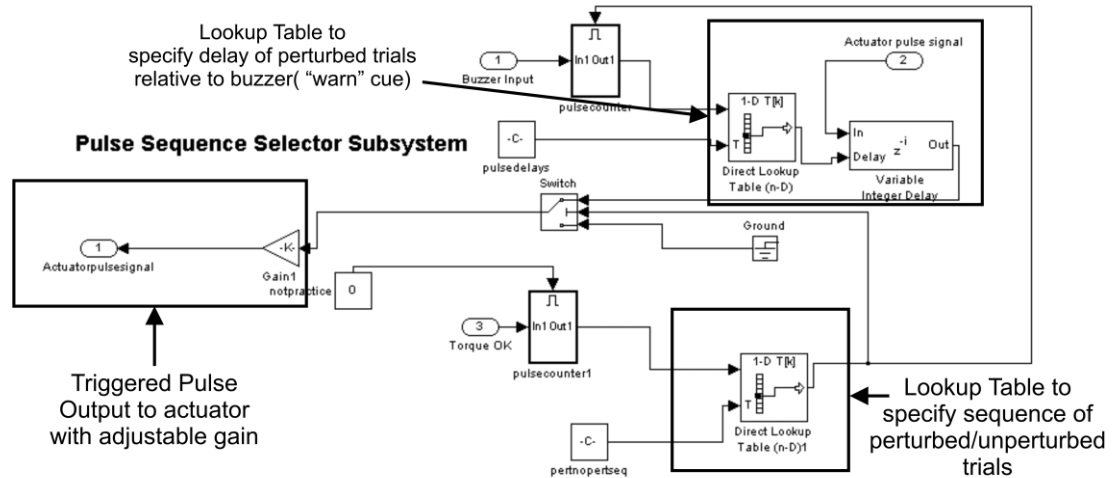


Figure 3.12. Perturbation sequence & delay selector subsystem which was used to specify the delay of perturbed trials with respect to the buzzer and sequence of perturbed/unperturbed trials.

This subsystem: 1) Specified the delay relative to the “warn” cue at which perturbations were applied to the ankle and 2) Selected the sequence of perturbed and unperturbed trials during the experiment.

1. Since the signals to the buzzer and actuator originated at the same time (refer to STATEFLOW chart in Section 3.5.5.2.1), this subsystem introduced a variable delay into the actuator input drive. This was done by using a 1-D lookup table, containing a sequence of delay times fed into a variable integer delay block.
2. A second lookup table, containing a combination of 1’s and 0’s, was used to specify the sequence of perturbed and unperturbed trials respectively. When an unperturbed trial was indicated by the lookup table (by a 0 in the table), the input signal for that trial was replaced by a ground (zero input), using a switching block.

Lastly, a gain block just before the output of this subsystem allowed the size of the triggered pulse sent to the actuator to be adjusted. During the experiment, a pulse input of 0.025 rad was used, which corresponded to an output voltage of 0.25V. As indicated previously, the output of this subsystem fed into the actuator real-time controller subsystem (Figure 3.12) to specify the position drive to the right pedal.

3.5.5.2.3 Actuator Real-Time Controller Subsystem

Figure 3.13 shows the actuator real-time controller subsystem. It controlled the position of the rotary pedals of the bilateral electro-hydraulic actuator.

Control algorithm

The control algorithm utilized proportional feedback, and feed-forward velocity control of a position error signal. The error signal was defined as the difference between the desired pedal position, and the actual position of the pedal obtained from the potentiometer, which was digitized using an A/D converter. The algorithm output was a command signal to the actuator servo, which was converted to the appropriate analog voltage using a D/A converter before being output. At the start of each experiment, the pulse size and width were monitored on an oscilloscope to ensure that all subjects were perturbed similarly.

Input selection

The inputs to the pedals could be specified in one of two ways. Before the start of the experiment, inputs from a pre-programmed buffer were used to warm up the hydraulics, test the apparatus to ensure that perturbations applied were of the correct size, and acclimatize the subject to the perturbations. However, during the experiment, we perturbed the ankle at specific times relative to the movement onset. Since the buffer did not allow for this precise timing, a switching mechanism was used whereby the command signal to the pedals could be specified with a triggered pulse. The timing of this pulse was specified in terms of a variable delay with respect to the onset of the buzzer “warn” cue, by using the *perturbation sequence & delay selector subsystem* (Section 3.5.5.2.2). Furthermore, the inputs to the left pedal were grounded to hold the pedal steady at a zero level. The major features of the subsystem, as discussed above, are annotated on Figure 3.13. Left pedal control blocks are shown in red and right pedal blocks in blue.

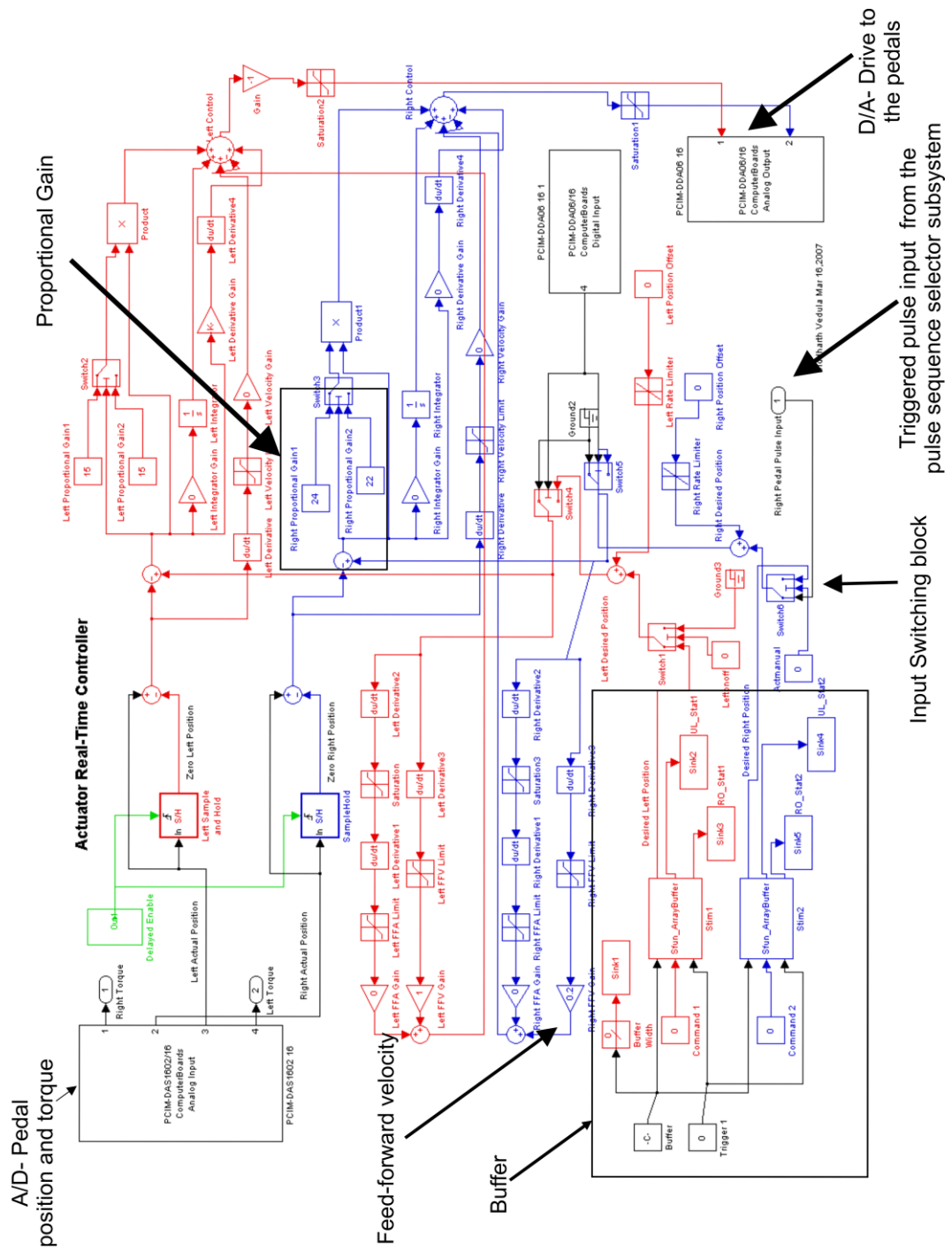


Figure 3.13. The Actuator Real-Time Controller incorporating proportional feedback and velocity feed-forward control. Inputs to the right pedal could be switched between a pre-programmed buffer and a triggered pulse input from the perturbation sequence & delay selector subsystem.

3.5.5.2.4 Sampling Subsystem

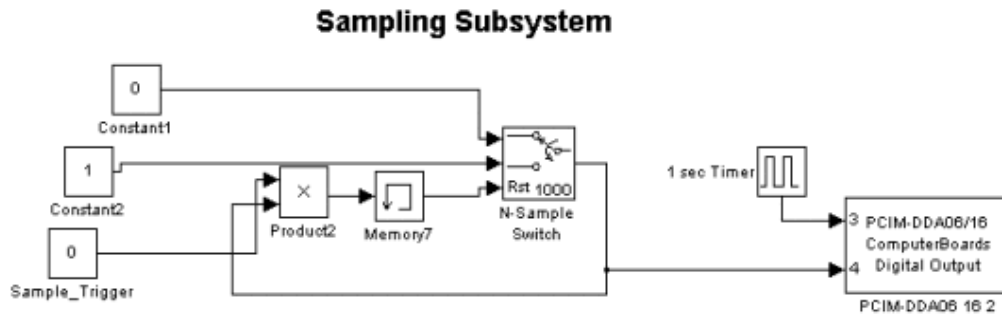


Figure 3.14. Sampling subsystem to initiate data collection.

Figure 3.14 shows the sampling subsystem. It operated independently of the others and triggered the DAQ when the base model was executed. Data sampling was initiated by sending out a 1ms pulse trigger to the four DAQ cards. Ancillary code polled the cards to check that all were triggered simultaneously.

3.5.5.3 Compiling and Executing the Real-Time Control Model

The second step of the control process was to compile the graphical SIMULINK model and execute it on a dedicated target workstation. *xPC Target* is a *MATLAB* based real-time digital signal processing (DSP) system that provides a host-target relationship allowing *SIMULINK* models to be executed in real-time on physical machines. Using this interface, the *SIMULINK* control model was compiled and loaded onto the target workstation via a TCP/IP Ethernet network connection. The target machine was equipped with digital I/O boards (D I/O), digital to analog (D/A) and analog to digital (A/D) converters. The schematic in Figure 3.15 illustrates the *xPC* host-target mechanism.

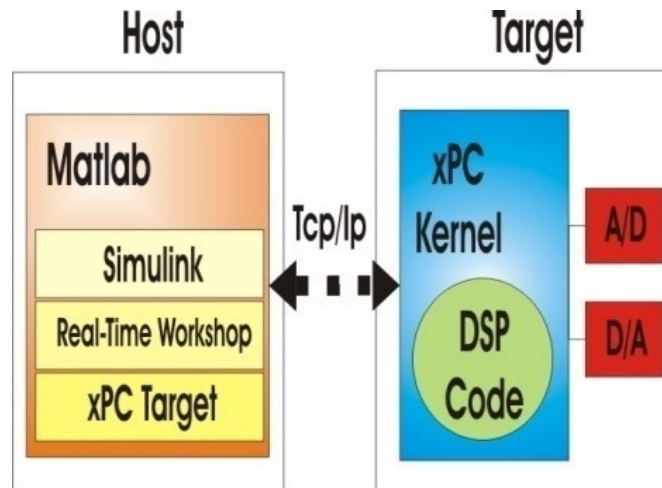


Figure 3.15. The xPC Target Framework, showing the host-target relationship. Adapted from [128].

The D/A converter (PCIM-DDA06/16) and A/D (PCIM-DAS1602/16) were purchased from *Measurement Computing*. Each had 8 differential channels. The A/D converter digitized the position and torque signals from both pedals for real-time feedback to the controller. For anti-aliasing purposes, the signals were routed through a custom built, 8th order, low-pass, constant delay filter bank with a cutoff frequency of 250 Hz. It had a gain of 1 and a stop-band attenuation of 80 dB. In turn, the D/A converter converted the computed servo-valve position signal output voltage and relayed it to the servovalves via a voltage to current converter. Associated D I/O cards were used to send and receive signals from the frame components.

3.5.6 Graphical User Interface for Experimental Control (GUI)

A GUI polled the real-time controller at 50 Hz, and also specified the parameters in the subsystems described above during the experiment. It is shown in Figure 3.16.

- A. The *trial monitor panel* displayed the total number of unperturbed and perturbed trials. It also displayed the movement time, reaction time, and an option to flag erroneous trials. It did this by accessing the counter blocks in *Target Frame Real-Time Controller Subsystem Level 2* (Section 3.5.5.2.1).
- B. The *torque monitor panel* set the steady-state baseline sway level for the subject, so that each trial could be initiated from a fixed starting position within a definable tolerance. The tolerance level could be adjusted individually for each foot ($\pm 10\%$ of

baseline level was used as a default in the experiment). It accessed the *Torquecheck subsystem* to specify the tolerance limits (Section 3.5.5.2.1).

- C. The *pulse perturbation panel* specified the perturbation parameters including the duration, size of the pulse, and the total number of pulses to be applied. It accessed the direct lookup tables in the *pulse-sequence selector subsystem* (Section 3.5.5.2.2).
- D. The *actuator input panel* switched the input to the actuator between the buffer and the triggered pulse perturbations inputs by accessing the switching block in the *actuator real-time controller subsystem* (Section 3.5.5.2.3).
- E. Using data from the *trial monitor panel*, a histogram of the reaction and movement times was computed to:
 - Find out when the subject was acquainted sufficiently with the task to produce a consistent movement, before starting the experiment. Practice trials were carried out till the subject could achieve a consistent reaction time of 0.15-0.25s and a movement time of 0.3-0.4s.
 - Flag erroneous trials during the experiment using a check box button incorporated in the *trial monitor panel*.



Figure 3.16. Graphical user interface (GUI) to monitor and control experimental parameters in real-time by interacting with SIMULINK block diagrams.

3.5.7 Data Acquisition System (DAQ)

Data were collected on the host workstation with four *National Instruments 4472* data acquisition cards, each with 8 A/D channels. They had a 24 bit resolution, giving a dynamic range of 110 dB. Each channel had a dynamic range of $\pm 10V$. Data were low-pass filtered with a cut-off frequency of 400 KHz and then digitized at a rate of 128 KHz. The data were then digitally filtered with a low-pass anti-aliasing brick-wall filter (cutoff 486.3 Hz), down-sampled to 1 KHz, and stored on the hard disk. For the analysis presented in Chapter 4, only data from the ipsilateral side of the body were analyzed. The data of interest are summarized in Table 3.3.

Table 3.3. Data of interest. Variables, transducers and relevant channels on the DAQ are indicated.

DAQ Channel	Variable	Transducer	Scale Factor	Resolution	Output Range of Sensor
3	Right Pedal Position	<i>Maurey Instruments 112-P19</i>	0.1rad/V	± 0.0087 rad	0-5.93 rad
4	Right Pedal Torque	<i>Lebow 2110-5k</i>	20Nm/V	± 0.04 Nm	0-565 Nm
5	LED (“move” cue)	Digital Out 1 on D I/O	N/A	N/A	N/A
6	Buzzer (“warn” cue)	Digital Out 3 on D I/O	N/A	N/A	N/A
11	Anterior Deltoid EMG	<i>Bagnoli-8 EMG Desktop System</i>	0.001 (amplifier gain was 1000)	± 1.2 μV	$(-4.8-4.8) * 10^6$ μV
13	TA EMG (Right Leg)	<i>Bagnoli-8 EMG Desktop System</i>	0.001	± 1.2 μV	$(-4.8-4.8) * 10^6$ μV
14	LG EMG (Right Leg)	<i>Bagnoli-8 EMG Desktop System</i>	0.001	± 1.2 μV	$(-4.8-4.8) * 10^6$ μV
15	MG EMG (Right Leg)	<i>Bagnoli-8 EMG Desktop System</i>	0.001	± 1.2 μV	$(-4.8-4.8) * 10^6$ μV
16	SOL EMG (Right Leg)	<i>Bagnoli-8 EMG Desktop System</i>	0.001	± 1.2 μV	$(-4.8-4.8) * 10^6$ μV
21	Right Pedal Force 1 (Top right corner)	<i>Omega LC302-100</i>	45 N/V	± 0.13 N	$0-4.5 * 10^2$ N
22	Right Pedal Force 2 (Top left corner)	<i>Omega LC302-100</i>	45 N/V	± 0.013 N	$0-4.5 * 10^2$ N
23	Right Pedal Force 3 (Bottom right corner)	<i>Omega LC302-100</i>	45 N/V	± 0.013 N	$0-4.5 * 10^2$ N
24	Right Pedal Force 4 (Bottom left corner)	<i>Omega LC302-100</i>	45 N/V	± 0.013 N	$0-4.5 * 10^2$ N
25	Angular arm position	<i>Microstrain Inc. FAS-G M</i>	87.9°/V	± 0.1 °	0-360 °
29	“Ready” switch	Digital Input from body switch	N/A	N/A	N/A
30	Target switch	Digital Input from target switch	N/A	N/A	N/A

3.5.8 Digital Signal Routing Enclosure

An enclosure housing a printed circuit board was used to interface the components on the frame with the D I/O and simultaneously route the signals to the DAQ. Since this was neither a sensor, nor part of the experimental control, its details are provided in Appendix A.

3.6 Data Pre-Processing

Data analysis techniques are described in Chapter 4. However, some pre-processing was carried out prior to these steps, and is described here.

3.6.1 Event Markers

Data were sampled at 1 KHz and stored in individual *MATLAB* *.mat* files, each 5 minutes (300,000 points) long. The files were segmented to extract the data of interest. This lay between the onset of the buzzer (“warn” cue) and the end of the movement, for each trial. The “warn” cue was identified from the rising edge of the real-time controller digital output to the buzzer (recorded on DAQ channel 6- Table 3.3). The “end” point was identified from the rising edge input from the target “end” switch (recorded on DAQ channel 30-Table 3.3). These events provided time stamps on the recorded *.mat* files. Data between trials were discarded. Note that this inefficient system of data collection was adopted since it was found that the workstation malfunctioned if it was used to frequently start and stop data collection.

Other time stamps of interest on the data files included:

- Onset of the light “move” cue, identified by a rising edge sent by the digital output of the controller, and sampled by the DAQ channel 5.
- Movement onset, identified by a falling edge input from the trigger “ready” switch, and sampled by the DAQ channel 29.
- The occurrence of a perturbation, identified by searching for a pulse onset in the right pedal potentiometer position, and sampled by the DAQ channel 3.

Figure 3.17 summarizes the process. Note that the schematic is not to temporal scale.

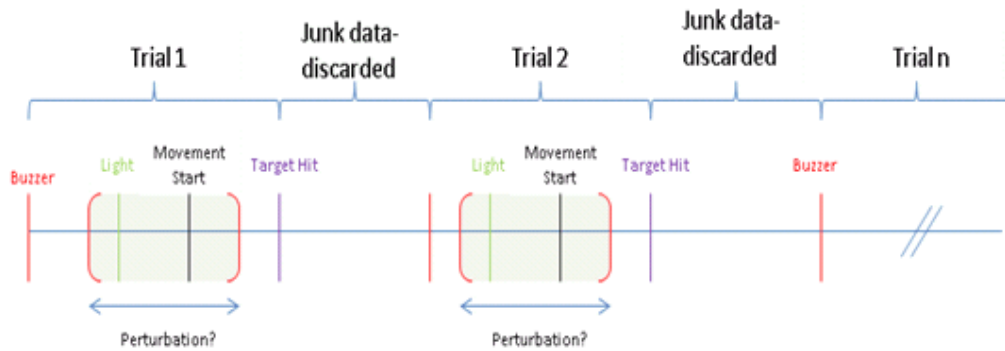


Figure 3.17. Event segmentation of data files.

3.6.2 Right Leg Center of Pressure

Most of the analog data of interest were obtained directly from the DAQ. However, the right leg center of pressure (CoP) was calculated from the right pedal load cell data.

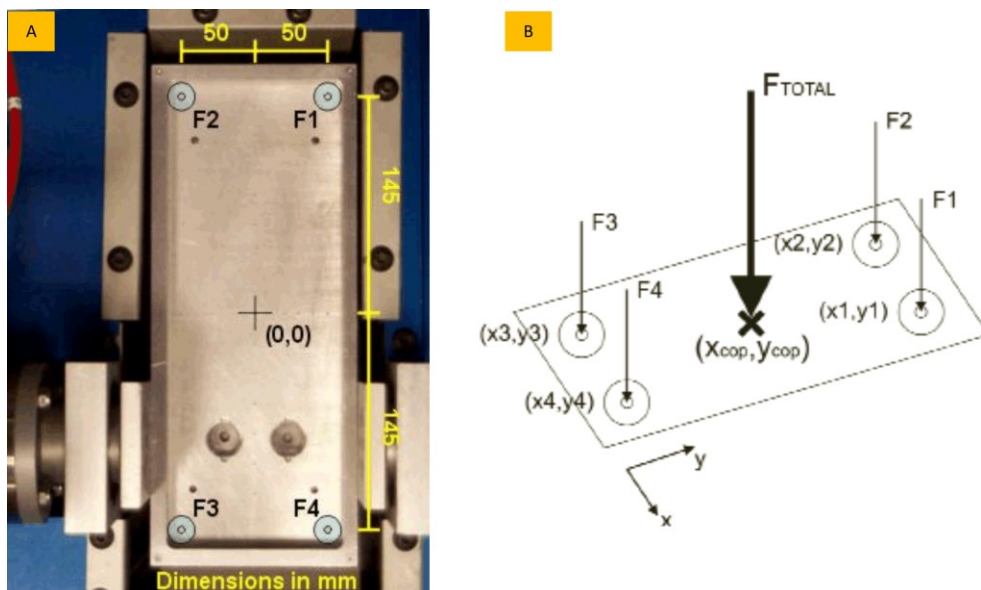


Figure 3.18. Calculation of the CoP. A) Picture of a foot pedal showing the location of the four load cells B) Schematic illustrating the co-ordinate map of the CoP.

Figure 3.18 shows the location of the four load cells (F1, F2, F3, F4), at each corner of the pedal. Distances relative to the center of the pedal in both x and y dimensions are shown in mm. The CoP refers to the single point at which the weighted

combination of these four forces at a given point in time can be localized. The origin of the CoP was defined as at the center of the rectangle formed by the four load cells, and is shown by the crosshair at 0, 0. Note that the weight of the pedal introduced a bias in the force reading of each load cell which was subtracted from the individual force sensor readings. The bias forces were obtained by measuring the load cell readings without any imposed load on them. Hence, as shown in equations 2 and 3, the CoP can be calculated in both x and y dimensions.

$$F_{TOTAL} = (F_1 - F_{BIAS1}) + (F_2 - F_{BIAS2}) + (F_3 - F_{BIAS3}) + (F_4 - F_{BIAS4}) \quad (1)$$

$$CoP_x = 50 * (F_1 - F_{BIAS1}) - 50 * (F_2 - F_{BIAS2}) - 50 * (F_3 - F_{BIAS3}) + 50 * (F_4 - F_{BIAS4}) \quad (2)$$

$$CoP_y = 145 * (F_1 - F_{BIAS1}) - 145 * (F_2 - F_{BIAS2}) - 145 * (F_3 - F_{BIAS3}) + 145 * (F_4 - F_{BIAS4}) \quad (3)$$

Where $x_1 = 50$ mm, $x_2 = -50$ mm, $x_3 = -50$ mm, $x_4 = 50$ mm, $y_1 = 145$ mm, $y_2 = 145$ mm, $y_3 = -145$ mm, and $y_4 = -145$ mm.

4. Data Analysis, Results & Discussion

In this chapter, a manuscript to be submitted to Experimental Brain Research is presented. For the purposes of this thesis, the manuscript is structured into sections. In Section 4.1, an abstract of the experiment is presented. Section 4.2 provides a summary of the relevant literature. Section 4.3 is a succinct summary of the experimental setup, experimental protocol and data analysis techniques (which followed the data pre-processing presented in Section 3.6). Results are presented in Section 4.4, followed by a discussion of these results in Section 4.5. Funding agencies are acknowledged in Section 4.6. References for the manuscript are consolidated with the rest of the thesis and presented at the end of the thesis.

**Stretch Reflex Changes Associated with Anticipatory Postural Adjustments
Preceding Voluntary Arm Movements in Standing Humans**

Siddharth Vedula, Paul J. Stapley, Ross Wagner and Robert E. Kearney

To be submitted to:
Experimental Brain Research

4.1 Abstract

Dynamic changes in stability, such as those induced by upper body movements, are preceded by anticipatory postural adjustments (APAs) in the rest of the body. For forward oriented upper body movements (e.g. arm raise), the APA is typically characterized by an inhibition of the triceps-surae (TS) before the activation of the deltoid, and a rebound of TS activity just before the onset of the arm movement. Biomechanically, this muscle pattern results in anticipatory forward sway, with the body then held at the new position.

Peripheral muscle stretch reflexes in the triceps-surae (TS) oppose forward sway. They are task-dependent, and vary based on the conditions at the joint and associated homonymous muscle activation levels. Hence during the APA, one might expect the reflexes (which oppose forward sway) in the calf to be initially inhibited and then rebound close to movement onset (to assist the slowing down of forward sway). However, to date, this has not been demonstrated.

Therefore, we devised a novel paradigm, where we measured the excitability of the stretch reflex at the TS at different times during the APA associated with unilateral right arm raises in standing humans. Our major results were: 1) The APA pattern was characterized by a repeatable pattern of change in the postural muscles consisting of an inhibition of the TS complex, followed by an activation of the TA muscle. 2) Reflexes were inhibited from their resting levels 80-100 prior to arm movement onset and rebounded to resting levels 0-40 ms before movement onset. 3) Reflex inhibitions were large-no subject had a reflex inhibition that was less than 50% of resting level-and were correlated with changes in reflex torques. 4) The reflex changes were dissociated from the changes in activity of the homonymous TS muscle. In particular, reflexes were inhibited 30-50 ms after the TS muscle activity but rebounded 20-40 ms before the TS muscle activity. Furthermore, the relative sizes of the reflex and muscle activity inhibitions were not correlated across subjects. The results indicated that TS stretch reflexes were inhibited during the APA as hypothesized, and that these changes were not solely caused by the descending central commands regulating the TS muscle activity.

4.2 Introduction

Standing humans are inherently unstable due to their high centre of mass (CoM) position above a relatively small base of support. Unless body position is completely static, and the CoM is aligned with the centre of vertical pressure (CoP), the downward force of gravity will produce a rotational torque about the ankle joint, causing it to sway forwards or backwards. The activities of the flexor and extensor muscles of the lower leg, primarily the triceps-surae (TS) complex comprising the gastrocnemius (GS) and soleus (SOL) muscles, and the antagonist tibialis anterior (TA) muscle counteract any forward or backward sway of the body by plantarflexing and dorsiflexing the foot, respectively. It is generally agreed that the resulting ankle torques are produced by a combination of the passive, visco-elastic properties of the ankle muscles, tendons and ligaments [2], active control from the CNS derived from visual, vestibular, and proprioceptive information [4-6, 74, 129], as well as peripheral stretch reflexes at the ankle [9, 125, 130].

It is known that stretch reflexes in the TS complex contribute to postural control. Typically, gastrocnemius (GS) stretch reflex dynamics have been associated with two components: a short latency reflex occurring at around 40 ms and a longer latency one between 100 and 120 ms [9]. The long latency component was deemed to be particularly useful for maintaining postural stability and thus called the functional stretch reflex [9-11]. Other studies have shown that the reflexes contribute significantly to overall ankle joint stiffness or the resistance of ankle muscles to sway [7, 8, 12]. However, reflex properties have been shown to be highly variable. Muscle activation level and joint position significantly influence reflex sensitivity [8, 13]. Studies have shown that reflexes are modulated during natural tasks such as walking and cycling, and more unnatural tasks (e.g. maintain a specific torque or position at a limb) [131, 132]. Others have suggested that reflexes can be modulated voluntarily if subjects are given appropriate feedback [15-17]. In summary, while it is agreed that TS stretch reflexes plays an important role in the control of sway, less is known about the underlying neural mechanisms regulating it and its functional contribution to postural stabilization.

Voluntary movements during stance result in internally generated destabilizations of the body. In such situations, it is widely accepted that a feed-forward mode of postural

control, mediated by descending commands from the CNS, is adopted. It has been shown that for a range of voluntary arm, trunk or leg movements, postural muscle activity precedes that of the focal muscles required to execute the movements [19-22]. This postural activity has been termed anticipatory postural adjustments (APAs). The classically used task adopted to study such feed-forward postural adjustments is the unilateral arm raise, during which the SOL shows an inhibition of activity approximately 60 ms before the activation of the deltoid (focal) muscle [20, 24, 25]. The antagonist flexor muscles (e.g. the TA or tensor faciae latae) do not typically show anticipatory activity, but are strongly activated at about the same time as the focal muscle. The actual physical movement of the arm starts 60-80 ms after the onset of the deltoid activity [19]. The biomechanical effect of this APA pattern is to cause a backward shift in the CoP, and a forward motion of the CoM. Functionally therefore; the APA has been traditionally interpreted as creating counteractive forces equal and opposite to those produced by the upcoming movement [23-26].

It would seem therefore, that active stretch reflexes in the TS complex will counter the forward motion of the body initiated by the APA to counteract the arm raise. Hence, it may be hypothesized that the TS stretch reflex should be inhibited during the APA period in order to enable the APA to perform its role. However, to our knowledge, no one has investigated this proposal. Woollacott et al. [126] indicated that overall sensitivities of the reflex pathways in these muscle groups were voluntary conditioned in preparation for an arm movement if subjects were given advance information on the nature of the arm movement (push vs. pull). However, they measured static reflex sensitivities prior to the APA phase as opposed to dynamic measures during the APA period. Ramos and Stark [101] predicted increased reflex activity prior to arm movement based on a two segment inverted pendulum simulation but did not provide any experimental evidence in support of this. A few analogous studies have investigated the SOL H-reflex during the APA phase of voluntary movements, such as arm raises, ballistic head movements, and stepping movements [29-31]. H-reflexes are caused by direct external electrical stimulation of the 1a afferent fibers, and assess the excitability of the α -motoneurons. Kasai [30] and Kawanishi [29] showed that SOL H-reflexes are inhibited

during the APA phase of voluntary arm raise movements. The authors suggested that these H-reflex changes might be due to a combination of feed-forward descending commands and pre-synaptic inhibition from 1a afferents projecting from the Brachialis Flexor (hamstring) muscles. However, since the methodology of H-reflex assessment bypasses the muscle spindles, their influence on the changes observed cannot be accounted for. Accordingly, it has also been shown that changes in the H-reflex do not exactly correspond to changes in the stretch reflex [32, 33].

Therefore, using a voluntary arm raise paradigm, we aimed to systematically document stretch reflex changes in the TS complex by applying small dorsiflexing pulse perturbations to the right ankle at different times during the APA period. The objective of this study was to investigate if TS stretch reflexes were inhibited during that period. We quantified the modulation in both time and amplitude of the reflexes and associated background muscle activity using EMG techniques, as well as the mechanical torque responses.

We found APA muscle patterns in the postural muscles that were consistent with previous reports. As hypothesized, we also found large inhibitions in the reflex during the APA. Interestingly, we found that the changes in the reflex were dissociated temporally from the corresponding changes in the TS muscle activity. The changes in the reflex were also correlated with reflex torque changes suggesting that they had significant mechanical effects.

4.3 Methods

4.3.1 Subjects

8 healthy subjects (4 males and 4 females aged between 21 and 26 years, mean weight 67.7 ± 12.9 kg, mean height 1.73 ± 0.113 m), with no reported history of neuromuscular disease, voluntarily participated in this study. Informed written consent was obtained following guidelines approved by the McGill Ethics Board.

4.3.2 Overview

The goal of the experiment was to investigate the behavior of the stretch reflex in the TS complex (the postural stabilizing muscles of the lower leg) during the APA phase of a voluntary movement. To this end, subjects stood upright and executed a unilateral right arm raise to a target anterior to the subject, positioned at arm's-length and shoulder height. At different times prior to and after the movement a small position perturbation was applied to the right ankle of the subject, to elicit a stretch reflex in the TS complex. Therefore, over a number of repetitions of the task, the reflex response as a function of time relative to the onset of the movement was determined.

4.3.3 Experimental Apparatus & Operation

Figure 4.1a shows a schematic of the experimental setup. The subject stood on two rotary foot pedals driven by hydraulic actuators. Each pedal was instrumented with four load cells (Omega LC302-100), one at each corner, that measured downward force and center of pressure (CoP), a potentiometer (Maurey Instruments- 112 P19) that measured the angular position, and a torque sensor (Lebow 2110-5k) that measured the pedal torque.

Figure 4.1a also shows a schematic of the adjustable aluminum frame bolted to the floor (55cm in front of the actuator), and fitted with the following components:

1. A piezoelectric buzzer (www.thesource.ca catalog # 2730059), and a LED (Active Electronics, model# 55-557-5), were used as audio “warn” cues and visual “move” cues to instruct the subject to execute the task.
2. A push button switch (RP Electronics, model 459512) was used as a movement “end” target for the arm raise
3. Two analog voltmeters (Nexxtech, www.thesource.ca catalog # 2218200) provided real-time feedback of the torque at each foot pedal, to help subjects maintain a steady-state torque level prior to the initiation of each trial.
4. A portable “ready” switch strapped to the subject’s thigh was used to detect the onset of movement.

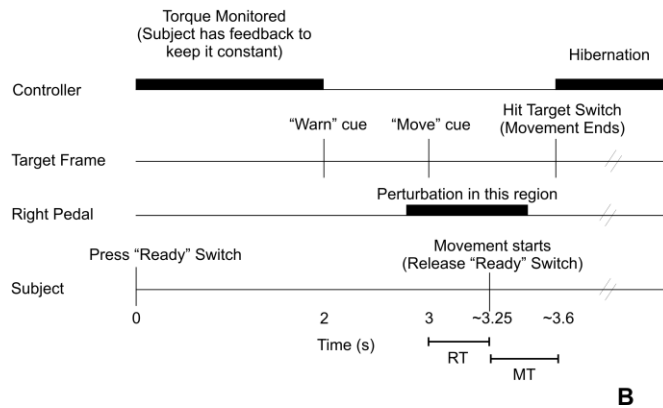
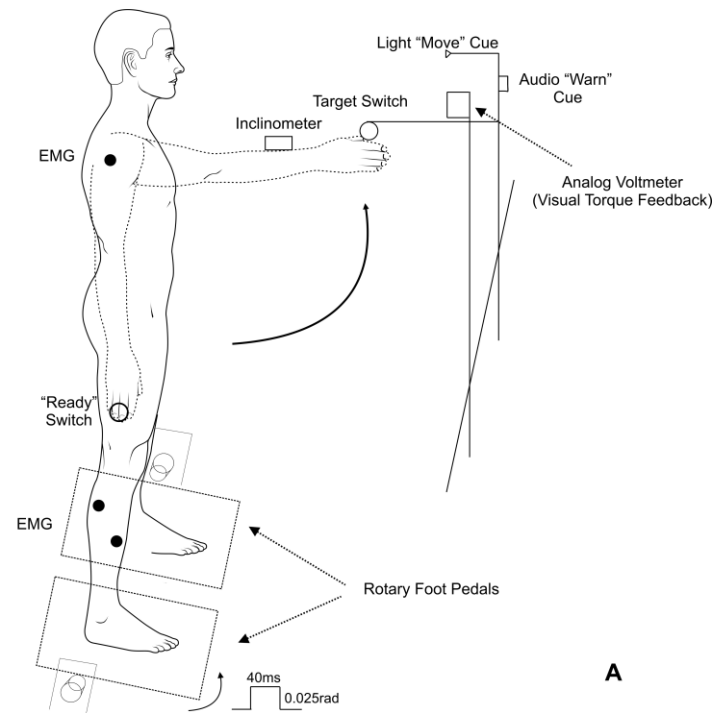


Figure 4.1. Experimental setup. A) Schematic illustrating the task carried out along with cues and sensors used. B) Chart indicating sequence of temporal events during the experiment.

EMGs were measured with an 8 channel differential EMG system (Delsys Bagnoli), having a bandwidth of 20-2000 Hz and a gain of 1000. Surface electrodes (D.E 2.1) were placed on the SOL, Lateral Gastrocnemius (LG), and TA of each leg, and the right Anterior Deltoid, the focal muscle of the arm movement. The last channel was used to record the EMG from the Medial Gastrocnemius (MG) of the right leg. A disposable, adhesive surface Ag/AgCl electrode (3M Red Dot) was placed on either the left or right knee cap to act as a reference. A single-axis inclinometer (Microstrain FAS-G) fixed to a

splint (Formedica Ergo-forme) on the right wrist and oriented orthogonally to the radial bone measured the angular position of the arm with respect to the vertical. The sensor output had a resolution of 0.1° and accuracy of $\pm 1^{\circ}$. A vertical arm position (fingers pointing down) was defined as 0° , and a horizontal arm position as 90° .

Two workstations, referred to as the host and target workstation, controlled the setup. The host workstation (AMD Athlon, 2.2 GHz, 2 GB RAM) had three functions. First, it was used to construct a real-time control model for the experimental apparatus. Second, it was used for data acquisition. Data were initially low-pass filtered with a cut-off frequency of 400 KHz. The data acquisition cards (National Instruments 4472) oversampled the data at 128 KHz, applied a low-pass digital brick wall filter (cutoff frequency 486.3 Hz), downsampled it to 1 KHz, and lastly saved it on the hard disk. Third, it housed a custom-built graphical user interface (GUI) which allowed the experimenter to monitor parameters during the experiment.

The target workstation (AMD Athlon 1.6 GHz, 256 MB RAM) was dedicated for apparatus control. It executed a compiled version of the graphical control model, which was uploaded from the host workstation via a TCP I/P Ethernet connection using the xPC Target Program. Pedal position was specified using a controller that implemented proportional position feedback and feed-forward velocity. Pedal position and torque were low-pass filtered with an 8th order, low-pass, linear phase, constant delay filter bank with a cut-off frequency of 250 Hz and unity gain (Frequency Devices 9064) and sampled at 1 KHz (Measurement Computing - PCIM-DAS1602/16). The control signal to the servovalve was provided by a D/A converter (Measurement Computing- PCIM-DDA06/16). D I/O channels on these cards were used to communicate with components on the aluminum target frame.

4.3.4 Experimental Protocol

Defining the Operating Point

Subjects were instructed to stand on the two foot pedals, maintain a relaxed stance, and a constant torque at both ankles using the real-time feedback from the analog voltmeters. At the start of each experiment, this torque was monitored for a period of 20

seconds. The average value was used as a baseline, along with a modifiable tolerance limit, by the real-time controller. This was typically set at $\pm 10\%$ of the baseline torque value, consistent with previous thresholds suggested by Macpherson et al. in feline experiments [133].

Experimental Paradigm

Figure 4.1b summarizes the experimental paradigm. Subjects were instructed to press down the “ready” switch strapped to the right thigh with their inner palm to initiate a trial. The torques at both ankles were monitored. Subjects were required to maintain torque levels within the defined baseline operating point and tolerance limit for a period of 2 seconds. Once this requirement was met, the controller issued an audio “warn” cue (10ms beep from the piezoelectric buzzer). One second later, the “move” cue LED (light) on the target frame was illuminated. Subjects were instructed to react by quickly raising their right arm to depress the target “end” switch with their right fist, which caused the LED to turn off immediately, and signaled the end of the trial. After a mandatory 2 second rest period, subjects depressed the “ready” switch to repeat the task.

In an initial practice period, subjects executed a number of trials, until a consistent movement was achieved. To this end, reaction times (RT- delay between light onset and release of “ready” switch) and movement times (MT- delay between release of “ready” switch and depression of target “end” switch) were monitored using the GUI. Once the subject had achieved a desirable movement pattern, with reaction times of 0.2-0.3s and movement times of 0.3-0.4s, usually after 25-30 trials, data collection was initiated. Subjects were able to execute the task comfortably with no fatigue.

In approximately 25% of the trials, no perturbations were applied. In the remainder, a small dorsiflexing pulse displacement (0.025 radians, 20 ms wide) was applied to the right ankle at a random delay (800ms-1400ms) from the “warn” cue, as shown in Figure 4.1b. Figure 4.2 shows the input perturbation profile for all subjects as a function of the delay with respect to the light (“move”) cue (shown by the vertical dotted line). The estimated RT window (0.2-0.3s after “move” cue) is shown by the grey window, and is approximately where movement onset is expected. The aim was to have a majority of perturbations in the APA window (i.e. ~ 200 ms before movement onset), with

a smaller number outside (i.e. before APA and after movement onset) acting as a reference. Limitations of this procedure are discussed in Chapter 5.

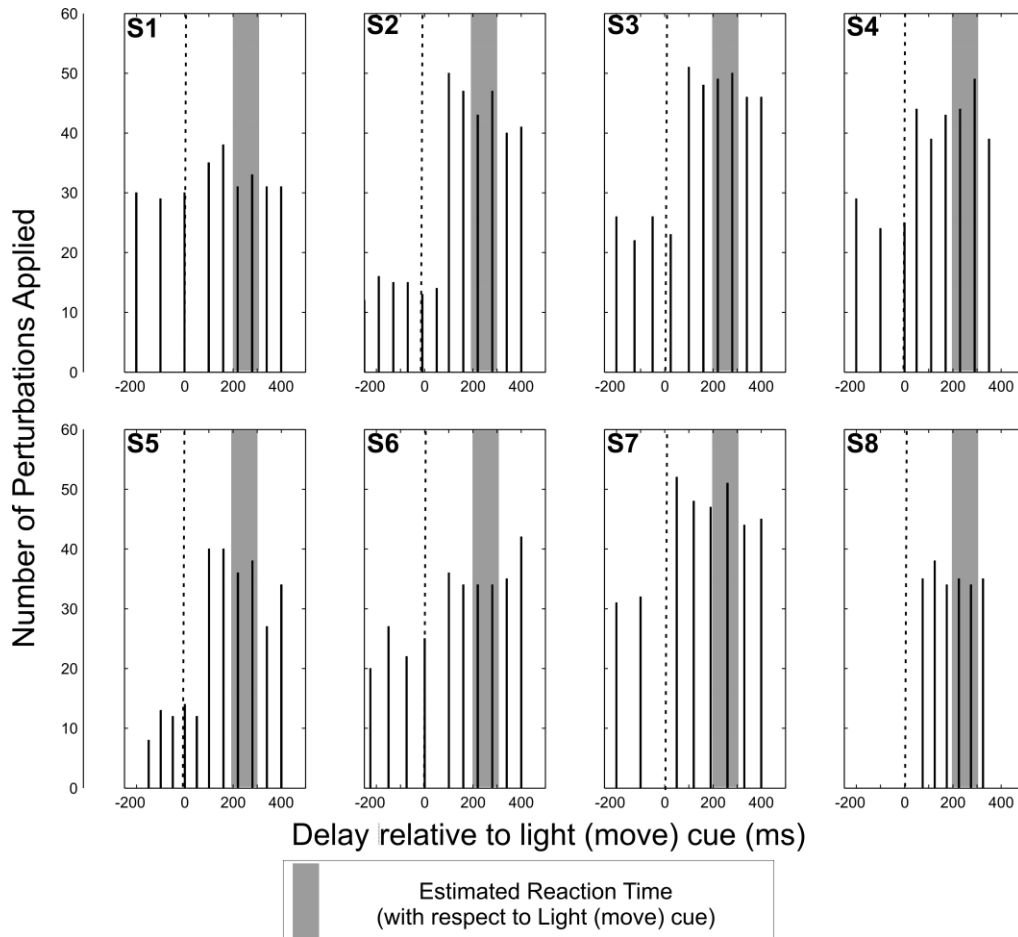


Figure 4.2. Input perturbation profiles for all subjects. Histograms show number of perturbations applied with respect to the go cue. Estimated RT region is shown by the grey window. Dotted line shows the onset of the “move” cue.

Perturbed and unperturbed trials were interspersed randomly. Each subject executed approximately 350-450 trials during one experiment. A mandatory 2 minute rest period was provided every 5 minutes to minimize the effects of fatigue.

The desirable range of RT and MT indicated above was found during a set of pilot experiments, and based on muscle force constraint studies done in the Balance and Voluntary Movement Laboratory (BVML, Department of Kinesiology, McGill). These studies investigated RT and MT’s during the APA phase of arm reach movements (data not published). It should also be noted that we did not actually monitor fatigue during the experiment.

4.3.5 Data Analysis

4.3.5.1 Trial Selection

The first step in the analysis process was trial selection. Since it was impossible to predict the precise RT for each trial, it was hoped that subjects would move consistently enough such that the RT's typically fell within the estimated RT zone (grey window, Figure 4.2).

Histograms of RT and MT were computed offline for all the trials. The mode RT and MT were identified, and the absolute distance to these mode values were computed for all trials. The cumulative probability function for these two distance metrics were calculated, and is shown below in Figures 4.3a and 4.3b for all subjects. Cutoff thresholds (i.e. the furthest tolerated distance to the mode values) to prune trials from the calculated histograms were chosen for RT and MT to be 100 ms and 60ms respectively. The data are summarized in Table 4.1 below.

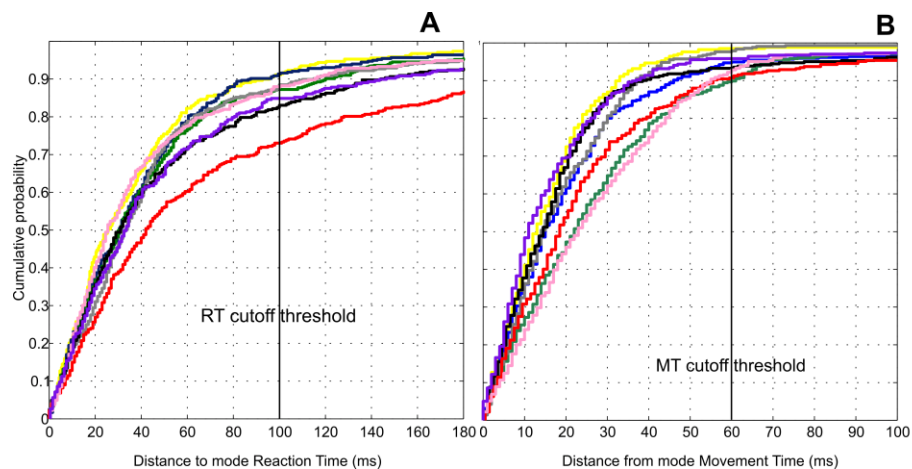


Figure 4.3. Cumulative distribution functions of the distance to the A) mode RT and B) mode MT for all trials and all subjects. Cutoff threshold values for trial rejection: mode RT \pm 100 ms, and mode MT \pm 60 ms.

These specific cutoff values were chosen so as to keep a large number of data points, with the subject exhibiting the greatest variability still retaining over 70% of trials. However, the analysis scripts were also structured so as to allow these thresholds to be easily adjusted in the future. The RT and MT histograms for all subjects are shown in Figure 4.4 below. Selected trials are shaded in black (overlying the grey bars for all trials). Limitations of this method and possible improvements are discussed in Chapter 5.

Table 4.1. Trial selection data. The total number of trials, along with the % rejected for each subject is indicated. The color legend corresponds to the curves in Figure 4.3.

Color Legend	Subject	Number of Trials	Number of Accepted Trials	% of Trials Rejected	RT mode (ms)	MT mode (ms)
Yellow	1	338	313	7.4	283	312
Blue	2	416	363	12.7	238	302
Green	3	455	362	20.4	248	328
Grey	4	425	382	10.1	233	313
Black	5	342	264	22.8	238	308
Red	6	367	261	28.9	228	328
Pink	7	449	370	17.6	248	308
Purple	8	337	283	16.0	273	273

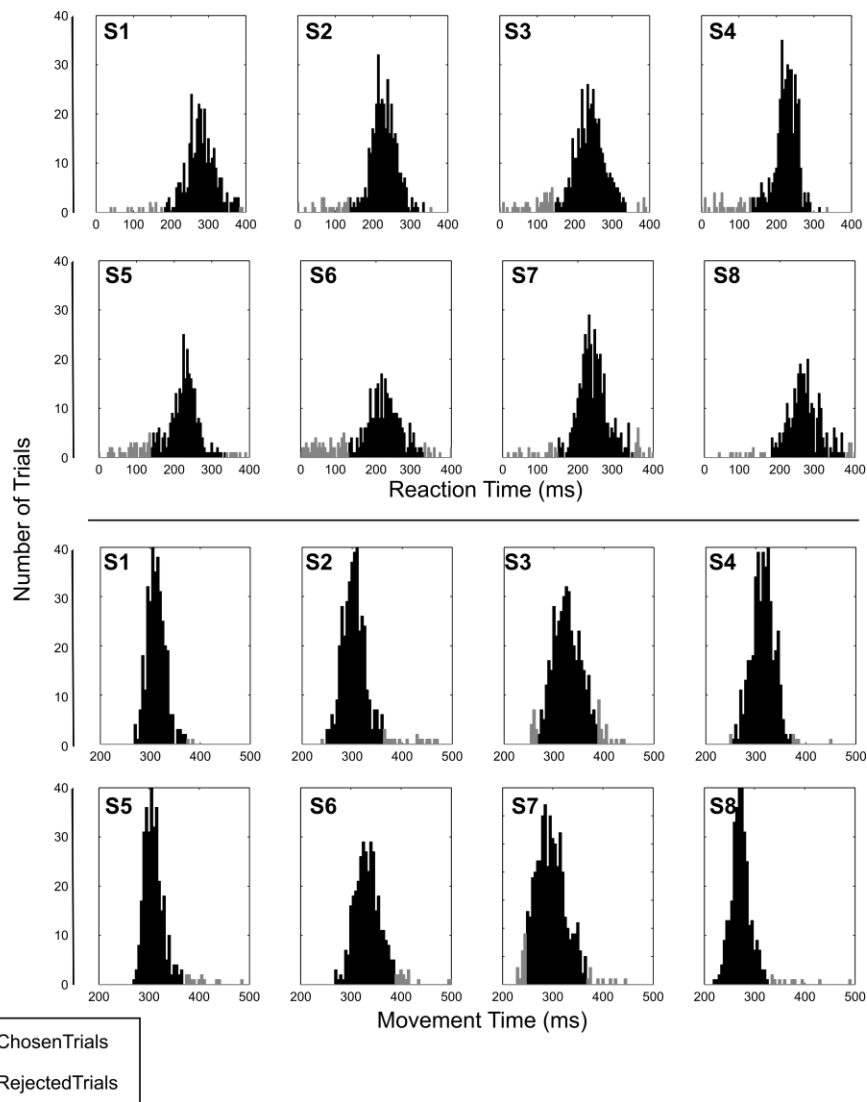


Figure 4.4. Reaction Time (top) and Movement Time (bottom) histograms for all subjects. The chosen trials are shaded in black overlaying all trials (grey).

The selected trials were segmented into perturbed and unperturbed trials. Figure 4.5 shows the distribution of perturbations applied with respect to the onset of movement from the selected trials (i.e. an indication of the times at which the reflex EMG values were measured).

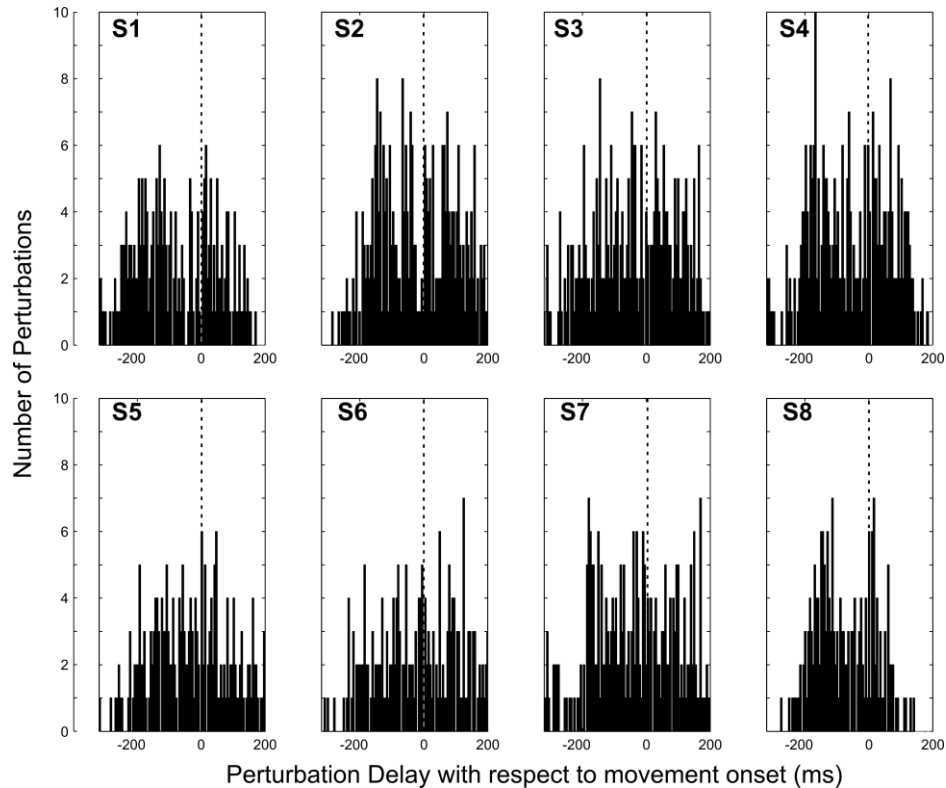


Figure 4.5. Perturbation profile with respect to movement onset after trial selection for perturbed trials. Dotted line signifies movement onset.

This report focuses on the analysis of the rectified EMG and torque responses from the ipsilateral side of the body. For all trials, movement onset of the arm was defined by the falling edge from the thigh “ready” switch output.

4.3.5.2 Unperturbed Trials

Unperturbed trials were aligned to the movement onset, defined by a step change in the signal from the “ready” switch (i.e. when switch is released) and ensemble averages were computed. Figure 4.7 shows an example of this. The data from these trials were used as controls to estimate changes in EMG and torques associated with the movement.

4.3.5.3 Perturbed Trials

The first measure computed for the perturbed trials was the *pulse delay* - the time delay at which the perturbation was applied with respect to movement onset.

Reflex EMG and Reflex Torque Computation

Figure 4.6 shows a data segment from a typical perturbed trial. Figure 4.6a shows the position signal of the pedal, with the dorsiflexing stretch indicated by the arrow. This resulted in a synchronized burst of activity in the TS, indicated by the arrow in Figure 4.6b. This typically started 40-50 ms after the stretch and lasted no longer than 100 ms [17]. Therefore, the reflex EMG for a particular trial was calculated by finding the maximum rectified EMG in the first 100 ms following the time at which the perturbation was applied (stretch onset).

Also, for each perturbed trial, the delay with respect to movement onset at which the reflex EMG peak occurred was computed, and defined as the *reflex EMG peak delay*. Along with the *pulse* delay defined above, this measure was used at a later stage in the analysis (Time modulation of Reflexes - Figures 4.9 and 4.10), and its use will be clarified when these figures are discussed (pages 92-94).

Torque responses in the perturbed trials were a combination of intrinsic torques due to mechanical visco-elastic joint properties, torques associated with the voluntary arm movement, and those caused by the reflex EMG. Since we were interested in the reflex contribution, it had to be extracted from the overall torque response. Figures 4.6c, 4.6d and 4.6e show this process for a sample perturbed trial.

Figure 4.6c shows the overall response from a sample perturbed trials; it was dominated by the large intrinsic component, 5-10 times greater than the other torques. This component occurred during the motion of the pedal, and could therefore be easily distinguished temporally from the reflex effect, which occurred much later. The reflex torque only occurred after the ankle stopped moving, in a region of interest 120-180 ms after the perturbation onset, and was characterized by a trough in the torque profile. However, during this time, the voluntary torque due to the arm movement was also changing, and had to be corrected for. We estimated this component from the ensemble average torque from the unperturbed trials (refer to Figure 4.6e). This component is

represented by the dotted line in Figure 4.6c. Figure 4.6d magnifies the scale, to focus on the region of interest, as defined above. The reflex component was extracted by subtracting the ensemble average voluntary torque from the overall perturbed torque response.

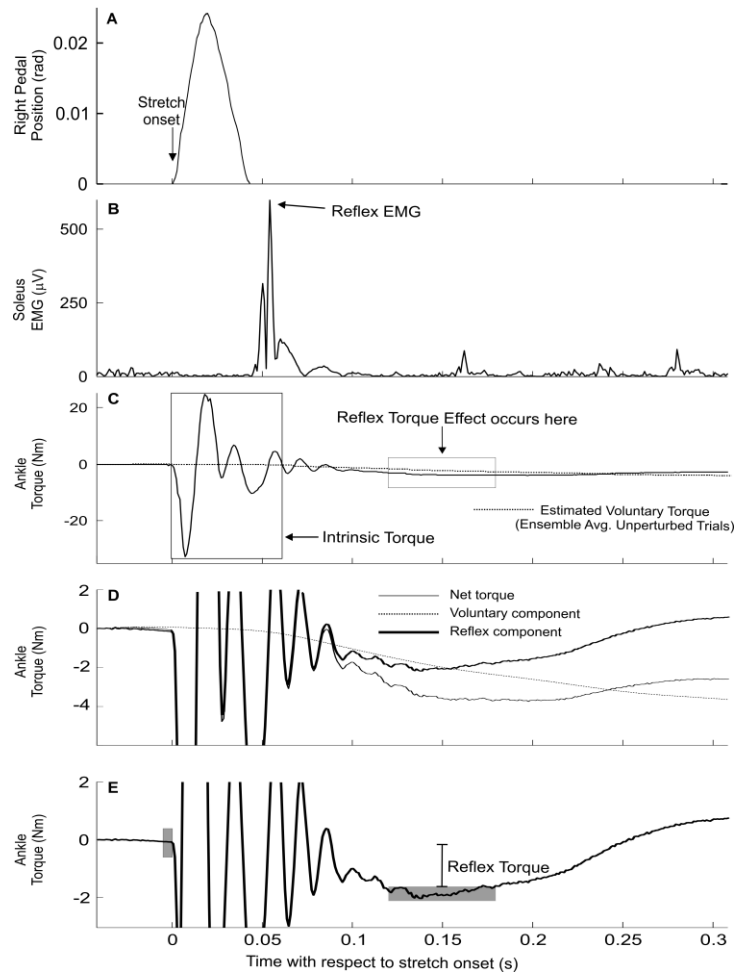


Figure 4.6. Calculation of the Reflex EMG and Reflex Torque. A) Foot pedal position. Dorsiflexing pulse of magnitude 0.025 radians causes a delayed reflex response shown in B) Soleus EMG. The EMG peaks at a lag of 50-60 ms from the pulse onset. The reflex EMG has a mechanical torque response which has to be separated from C) the overall torque response with D) intrinsic, reflex, and voluntary components, so as to compute the E) reflex torque.

Lastly, Figure 4.6e shows how the reflex torque value was calculated from the extracted reflex component. Reflex torque values were calculated by subtracting the average of the extracted reflex component in a 5ms window prior to pulse onset from the average of the same profile over a window, 120-180 ms after stretch onset.

The reflex torque value, as indicated on Figure 4.6e, should always be a negative number (corresponding to a plantarflexion) with more negative values signifying larger reflex torques. Across subjects, $3\pm 2\%$ of selected trials had reflex torque values that were computed to be positive and nonsensical (because the background torque during those trials deviated significantly from the ensemble control average, resulting in an incorrect subtraction of the control profile). The EMG and torque data from these trials were discarded from further analysis.

Time Modulation of Reflexes- Ensemble Changes

We initially investigated the ensemble reflex EMG and reflex torque variability as a function of the movement onset, to have a broad understanding of the reflex modulation pattern during the APA. Results are shown in Figure 4.8. Trials were segmented into 20 ms bins according to the *pulse delay* as defined previously. In each bin, EMG and torque profiles were re-aligned on the onset of the pulse and ensemble averaged. Since the reflex responses were synchronized to the onset of the pulse, this technique separated the reflex components from asynchronous non-reflex activity (e.g. EMG due to postural muscle activity).

Time Modulation of Reflexes- Onset of Inhibitions and Rebounds

To follow up on this analysis we computed the onset of inhibition and rebound in activity for both the reflex and background EMG measures. For this purpose, we used the reflex EMG values computed from each perturbation trial (as opposed to an ensemble average as in Figure 4.8), as a function of movement onset. Furthermore, to explore the etiology of these reflex changes, we also compared them to that of the associated background muscle activity EMG. As in Figure 4.8, data were segmented into bins.

Three different bin sizes (20, 15 and 10 ms) were used to ensure that detected changes were not artifacts of the binning procedure. Using a smaller bin increases the time resolution to detect the onset of inhibitions and rebounds, but decreases the number of points in the bin, as can be seen from Figure 4.5.

The data points within each bin were then graphically represented as a box-and-whisker plot showing the lower quartile, median and upper quartile, with dotted (whisker)

lines extending to the furthest data point within the whisker length. Any outliers beyond the whisker length, set to a maximum length of 1.5 times the inter-quartile range, were represented as a plus (+) sign. Inhibitions and rebounds for reflex and background muscle activity were then defined as follows:

- Inhibitions were identified by detecting the bin where at least 75% of the data (i.e. the entire box minus the upper whiskers) were below the baseline resting level. Furthermore, all bins for the next 40-45ms (i.e. 2 bins with a 20 ms bin size) had to also be below the baseline activity. This was done to ensure that the inhibition detected was a sustained inhibition and not just a transient change.
- Rebound times (i.e. return to the baseline level) were identified by detecting the first bin which no longer satisfied the inhibition criterion (i.e. a part of the box intersected the baseline level). Again, successive bins (for 40-45 ms) had to also have a box plot either intersecting the baseline level or greater than it.

This binning procedure was used primarily since the reflex data were not evenly sampled throughout the APA period (as can be seen in Figure 4.5). In a preliminary analysis, the data points were fit with an interpolated smoothing spline (data not shown), and we attempted to detect inhibitions using a mean \pm std relative to the resting level (i.e. the average activity before the APA onset, e.g. 400 to 200 ms before movement onset). However, since the reflex data at these times were sparsely sampled, the spline trends were easily distorted by outliers, and also carried a large residual error estimate. It was therefore felt that an analysis that quantized the data into bins, with a representation of the distribution within each bin, would allow more valid comparisons between unequally sampled data.

Results from a representative subject, with a 20 ms bin width, are shown in Figure 4.9. Results for all subjects, and for all three bin sizes, are shown in Figure 4.10.

Lastly, it is important to note in this analysis, since we were comparing reflex changes to the background muscle activity, the reflex EMG data (i.e. Figure 4.9a) were

not segmented based on the *pulse delay*. Instead, the measure used for segmentation was the *reflex EMG peak delay* (as defined above on page 90).

This differs from what was done in Figure 4.8 (which uses the *pulse delay*). This was done, following a preliminary analysis, which showed that using the *pulse delay* criterion in this situation would make comparisons with the background muscle EMG erroneous. This is because, as shown in Figure 4.6b, the reflex EMG peak typically occurred 40-50 ms after stretch (*pulse*) onset. Unlike Figure 4.8, where only the ensemble response was looked at within each bin, this analysis looked at the individual responses. When the *pulse delay* criterion was used in this situation, it introduced an artifact in the analysis, with each reflex response being shifted back in time by about 40-50ms (the neural conduction delay), and made comparisons with background EMG changes erroneous. Therefore, *the reflex EMG peak delay* was used to bin the reflex data in Figures 4.9 and 4.10.

4.4 Results

Data shown are from the SOL used as a representative muscle for the TS complex. Furthermore, data for all figures (except Figures 4.10-4.12 which show data from all subjects) is from one representative subject (Subject S1 in Table 4.1).

4.4.1 Unperturbed Trials

Figure 4.7 shows the ensemble average of the unperturbed trials aligned to the movement onset (vertical black line). The dotted error lines, below and above the ensemble average line, are the 25% and 75% quartiles of the datasets. This measure was used (as opposed to showing the ensemble average \pm std), since the rectified EMG values (Figures 4.7b, 4.7c, and 4.7d) do not have Gaussian distributions (rectifying the raw EMG, which has a Gaussian distribution, gives a folded normal distribution). For the purposes of continuity, the same error estimates are also used for the data in figures 4.7a and 4.7e.

Figure 4.7a shows the trajectory of the arm movement. All three TS muscles exhibited a characteristic APA defined by an initial inhibition followed by activation prior to movement onset. Thus, the start of the APA was indicated by the onset of inhibition in

the SOL, as shown by the arrow in Figure 4.7d. Note that all arrows show approximate times at which changes occurred. For the purposes of comparing these changes with reflex changes we used a box-whisker plot analysis (Figure 4.9). The SOL inhibition was followed by activation of the agonist TA (Figure 4.7c), and finally by activation of the Anterior Deltoid (Figure 4.7b) -the muscle responsible for the arm movement. Close to movement onset, there was a recovery of the SOL muscle activity and a reciprocal pattern of the TA (return to resting level). Biomechanically, during the APA, there was a small dorsiflexing torque on the right pedal (Figure 4.7e).

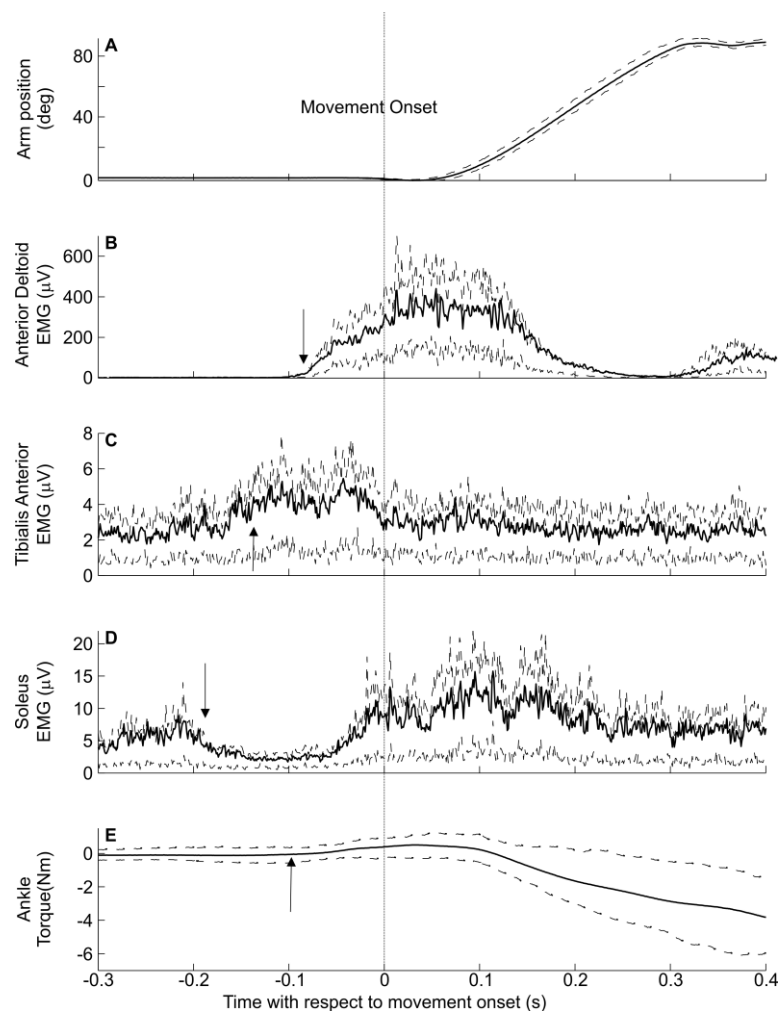


Figure 4.7. Ensemble average of unperturbed trials for a typical subject. A) Arm position. B) Anterior Deltoid, C) TA D) and SOL EMG's. E) Ankle Torque. Signals were aligned on movement onset (black line). Arrows indicate approximate start of change in each signal. Arm position 0° is defined as perpendicular, and 90° as parallel to the floor. Dorsiflexing torques are taken as positive. Postural muscle changes preceded focal (deltoid) muscle activity.

4.4.2 Perturbed Trials

4.4.2.1 Time Modulation of Reflexes

Figures 4.8a and 4.8b show the variation of the binned (bin width of 20 ms) ensemble reflex EMG and reflex torque component (refer to Figure 4.6d) with respect to the time at which the arm movement started. For clarity, the curves are offset vertically. Furthermore, to decrease image clutter (prevent torque profiles from overlapping), every second bin is shown (i.e. delay between successive bins shown in Figure 4.8 is 40 ms). During the APA phase (~200 to 0 ms), the amplitude of the reflex EMG peak first decreased to a minimum value and then rebounded close to movement onset. The ensemble reflex torque component responses also changed with time in a similar manner to the EMG. As in Figure 4.6e, the torque traces are truncated so as to focus on the trough, from which the reflex torque is computed. The intrinsic torque response in Figure 4.8b is shaded lighter, as it is not of interest.

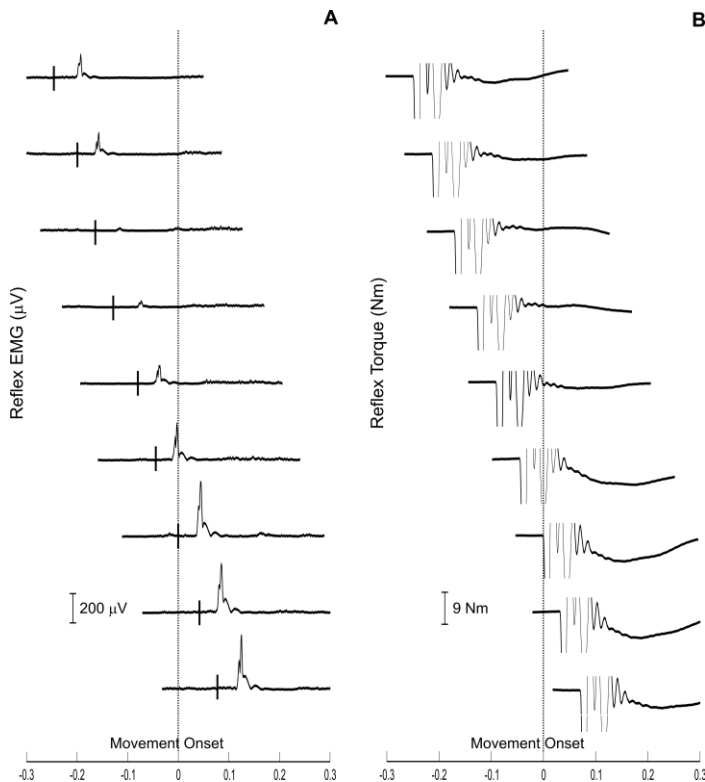


Figure 4.8. Reflex modulation in time. A) Reflex EMG modulation. Data was binned into 20 ms bins and pulses within each bin were aligned, at times indicated by vertical dashes. Every alternate bin is shown. EMG peaks show a biphasic pattern with an initial decrease followed by an increase closer to movement onset. B) Reflex Torque Component modulation. Torques profiles were aligned similarly in 20 ms bins. It follows a pattern similar to the EMG with an initial decrease followed by an increase.

Figure 4.8 demonstrated that there were systematic changes in the reflex response to perturbations during the APA. To detect the onset of reflex and background muscle activity inhibitions and rebounds, we used a box-whisker plot representation, with the inhibition and rebound criteria defined in Section 4.3.5.3. Figure 4.9a shows that, for this subject, the significant reflex inhibition occurred 140-160ms before movement onset, while significant reflex rebound occurred 20-40 ms before movement onset. The period of inhibition is indicated by the ruler line with downward arrows. Furthermore, to explore the etiology of these changes we compared their latencies to those of the background muscle activity from the unperturbed trials. Figure 4.9b shows that significant inhibition in background muscle activity occurred 180-200ms before movement onset, while significant rebound in background muscle activity occurred 20-40ms before movement onset. Hence for this subject, reflex inhibition occurred approximately 40 ms after background muscle activity inhibition, while the reflex rebound occurred at approximately the same time as the rebound in muscle activity.

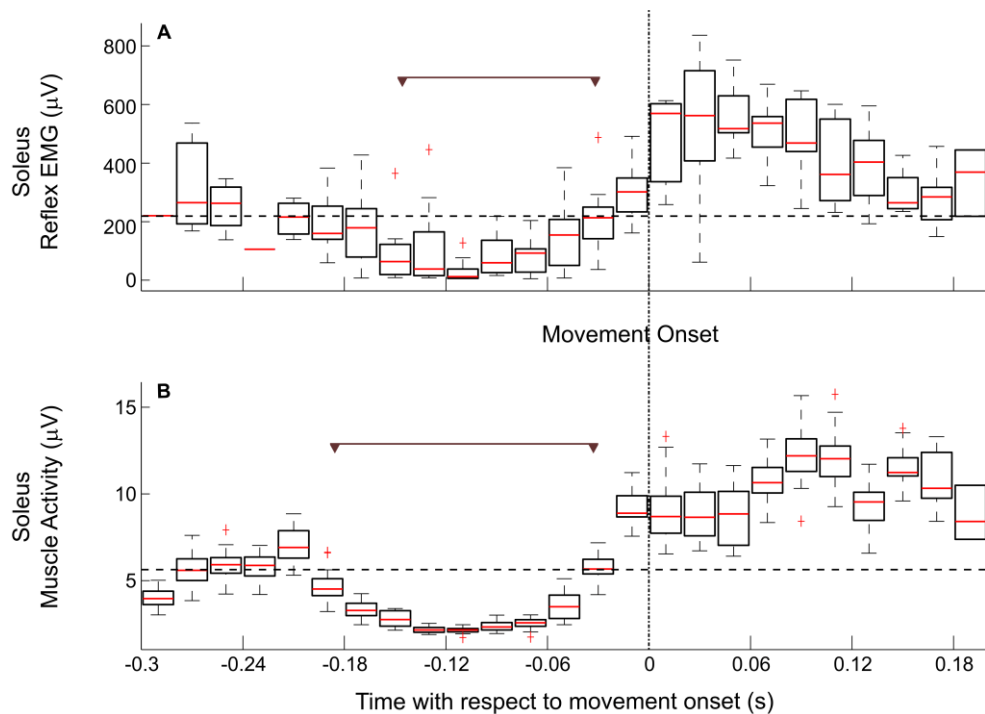


Figure 4.9. Box-Whisker Plot Analysis. Data was segmented into 20 ms bins. Box boundaries are at the lower and upper quartile, encompassing the median (red). The dashed ‘whisker’ lines represent 1.5 times the inter-quartile range and outliers are shown by crosses. A) Reflex B) SOL muscle activity. Downward arrows highlight periods of inhibition and rebound in each parameter. Reflex inhibition occurs after muscle activity inhibition while reflex rebound occurs at the same time as muscle activity rebound.

We similarly computed box-whisker plots for all 8 subjects for all three muscles of the TS. In addition, to validate our analysis procedure, we reduced the bin sizes to 15 ms, and 10 ms, and repeated the analysis. Figure 4.10a (I-III) shows the inhibition and rebound times for both the reflex and background activity across the 20 ms, 15ms, and 10 ms bin sizes respectively. Reflexes are represented by squares, and inhibitions are indicated by filled symbols. Figure 4.10b (I-II) summarizes these findings showing histograms of the differences between inhibition times and rebound times.

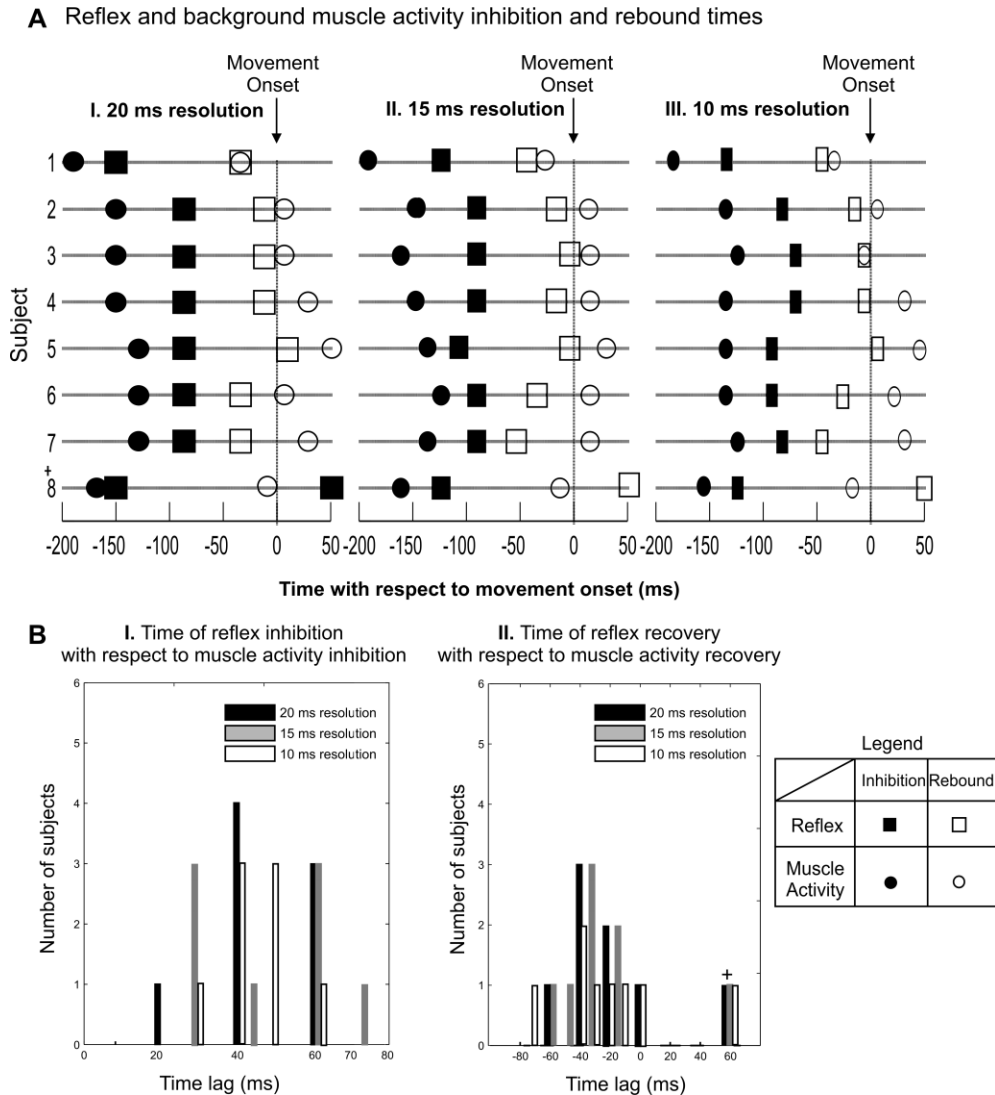


Figure 4.10. Modulation of reflex activity with respect to muscle activity across subjects. Data are quantized into 20 ms bins. A) Reflex and muscle activity inhibition and rebound times for the SOL. B) I. Onset of reflex inhibition with respect to muscle activity inhibition. All histogram bars are located at positive lags, indicating that reflex inhibitions followed muscle activity inhibitions. II. Onset of reflex rebound with respect to muscle activity rebound. Most subjects had reflex rebound times that were equal or less than muscle activity rebound times. Subject flagged with (+) behaved differently.

As observed in Figure 4.10a, using different bin sizes will alter the detected inhibition and rebound times slightly. However, the general pattern is consistent across all three bin sizes. First, from Figure 4.10a, it was observed that across subjects, the reflex was generally inhibited 80-100 ms before movement onset. Second, as shown in Figure 4.10b (I), the reflex inhibitions typically occurred 30-50ms after the inhibitions in background muscle activity. Third, as shown in Figure 4.10b (II) reflex rebounds also typically preceded muscle activity rebounds by 20-40ms.

It should be noted that we had one piece of anomalous data, flagged by the plus (+) sign. Subject 8 behaved oppositely to the rest of subjects, in terms of reflex rebound times (S8 reflexes rebounded after rebound in S8 background muscle activity). This subject had larger resting reflex levels, compared to the other subjects (2-3 times greater in magnitude than any other subject), but the cause for this phenomenon was not determined.

4.4.2.2 EMG Amplitude Modulation of Reflexes

Table 4.2. Reflex and muscle activity inhibitions for the SOL, represented as a percent change with respect to baseline levels.

Subject	% Reflex inhibition	% Muscle Activity inhibition
1	95	86
2	49	81
3	58	61
4	69	98
5	84	76
6	56	87
7	52	58
8	65	70

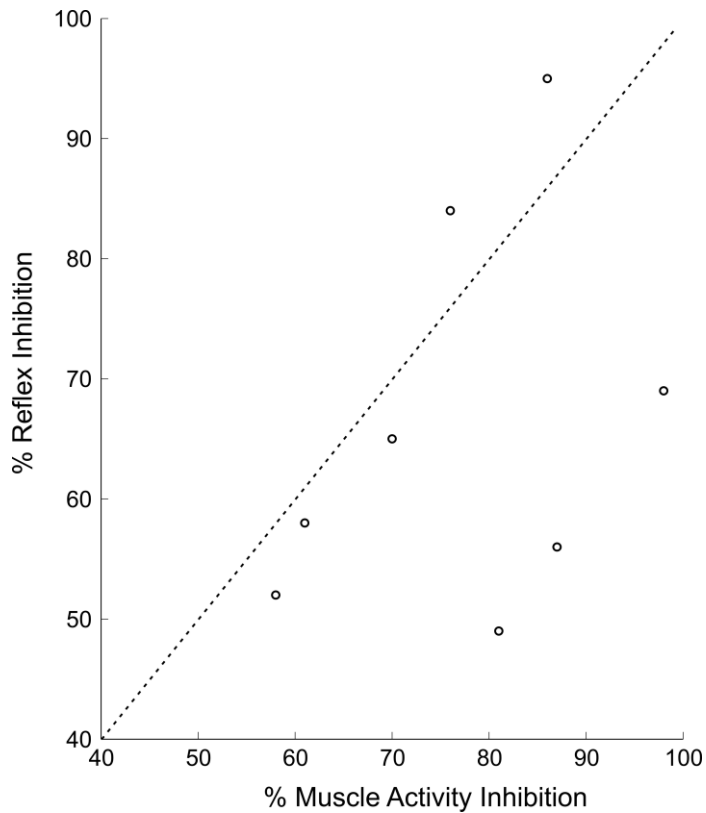


Figure 4.11. Percent SOL reflex inhibition versus percent inhibition in SOL muscle activity for all subjects, with respect to resting levels. The dotted line represents a linear relationship with unity gain. The results indicate that no direct linear relationship ($R=0.35$) exists between the reflex and muscle activity inhibition.

We also analyzed the amplitudes of reflex and muscle activity inhibitions for all three muscles of the TS. Data were normalized with respect to the resting levels to compute the percentage of inhibition for each parameter. Data from the SOL are summarized in Table 4.2 and illustrated in Figure 4.11. We found large reflex inhibitions during the APA in all subjects ($> 50\%$). However, we did not find any consistent unifying pattern across subjects, or across muscle groups, which would indicate that relative amplitude changes in background and reflex activity were strongly linked in any fashion (a correlation analysis gave a coefficient of 0.35). We also compared the size of the reflex inhibition as a function of initial resting background muscle and reflex activity and found no consistent correlation (data not shown).

4.4.2.3 Reflex Torque Changes

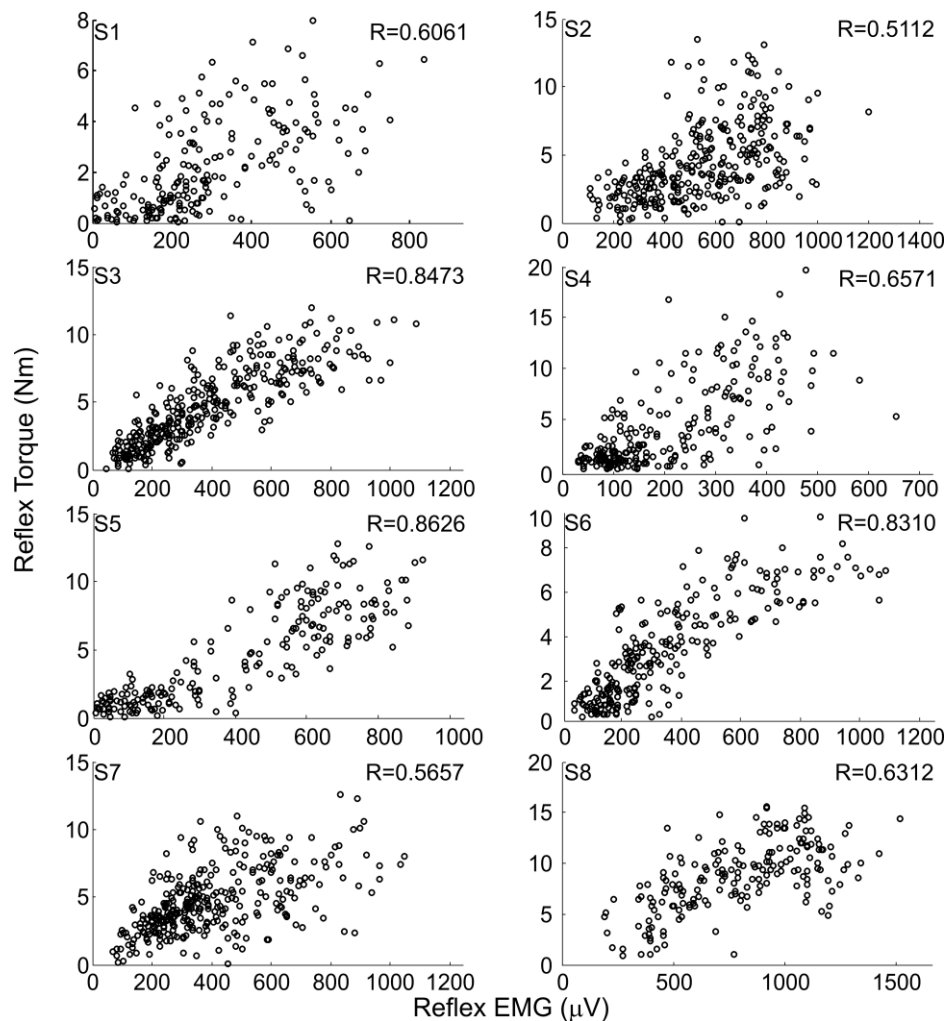


Figure 4.12. Relationship between reflex EMG and rectified reflex torques. Data from all subjects is shown, along with respective correlation coefficients.

Lastly, we explored whether these large changes in the reflex EMG had any mechanical reflex torque effect. This is important to show, since past studies in our laboratory have indicated that changes in reflex EMG do not necessarily directly correlate to mechanical changes in reflex torque [8]. Therefore, the correlation coefficient between the reflex EMG and absolute value of the reflex torque were computed. Figure 4.12 shows a scatter plot between these two parameters for each subject. In all cases, there was a positive correlation with correlation coefficients ranging from 0.5 to 0.8. The

relationship is by no means strictly linear; there was a saturation of the torque at low levels and the torque estimates were very noisy. However, we suggest that this is nevertheless strong evidence that the reflex EMG changes had significant mechanical effects.

4.5 Discussion

4.5.1 Summary

A novel experiment was conducted to investigate the role of the ankle stretch reflex in counteracting self-induced destabilizations of posture. We measured the EMG and associated torque response of the TS stretch reflex in the time period just preceding a voluntary arm raise movement. In this period, known as the anticipatory postural adjustment phase (APA), descending commands from the CNS are used to regulate postural muscle activity, in anticipation of the upcoming disturbance. This is typically characterized by an inhibition of the SOL muscle and an activation of the TA muscle. Biomechanically, this causes a forward sway of the body. Since the stretch reflex inhibits such forward sway, we hypothesized that it might be inhibited during the APA period, and investigated whether this was indeed the case.

We first showed that the arm movement resulted in an APA pattern, whose EMG pattern was defined by a consistent inhibition of the TS, and an activation of the TA muscle. As shown by Figure 4.10, SOL inhibitions generally occurred in a range of 120-160 ms prior to movement onset. Across subjects, focal (Deltoid) muscle onset typically occurred 80-90 ms prior to movement onset (data not shown) In terms of SOL inhibition times, the data are consistent with that of previous studies investigating arm raises which have shown that SOL inhibitions take place 40-60 ms prior to the activation of the focal muscle for such a movement [20, 29]. The SOL inhibition, followed by TA activation pattern is also consistent with the general anticipatory muscle activation pattern defined by Crenna and Frigo for forward oriented movements [19].

We first studied the time course of reflex changes during the APA and showed that the reflexes were modulated during the APA phase, with an initial decrease followed by a rebound close to movement onset. We also found that these reflex changes were not

strictly time-locked with the corresponding muscle activity changes during the APA. Reflex inhibitions typically lagged muscle inhibitions by 30-50 ms while reflex rebound times preceded muscle activity rebounds by 20-40ms.

Next, we analyzed the amplitudes of the detected inhibitions and found that reflexes inhibited in a range of approximately 50-95% of their resting levels, but that the amplitudes of the inhibitions were not linked to the amplitudes of background muscle activity inhibitions.

Last, we showed that the changes detected in the reflex EMG did correlate to mechanical reflex torque responses.

In summary, our results demonstrate that reflexes are strongly inhibited during the APA. Furthermore, there is evidence that these inhibitions are not solely due to the associated inhibitions in background muscle activity, as indicated by the temporal differences between reflex and background EMG (Figure 4.10), and absence of correlation in the amplitudes of the inhibitions (Table 4.2 and Figure 4.11).

4.5.2 Possible Neural Mechanisms of Reflex Modulation

There has been much debate about how reflex modulation might be achieved. Possible physiological mechanisms that have been postulated for reflex modulation include changes in α -motorneuron activity, inter-limb spinal effects, inputs from long-loop transcortical pathways, altered γ -motorneuron drive, and interneuronal polysynaptic reflex pathways influenced by local pre-synaptic inhibition [13, 29, 30, 57, 62, 64, 134-137].

While our experiment was not designed to pinpoint the exact neural causes of the observed changes, we were able to rule out certain possibilities. Specifically, of the mechanisms mentioned in the previous paragraph, we can rule out the first three due to the following reasons:

1. Our results would discount the possibility that reflex changes during the APA merely reflect changes in α -motor neuron excitability, due to direct monosynaptic connections from the descending feed-forward commands resulting in the changes in postural muscle activity. In that event, we

should have found no temporal differences between the reflex EMG and background muscle activity changes. This was not the case.

2. Inter-limb spinal effects can be discounted due to the fact that we were studying changes in the anticipatory phase of the movement.
3. The influence of long-loop pathways can be rejected on the basis that the reflexes measured in our experiment consisted of a unimodal peak which occurred 50-60 ms after stretch onset. These latencies are incompatible with long-loop pathways.

In addition, we also rule out the possibility that the 30-50 ms reflex inhibition delays with respect to background muscle activity inhibition are simply due to the neural delays involved in the stretch reflex conduction pathway (i.e. the delay between applying a perturbation and the detection of the EMG peak as the signal propagates from the spindles to the afferent and finally the efferent) on two counts. While comparing reflex EMG changes with background EMG muscle activity changes, we accounted for the stretch reflex conduction times by measuring the *reflex EMG peak delay* as opposed to the *pulse delay*, as indicated in Figure 4.9. Moreover, in general, the possibility of either the reflexes or muscle activity having a simple direct causal effect (i.e. a direct delay between the two factors) on the other is ruled out by the fact that reflex inhibitions *followed*, while the reflex rebounds *preceded* muscle activity changes during the APA.

Therefore, the mechanisms that could potentially play role are changes in γ -neuron activity, and pre-synaptic inhibition.

First, altered γ -motorneuron activity has been well established as a source for the regulation of muscle spindle sensitivity. Nuclear bag and nuclear chain intrafusal fibers within the muscle spindles are innervated by γ - fibers. The γ -neurons are thought to be influenced by descending commands from higher brain centers, such as the cerebellum, either directly or via interneurons synapsing from the corticospinal tract [62].

Second, as opposed to strictly monosynaptic stretch reflex pathways directly between 1a afferent and the α -motorneurons, there are many polysynaptic reflex cord pathways utilizing an intermediary interneuron between the sensory and

motor neurons. It is possible that changes in the gains of these interneurons could alter the reflex sensitivities. A number of studies have suggested that local GABA mediated pre-synaptic modulation plays a vital role in reflex modulation. At the spinal level, this mechanism is mediated by interneurons that are innervated by Ia afferents of antagonist muscles and also by flexion reflex afferents [64]. It has been shown to be involved in topically inhibiting the SOL H-reflex in stance as opposed to prone or supported conditions [134, 135]. Stewart and Brooke [136] showed that a stimulation of the common peroneal nerve led to an inhibition of the H-reflex. Capaday [137] also showed that injecting baclofen, which binds and acts as an agonist at GABA_B receptors, resulted in a decrease in the cat SOL stretch reflex.

4.5.3 Analogous Studies

We believe this is the first study to measure the stretch reflex excitability during the APA period. In related studies, Kasai [30] and Kawanishi [29] investigated the SOL H-reflex changes in the APA phase of voluntary upward arm movements in both normal upright stance and counterbalanced (supported at the back) stance. Their results were reported using the activation of the deltoid muscle as a zero reference. They found that the SOL H-reflex inhibited approximately 60-80 ms before the activation of the focal deltoid muscle and rebounded approximately 60 ms after, corresponding to reflex inhibition times of 120-140 ms. Furthermore, the conclusion from these experiments was that the inhibition could be divided into two phases, pre-deltoid activation and post-deltoid activation, mediated by descending central commands and pre-synaptic inhibition respectively.

In the first inhibition phase, Kasai (1996) found that the H-reflex inhibition occurred in both normal and counterbalanced stance, but that it was larger in the normal stance condition. Using a low-intensity conditioning stimuli on the common peroneal nerve, they found no changes with a control condition, suggesting that local pre-synaptic inhibition was not responsible for this initial inhibition. Instead, they showed that the H-reflex changes prior to deltoid muscle activation were closely linked to the anticipatory

excitation of the biceps femoris (BF) muscle (hamstring), and the inhibition of the SOL muscle.

Kawanishi et al. (1999) followed up on these experiments by conducting a set of experiments where the BF tendon was vibrated at 30 Hz at various times during the APA. This artificially induces pre-synaptic inhibition of the 1a afferents of the SOL by the 1a afferents of the BF and can be detected by a reduction in the SOL H-reflex. However, if large pre-synaptic inhibitory mechanisms between these two afferents are naturally in effect, then the vibration should have no additional influence as the GABA mediated pathway will be saturated. Between vibration and non-vibration cases, they only found significant differences in the reflex in the time period prior to focal deltoid muscle activation. They suggested that this was evidence that the inhibition phase after deltoid muscle onset was naturally mediated by local pre-synaptic inhibition.

Our results do not agree with these findings. As shown in Figure 4.10a, our reflex inhibition periods were almost 50% shorter, typically in the range of 40-80 ms (time difference between the filled in squares), as opposed to 140-160 ms in their experiments. Also, with regards to the initial inhibition times, we found that stretch reflex inhibitions typically occurred 80-100 ms before movement onset (or approximately at the same time as deltoid muscle activity), while their initial H-reflex inhibitions occurred about 80-100 ms before deltoid muscle activity. Lastly, we consistently found that the start of the stretch reflex inhibition lagged the muscle inhibition and was not a direct result of feed-forward commands as they suggested.

In terms of the reflex rebound phase, the results are more similar. As shown in Figure 4.10a, we typically found that reflexes rebounded 0-40ms before movement onset. With respect to the deltoid activation time, this corresponds to a lag of approximately 40-60ms. This time period is similar to the 60ms period reported for the second phase of inhibition in the aforementioned literature.

Therefore, although we might expect a generally similar pattern of changes, there is no reason to expect that H-reflex changes should directly translate to stretch reflex changes. Andersen [33] investigated the two reflex mechanisms during walking, and found significant differences during the late phase of stance which is associated with the

unloading of the muscle spindles. Morita [32] investigated differences between the effects of pre-synaptic inhibition on H-reflexes and stretch reflexes, and found that H-reflexes were more sensitive to pre-synaptic inhibitory mechanisms. Since the effects of the spindle are ignored in the H-reflexes, they suggested that mechanical and electrical stimuli might cause differences in the composition and/or temporal dispersion of the 1a afferent signals. To be more precise, during an electrical stimulation (H-reflex) the 1a afferents are all activated almost simultaneously. This leads to a motor volley at the spinal cord that is highly synchronized in time. However, during a mechanically elicited stretch-reflex the 1a afferents are not activated synchronously; some afferents may also discharge multiple times, and the measured α -motor neuron EMG activity is a factor of the size, velocity, and acceleration of the spindle stretch [32].

In general, our experimental paradigm did not allow us to precisely isolate the neural causes underlying the stretch reflex modulation. Given the latencies of our reflex inhibitions with respect to movement onset, we suggest that descending feed-forward central commands are definitely involved. However, the fact that the reflexes inhibit after the muscle activity and rebound before it makes it unlikely that central commands alone can explain these changes.

4.5.4 Functional Role of Reflex Modulation during the APA

Traditionally, the functional role of the APA was thought to be one of CoM stabilization [23, 25]. A number of other experiments have suggested otherwise. For example, similar APA patterns have been found in locomotion initiation where the goal is to move the CoM forwards [19]. With respect to the arm raise paradigm, Patla et al. [28] suggested that the APA activity would be more useful for joint stabilization, and that initial control near movement onset was entirely passive, given that the CoM profiles of a simulated passive inverted pendulum model did not deviate from the measured CoM profile till 200 ms after the arm movement. Similarly, using a more complex four joint model, Pozzo et al. [21] showed that overall CoM disturbances were minimal for the arm raise action (1.5 mm anterior displacement), and hence did not necessarily warrant any compensation for it. They also indicated that the deceleration of the arm would change

the direction of the initially de-stabilizing reaction forces on the body and hence lead to self-stabilization.

Our findings confirm our initial hypothesis that reflexes should be generally inhibited during the APA. They also confirm the hypotheses suggested by simulation studies [101], which suggest that reflexes should be activated just before movement onset; and play a crucial role in regulating the amount of forward APA mediated sway (i.e. to help hold the CoM in a new position). We also showed that the reflex EMG changes were large (>50% of resting levels) and did translate to significant changes in reflex torque. This was important to demonstrate, since previous work in our laboratory has shown that reflex EMG changes do not necessarily directly translate to reflex torque changes [8]. The magnitudes of these plantarflexing torque responses near movement onset were about 1-3 Nm which is of an order of 2-3 times greater than the dorsiflexing APA torque magnitudes at the same time. Hence, the reflex torques could definitely have had a significant impact on mediating the degree of forward sway initiated by the APA

We propose a series of future studies to better investigate the association of the reflex with the APA, and to better understand their functional roles with regards to postural stabilization. The experimental frame was designed so that similar studies could be conducted for other voluntary arm movements, such as a forward arm reach. This movement requires a deliberate forward shift in the CoM [108]. As shown by Crenna and Frigo [19], the general APA pattern observed for different forward oriented movements is similar; however the time course of postural muscle inhibitions and activations is different. Given that the two movements have different biomechanical goals (CoM stabilization for an arm raise vs. CoM movement for an arm reach); a comparison of the APA and reflex properties between the two movements would be very interesting.

4.6 Acknowledgments

The authors would like to thank the rest of the research team at REKLAB (Department of Biomedical Engineering, McGill) and BVML (Department of Kinesiology, McGill) for their support and input during this project. This study was supported by the Natural Sciences and Engineering Research Council of Canada (NSERC) and the Canadian Institutes of Health Research (CIHR).

5. Conclusions

5.1 Summary

A novel experiment was conducted to investigate the role of the ankle stretch reflex in counteracting self-induced destabilizations of posture. We measured the EMG and associated torque response of the TS stretch reflex in a phase of time just preceding a voluntary arm raise movement. In this period of time, known as the anticipatory postural adjustment phase (APA), descending commands from the CNS are used to regulate postural muscle activity, in anticipation of the upcoming disturbance. This is typically characterized by an inhibition of the SOL muscle and an activation of the TA muscle. Biomechanically, this causes a forward sway of the body. Since the stretch reflex in the TS inhibits forward sway, we hypothesized that it might be inhibited during the APA period, and investigated whether this was indeed the case.

5.2 Main Findings

- The APA pattern was characterized by a consistent, repeatable pattern of change in the postural muscles consisting of an inhibition of the TS complex, followed by an activation of the TA muscle. The inhibition of the TS consistently preceded the activation of the deltoid muscle, which was responsible for the arm movement.
- Typically reflexes inhibited from their resting levels 80-100 ms prior to arm movement onset and rebounded to resting levels 0-40 ms before arm movement onset.
- The reflex inhibitions were large- no subject had a reflex inhibition that was less than 50% of resting level- and were correlated with changes in reflex torques. This showed that the reflexes had significant mechanical effects.
- Although the homonymous muscle activity (TS) was also inhibited and then rebounded during the APA, the reflex changes were dissociated from these changes. In particular:
 - Reflexes were inhibited 30-50 ms after muscle activity inhibitions and rebounded 20-40 ms before muscle activity rebounds.
 - The relative sizes of the reflex and muscle activity inhibitions were not correlated in amplitude across subjects.

5.3 Limitations of the Study & Suggestions for Improvement

The results of the study were novel and encouraging. However, the experiment had a number of limitations which are important to elucidate for improvements in the future.

5.3.1 Input Perturbations Profile

We attempted to design the input perturbation profile so as to have a large number of trials during the APA period and a smaller subset outside (before APA and after movement onset). Furthermore, the delays of the perturbed trials (and the occurrence of the unperturbed trials) were entirely randomized.

The nature of the task itself brings forth two issues:

- There is inevitably some variability with respect to the RT. Some subjects performed better than others in terms of this (refer to Figure 4.4, e.g. S4 vs. S5).
- Furthermore, it is impossible to predict what the exact RT will be for a given trial in advance.

Therefore, given that the input perturbation delays are randomized, we would want the RT to show as little variability as possible. If this is the case, then the distributions of the input perturbations (chosen with respect to the onset of movement) would more accurately reflect what we intended as an input.

The recommendations for future work in this regard are as follows:

- Make the subject training procedure more rigorous so that subjects react with RT with minimal variability. This could be implemented through a longer period of training prior to the experiment.
- Increase the number of input perturbations. Analysis of the data (Figures 4.5 and 4.10) suggests that more input perturbations are needed in the APA window especially in the regions where the onsets of inhibitions occur. In particular, once bin sizes are reduced to less than 10 ms, on average there were less than 4 points per bin in this region. This severely limits our ability to determine an inhibition.

As shown in Figure 4.2, for subjects S1 to S7 about 15-20% of input perturbations were input before the onset of the light “go” cue (0 to 200 ms before light onset). The idea was to use these perturbations as a baseline. However the temporal

spacing of these inputs was probably too large (usually around 50ms) and should be decreased, along with a shift of the whole profile closer to the onset of the light cue.

The major problem with increasing the number of input perturbations is an extension of the experimental time. On average most experiments took 2.5-3 hrs (including time for subject setup). Regardless, it is recommended that 1) the input perturbation should be re-organized to increase the temporal resolution for inhibition detection (Figure 4.9) and 2) sampling in both the baseline area and in the region 0-100 ms after light onset time should be increased (which would be in the region of APA onset, assuming a 225-275ms RT).

5.3.2 Trial Rejection Procedure

In general, constraining the data with respect to the RT and MT is important for the following reasons:

- A change in RT should cause a shift in the onset time of the APA in the same direction. For instance, for a subject with consistently smaller RT, we should expect an earlier onset time in the APA (assuming that the movements are consistent enough to evoke the same muscle mechanics).
- A change in MT should alter the size (amplitude) of the APA inhibition. For example, with a very slow movement, the angular acceleration of the arm would be slower and hence result in a smaller reactive moment being transferred to the body, and hence reduce the need for an APA. Conversely, a very quick movement should produce a larger APA, Note that between subjects, anthropometric factors (e.g. the inertial mass of the subject) would also play a role.

In general, there a couple of possible approaches to rejecting faulty trials on the basis of RT and MT:

- Analogous experiments in the BVML (Dept. of Kinesiology, McGill) with arm reach movements have discarded trials on the basis of RT and MT being greater than \pm std from the mean value. We did not adopt this approach for a couple of reasons

- The distributions were not normal- they exhibited left skewness for RT and right skewness for MT. Hence, it is more appropriate to choose a mode as opposed to a mean.
- With such an approach, ~33% of trials from all subjects are always rejected (mean \pm std incorporates ~67% of the variability). Therefore, for subjects that perform well (with little variability), perfectly good trials would be thrown out.
- Hence, it was decided to choose absolute thresholds (i.e. \pm x ms from the mean (or mode in our case)) beyond which trials could be rejected. To ensure that the threshold distance was chosen uniformly across all subjects, the current analysis process plotted a CDF of the errors for the MT and RT variables (Figure 4.3), and chose the cutoff based on these plots (to maximize the number of trials selected). However, in effect, these choices were arbitrary (although easily customizable), with the rationale for choosing the cutoffs based on keeping at least 67% of the trials for the subject with the greatest variability (and subjects who performed ‘better’ keep a greater percent of the trials).

Hence, the trial selection process could be improved by carrying out an analysis to investigate the effect of RT and MT on the APA (i.e. curves of APA onset time versus RT, and APA inhibition size versus MT). This should give an estimate of whether there is truly a change in response variability with changes in RT and/or MT, and allow thresholds to be chosen less arbitrarily. A preliminary analysis was begun with a representative subject (S1). However, we encountered the following issues:

- Not all trials could be used. For trials where perturbations were applied during the APA, it was not possible to detect the onset of the APA or the size of the inhibition due to the reflex peak in the EMG profile.
- If only unperturbed trials were used instead, the sample size drops down to 44 trials (for subject S1), hardly an ideal sample size to study the effect of RT and MT on the onset time and the size of the APA respectively.

- Still considering only these control trials, we defined an inhibition to occur when the EMG trace for a single trial decreased to less than one std below its resting value (mean from the buzzer to 500 ms after buzzer). After low-pass filtering the EMG data (2nd order Butterworth, cutoff frequency 5 Hz), this approach still did not work for all the trials, as some trials had large standard deviations, and noticeably picked wrong points for an inhibition or could not detect an inhibition at all (i.e. when ensemble averages are considered inhibitions are clearly visible, but individual trials are variable).
- Alternately the trials could also be binned and their effects analyzed as a group (e.g. 10 ms RT bins), but this was not done.

As a whole, this approach will have to be carried out more thoroughly in the future with all subjects in case a re-analysis of the data and/or a modified trial rejection procedure is adopted.

5.3.3 Determination of Inhibition and Rebound Times

As indicated in Figure 4.9, the periods of reflex and muscle activity inhibition were determined by graphically inspecting bins, such that at least 75% of the data points in that region were below baseline (resting) levels. As indicated in Section 4.3.5.3 (page 93), the binning approach was preferred to a spline-based interpolation analysis.

However, the box-whisker plot analysis can also be extended to compare two bins for statistically significant differences. In fact, the binning analysis was initially conducted using a Kruskal-Wallis non parametric ANOVA. This test compares the medians of different groups of data, and returns a P value for the null hypothesis that all samples come from the same distribution, with a 95% confidence interval. The inhibition time (i.e. bin where inhibition occurred) was then defined as follows:

1. The median of the chosen bin had to be *significantly* less than the median of the preceding bin.
2. The median of the bin following the chosen bin had to be *less* than the median of the chosen bin. It had to also be *significantly less* than the median of the first bin (i.e. the bin preceding the chosen bin).

The rebound time was defined as follows:

1. The median of the chosen bin had to be *significantly greater* than the preceding bin, and greater than the resting level.
2. The median of the bin following the chosen bin had to be greater than the median of the chosen bin. It had to also be *significantly greater* than the very first bin (i.e. the bin preceding the chosen bin).

However, after the initial review of this thesis, this approach was discarded for the following reasons:

1. We were not able to determine the power of the Kruskal-Wallis test.
2. With bin sizes of 10 ms, there were far too points to have *statistically significant* differences in the bins close to the onset of inhibitions and satisfy the defined criterion for changes. Hence, although it was graphically clear that the data points were below resting levels, the Kruskal-Wallis analysis would fail for this bin width and the results were inconsistent with the larger bin widths. Note that, as indicated in Section 5.3.1, increasing the number of trials might resolve this issue.
3. There was also no real rationale for defining the criteria for significant changes in terms of the number of consecutive bins used for the analysis. Furthermore, it was found that changing the location of the bin edges would affect the KW analysis results, which was not the case with the box-whisker plot analysis. Since there was no real justification for picking the bin edges that I did, this could be another potential source of error.

In general, as indicated in Section 5.3.1, unless the number of samples is greatly increased, it is futile in my opinion to look for *statistical* differences in the parameters. However, I believe that the current analysis, although not strictly a statistical measure, does well in representing the general trend apparent in all subjects (i.e. reflexes inhibit after and rebound before background muscle activity).

5.3.4 Measures of Fatigue

We are reasonably confident that fatigue was minimized throughout the experiment due to the rest periods provided (2 seconds between movements) and a 3-4 minute break every 5 minutes. Subjects were able to execute the task comfortably and did not physically report any fatigue.

However, it would be ideal to monitor fatigue throughout the experiment. This could potentially be done by taking maximum voluntary contraction (MVC) measures of the postural limb sets at different times during the study.

5.3.5 Measurements of Body Sway & Joint Angles

We attempted to ensure that all trials were executed from the same ankle joint angle, by monitoring the torques at both foot pedals before the start of each trial. However, ideally it would have been appropriate to have some kinematic data as well of the individual body segments (e.g. trunk, thighs, lower leg). For example, we could monitor the position of each segment in space through visual tracking with reflective markers, or inclinometers placed on the segments.

Secondly, we have no way of precisely ensuring that subjects stood absolutely upright (i.e. did not flex their knees while raising their arms). However, we expect that any such movements would have produced unusual readings in the load cells implanted in the foot pedals, which we did not observe.

5.3.6 Data from the Contralateral Side of the Body

We recorded data from the contralateral limb. However, the data were not analyzed in the interests of time. Given that the focal movement is asymmetric (i.e. unlike a bilateral raise), we would not expect stretch reflexes of the same magnitude in the contralateral limb. However, this would be an interesting topic to explore.

5.4 Final Conclusions

We demonstrated that reflexes were significantly inhibited during the APA. This confirmed our hypothesis in terms of the functional benefit of a reflex inhibition during the APA period, such that it should be inhibited so as not to oppose the forward sway

initiated by the APA. Moreover, the reflex rebound was linked closely to movement onset, suggesting that it could also significantly contribute to the reduction of forward sway at the end of the APA. These reflex changes have been postulated previously- but we believe this is the first study to empirically demonstrate them.

Our experiments did not allow us to specifically pinpoint the neural mechanisms underlying the changes we observed. However, given that the reflex changes were not linked to the changes in muscle activity (inhibited after, rebounded before, and no amplitude correlation), we were able to rule out the direct effect of feed-forward descending commands (i.e. altered α -motorneuron activity). We postulate that the reflex changes we observed during the APA could be mediated by other sources of central command (e.g. γ -drive), and also possibly influenced by local mechanisms such as GABA mediated pre-synaptic inhibition.

References

1. Winter, D.A., et al., *Stiffness control of balance in quiet standing*. Journal of Neurophysiology, 1998. **80**(3): p. 1211-21.
2. Winter, D.A., et al., *Unified theory regarding A/P and M/L balance in quiet stance*. Journal of Neurophysiology, 1996. **75**(6): p. 2334-43.
3. Weiss, P., R.E. Kearney, and I.W. Hunter, *Position dependence of stretch reflex dynamics at the human ankle*. Experimental Brain Research, 1986. **63**: p. 49-59.
4. Day, B.L., et al., *Effect of vision and stance width on human body motion when standing: implications for afferent control of lateral sway*. Journal of Physiology, 1993. **469**: p. 479-99.
5. Peterka, R.J., *Sensorimotor integration in human postural control*. Journal of Neurophysiology, 2002. **88**(3): p. 1097-1118.
6. Jeka, J., K.S. Oie, and T. Kiemel, *Multisensory information for human postural control: integrating touch and vision*. Experimental Brain Research, 2000. **134**(1): p. 107-25.
7. Sinkjær, T., et al., *Muscle stiffness in human ankle dorsiflexors: Intrinsic and reflex components*. Journal of Neurophysiology, 1988. **60**: p. 1110-1121.
8. Mirbagheri, M.M., H. Barbeau, and R.E. Kearney, *Intrinsic and reflex contributions to human ankle stiffness: variation with activation level and position*. Experimental Brain Research, 2000. **135**(4): p. 423-36.
9. Nashner, L.M., *Adapting reflexes controlling the human posture*. Experimental Brain Research, 1976. **26**(1): p. 59-72.
10. Gielen, C.C.A.M., Ramaekers, L., and E.J. van Zuylen, *Long-latency stretch reflexes as co-ordinated functional responses in man*. Journal of Physiology, 1988. **407**: p. 275-292.
11. Freedman, W., S. Minassian, and R. Herman, *Functional stretch reflex (FSR) - a cortical reflex?* Progress in Brain Research, 1976. **44**: p. 487-490.
12. Allum, J.H.J., K.H. Mauritz, and H. Vogele, *Stiffness regulation provided by short-latency reflexes in human triceps surae muscles*. Brain Research, 1982. **234**: p. 159-164.

13. Stein, R.B. and R.E. Kearney, *Nonlinear behavior of muscle reflexes at the human ankle joint*. Journal of Neurophysiology, 1995. **73**: p. 65-72.
14. Grey, M.J., B. Larsen, and T. Sinkjaer, *A task dependent change in the medium latency component of the soleus stretch reflex*. Experimental Brain Research, 2002. **145**(3): p. 316-22.
15. Wolf, S.L. and R.L. Segal, *Reducing human biceps brachii spinal stretch reflex magnitude*. Journal of Neurophysiology, 1996. **75**(4): p. 1637-46.
16. Segal, R.L. and S.L. Wolf, *Operant conditioning of spinal stretch reflexes in patients with spinal cord injuries*. Experimental Neurology, 1994. **130**(2): p. 202-13.
17. Ludvig, D., I. Cathers, and R.E. Kearney, *Voluntary modulation of human stretch reflexes*. Experimental Brain Research, 2007. **183**(2): p. 201-13.
18. Bernstein, N., *The co-ordination and regulation of movements*. 1967: Oxford.
19. Crenna, P., and C. Frigo, *A motor program for the initiation of forward-oriented movements in humans*. Journal of Physiology, 1991. **437**: p. 635-53.
20. Bouisset, S. and M. Zattara, *A sequence of postural movements preceded voluntary movement*. Neuroscience Letters, 1981. **22**: p. 263-270.
21. Pozzo, T., M. Ouamer, and C. Gentil, *Simulating mechanical consequences of voluntary movement upon whole-body equilibrium: the arm-raising paradigm revisited*. Biological Cybernetics, 2001. **85**(1): p. 39-49.
22. Patla, A.E, *Adaptation of postural response to voluntary arm raises during locomotion in humans*. Neuroscience Letters. 1986. **68**: p. 334-338.
23. Marsden, C.D, P.A. Merton, and H.B. Morton, *Anticipatory postural responses in the human subject*. Journal of Physiology, 1977. **273**: p. 64P.
24. Belenkii, V.Y., V.S. Gurfinkel, and Y.I. Paltsev, *Elements of control of voluntary movements*. Biophysics, 1967. **12**: p. 154-161.
25. Bouisset, S. and M. Zattara, *Biomechanical study of the programming of anticipatory postural adjustments associated with voluntary movement*. Journal of Biomechanics, 1987. **20**(8): p. 735-42.
26. Mouchnino, L., et al., *Coordination between equilibrium and head-trunk orientation during leg movement: a new strategy build up by training*. Journal of Neurophysiology, 1992. **67**(6): p. 1587-98.

27. Stapley, P., T. Pozzo, and A. Grishin, *The role of anticipatory postural adjustments during whole body forward reaching movements*. Neuroreport, 1998. **9**(3): p. 395-401.
28. Patla, A.E., M.G. Ishac, and D.A. Winter, *Anticipatory control of center of mass and joint stability during voluntary arm movement from a standing posture: interplay between active and passive control*. Experimental Brain Research, 2002. **143**(3): p. 318-27.
29. Kawanishi, M., S. Yahagi, and T. Kasai, *Neural mechanisms of soleus H-reflex depression accompanying voluntary arm movement in standing humans*. Brain Research, 1999. **832**(1-2): p. 13-22.
30. Kasai, T. and T. Komiyama, *Soleus H-reflex depression induced by ballistic voluntary arm movement in human*. Brain Research, 1996. **714**(1-2): p. 125-34.
31. Komiyama, T. and T. Kasai, *Changes in the H-reflexes of ankle extensor and flexor muscles at the initiation of a stepping movement in humans*. Brain Research, 1997. **766**(1-2): p. 227-35.
32. Morita, H., et al., *Sensitivity of H-reflexes and stretch reflexes to presynaptic inhibition in humans*. Journal of Neurophysiology, 1998. **80**(2): p. 610-20.
33. Andersen, J.B. and T. Sinkjaer, *The stretch reflex and H-reflex of the human soleus muscle during walking*. Motor Control, 1999. **3**(2): p. 151-7.
34. Seeley, R.R., et al., *Anatomy & physiology*. 6th ed. 2003, Boston: McGraw-Hill. 1 v. (in various pagings).
35. Gray, H., *Anatomy of the Human Body*, W.H. Lewis, Editor. 1918, Bartleby.com.
36. Specialists, S.O.S. *Ankle Anatomy*. 2008 [cited 2008 07/21/2008]; Available from: <http://www.southwest-ortho.com/ankle/anatomy-3.html>.
37. Gross, J.M., J. Fetto, and E. Rosen. *Musculoskeletal examination*. 2002 [cited 2008 21/8/2008]; Available from: http://books.google.ca/books?id=REptMwoQ6PMC&pg=PT384&lpg=PT384&dq=degree+of+foot+eversion+in+normal+people&source=web&ots=j6WIIAj1xq&sig=NgVqhiDet1q1IQjUoP84IzsaMQ&hl=en&sa=X&oi=book_result&resnum=6&ct=result.
38. Guyton, A.C. and J.E. Hall, *Textbook of medical physiology*. 10th ed. 2000, Philadelphia: Saunders. xxxii, 1064 p.

39. Guyton, A.C. and J.E. Hall, *Textbook of medical physiology*. 2006, Elsevier Saunders: Philadelphia. p. xxxv, 1116 p.
40. Fawcett, D.W. and W. Bloom, *A textbook of histology*. 11th ed. 1986, Philadelphia: Saunders. xi, 1017 p.
41. Guyton, A.C., *Textbook of medical physiology*. 8th ed. 1991, Philadelphia: Saunders. xli, 1014 p.
42. Huxley, A.F. and R. Niedergerke, *Measurement of muscle striations in stretch and contraction*. *Journal of Physiology*, 1954. **124**(2): p. 46-7P.
43. Huxley, A.F. and R. Niedergerke, *Structural changes in muscle during contraction; interference microscopy of living muscle fibers*. *Nature*, 1954. **173**(4412): p. 971-3.
44. Hole, J.W., *Human anatomy and physiology*. 2nd ed. 1981, Dubuque, Iowa: W.C. Brown Co. xxxi, 791, [63] p., [12] p. of plates.
45. Tarnakin, D.A., *Sliding Filament Theory*. 2006.
46. Huxley, H.E., *Fifty years of muscle and the sliding filament hypothesis*. *European Journal of Biochemistry*, 2004. **271**(8): p. 1403-15.
47. Widmaier, E.P., et al., *Vander, Sherman, & Luciano's human physiology: the mechanisms of body function*. 9th ed. 2004, Boston: McGraw-Hill Higher Education. xxv, 825 p.
48. Burke, R.E., et al., *Physiological types and histochemical profiles in motor units of the cat gastrocnemius*. *Journal of Physiology*, 1973. **234**(3): p. 723-48.
49. Gordon, A.M., A.F. Huxley, and F.J. Julian, *The variation in isometric tension with sarcomere length in vertebrate muscle fibers*. *Journal of Physiology*, 1966. **184**(1): p. 170-92.
50. Huxley, H.E. and M. Kress, *Crossbridge behaviour during muscle contraction*. *Journal of Muscle Research and Cell Motility*, 1985. **6**(2): p. 153-61.
51. Kandel, E.R., J.H. Schwartz, and T.M. Jessell, *Principles of neural science*. 4th ed. 2000, New York: McGraw-Hill Health Professions Division. xli, 1414.
52. Adrian, E.D. and D.W. Bronk, *The discharge of impulses in motor nerve fibers: Part II. The frequency of discharge in reflex and voluntary contractions*. *Journal of Physiology*, 1929. **67**(2): p. i3-151.

53. Hodson-Tole, E.F. and J.M. Wakeling, *Motor unit recruitment for dynamic tasks: current understanding and future directions*. Journal of Computational Physiology [B], 2008.
54. Kennedy, P.M. and A.G. Cresswell, *The effect of muscle length on motor-unit recruitment during isometric plantar flexion in humans*. Experimental Brain Research, 2001. **137**(1): p. 58-64.
55. Pasquet, B., A. Carpentier, and J. Duchateau, *Change in muscle fascicle length influences the recruitment and discharge rate of motor units during isometric contractions*. Journal of Neurophysiology, 2005. **94**(5): p. 3126-33.
56. Pasquet, B., A. Carpentier, and J. Duchateau, *Specific modulation of motor unit discharge for a similar change in fascicle length during shortening and lengthening contractions in humans*. Journal of Physiology, 2006. **577**(Pt 2): p. 753-65.
57. Friedman, W.A., et al., *Recurrent inhibition in type-identified motoneurons*. Journal of Neurophysiology, 1981. **46**(6): p. 1349-59.
58. Brown, I.E., E.J. Cheng, and G.E. Loeb, *Measured and modeled properties of mammalian skeletal muscle. II. The effects of stimulus frequency on force-length and force-velocity relationships*. Journal of Muscle Research and Cell Motility, 1999. **20**(7): p. 627-43.
59. Netter, F.H. and A.F. Dalley, *Atlas of human anatomy*. 2nd ed. 1997, East Hanover, N.J.: Novartis. [xiv, 525 p. of plates].
60. Stein, R.B., *Nerve and muscle: membranes, cells, and systems*. 1980, New York: Plenum Press. ix, 265 p.
61. Hulliger, M., et al., *Flexible fusimotor control of muscle spindle feedback during a variety of natural movements*. Progress in Brain Research, 1989. **80**: p. 87-101; discussion 57-60.
62. Ribot-Ciscar, E., et al., *Post-contraction changes in human muscle spindle resting discharge and stretch sensitivity*. Experimental Brain Research, 1991. **86**(3): p. 673-8.
63. Matthews, P.B., *What are the afferents of origin of the human stretch reflex, and is it a purely spinal reaction?* Progress in Brain Res, 1986. **64**: p. 55-66.
64. Katz, R., *Presynaptic inhibition in humans: a comparison between normal and spastic patients*. Journal of Physiology Paris, 1999. **93**(4): p. 379-85.

65. Hermens, H.J. *SENIAM- Surface Electromyography for the Non-Invasive Assessment of Muscles*. 2008 [cited; Available from: www.seniam.org].
66. Kearney, R.E., R.B. Stein, and L. Parameswaran, *Identification of intrinsic and reflex contributions to human ankle stiffness dynamics*. IEEE Transactions on Biomedical Engineering, 1997. **44**(6): p. 493-504.
67. Kearney, R.E. and I.W. Hunter, *System identification of human joint dynamics*. Critical Reviews in Biomedical Engineering, 1990. **18**: p. 55-8.
68. Loram, I.D., S.M. Kelly, and M. Lakie, *Human balancing of an inverted pendulum: is sway size controlled by ankle impedance?* Journal of Physiology, 2001. **532**(Pt 3): p. 879-91.
69. Schweigart, G. and T. Mergner, *Human stance control beyond steady state response and inverted pendulum simplification*. Experimental Brain Research, 2008. **185**(4): p. 635-53.
70. Gage, W.H., et al., *Kinematic and kinetic validity of the inverted pendulum model in quiet standing*. Gait & Posture, 2004. **19**(2): p. 124-32.
71. Winter, D.A., *Biomechanics and motor control of human movement*. 3rd ed. 2005, Hoboken, N.J.: John Wiley & Sons. xvi, 325 p.
72. Hunter, I.W. and R.E. Kearney, *Respiratory components of human postural sway*. Neuroscience Letters, 1981. **25**: p. 155-159.
73. Hodges, P.W., et al., *Coexistence of stability and mobility in postural control: evidence from postural compensation for respiration*. Experimental Brain Research, 2002. **144**(3): p. 293-302.
74. Morasso, P.G. and M. Schieppati, *Can muscle stiffness alone stabilize upright standing?* Journal of Neurophysiology, 1999. **82**(3): p. 1622-6.
75. Casadio, M., P.G. Morasso, and V. Sanguineti, *Direct measurement of ankle stiffness during quiet standing: implications for control modeling and clinical application*. Gait & Posture, 2005. **21**(4): p. 410-24.
76. Rao, G.P. *Elements of Control Systems*. [cited 23/07/2008]; Available from: <http://www.eolss.com/eolss/images/6.43.1.0Figure15.JPG>.
77. Nashner, L.M., *Fixed patterns of rapid postural responses among leg muscles during stance*. Experimental Brain Research, 1977. **30**: p. 13-24.

78. Horak, F.B. and L.M. Nashner, *Central programming of postural movements: adaptation to altered support-surface configurations*. Journal of Neurophysiology, 1986. **55**(6): p. 1369-81.
79. Iles, J.F. and J.V. Pisini, *Vestibular-Evoked Postural Reactions in Man and Modulation of Transmission in Spinal Reflex Pathways*. Journal of Physiology-London, 1992. **455**: p. 407-424.
80. Markham, C.H., *Vestibular control of muscular tone and posture*. Canadian Journal of Neurological Sciences, 1987. **14**: p. 493-496.
81. Schor, R.H. and A.D. Miller, *Vestibular reflexes in neck and forelimb muscles evoked by roll tilt*. Journal of Neurophysiology, 1981. **46**: p. 167-178.
82. Vidal, P.P., A. Berthoz, and M. Millanvoye, *Difference between eye closure and visual stabilization in the control of posture in man*. Aviation, Space, and Environmental Medicine, 1982. **53**(2): p. 166-70.
83. Nashner, L., and A. Berthoz, *Vision contribution to rapid motor responses in the control of posture*. Proceedings of the 27th international Congress of Physiological Sciences, 1977.
84. Fitzpatrick, R., D.K. Rogers, and D.I. McCloskey, *Stable human standing with lower-limb muscle afferents providing the only sensory input*. Journal of Physiology, 1994. **480**(Pt 2): p. 395-403.
85. Maurer, C., T. Mergner, and R.J. Peterka, *Multisensory control of human upright stance*. Experimental Brain Research, 2006. **171**(2): p. 231-50.
86. Rushton D.N, J.C. Rothwell, and M.D. Craggs, *Somatosensory evoked potential of gating during different kinds of movement in man*. Brain, 1981. **104**: p. 465-491.
87. Nashner L.M., F.O. Black, and C. Wall, III, *Adaptation to altered support and visual conditions during stance: patients with vestibular deficits*. Journal of Neuroscience, 1982. **2**: p. 536-544.
88. Oie, K.S., T. Kiemel, and J.J. Jeka, *Multisensory fusion: simultaneous re-weighting of vision and touch for the control of human posture*. Cognitive Brain Research, 2002. **14**(1): p. 164-76.
89. ECOSSE. [cited; Available from:
<http://eweb.chemeng.ed.ac.uk/courses/control/restricted/course/second/course/figures/6/feedforward1.gif>

90. von Holst, E. and H. Mittelstaedt, *Das Reafferenzprinzip*. Naturwissenschaften, 1950. **37**: p. 464-476.
91. Roy, J.E. and K.E. Cullen, *Dissociating self-generated from passively applied head motion: neural mechanisms in the vestibular nuclei*. Journal of Neuroscience, 2004. **24**(9): p. 2102-11.
92. Johansson, R.S. and Westling, G., *Programmed and triggered actions to rapid load changes during precision grip*. Experimental Brain Research, 1988. **71**: p. 72-86.
93. Davidson, P.R. and D.M. Wolpert, *Widespread access to predictive models in the motor system: a short review*. Journal of Neural Engineering, 2005. **2**(3): p. S313-9.
94. Pigeon, P., et al., *Coordinated turn-and-reach movements. I. Anticipatory compensation for self-generated coriolis and interaction torques*. Journal of Neurophysiology, 2003. **89**(1): p. 276-89.
95. Wolpert, D.M. and R.C. Miall, *Forward Models for Physiological Motor Control*. Neural Networks, 1996. **9**(8): p. 1265-1279.
96. Ito, M., *Neurobiology: internal model visualized*. Nature, 2000. **403**(6766): p. 153-4.
97. Kawato, M., *Internal models for motor control and trajectory planning*. Current Opinions in Neurobiology, 1999. **9**(6): p. 718-27.
98. Wolpert, D.M. and M. Kawato, *Multiple paired forward and inverse models for motor control*. Neural Networks, 1998. **11**(7-8): p. 1317-1329.
99. Gatev, P., et al., *Feedforward ankle strategy of balance during quiet stance in adults*. Journal of Physiology, 1999. **514**(Pt 3): p. 915-28.
100. Masani, K., A.H. Vette, and M.R. Popovic, *Controlling balance during quiet standing: proportional and derivative controller generates preceding motor command to body sway position observed in experiments*. Gait & Posture, 2006. **23**(2): p. 164-72.
101. Ramos, C.F. and L.W. Stark, *Postural Maintenance During Movement - Simulations of a 2 Joint Model*. Biological Cybernetics, 1990. **63**: p. 363-375.
102. Cordo P.J. and L.M. Nashner, *Properties of postural adjustments associated with rapid arm movements*. Journal of Neurophysiology, 1982. **47**: p. 287-302.
103. Horak, F. and J.M. Macpherson, *Postural Orientation and Equilibrium*, in *Handbook of Physiology*, L.B. Rowell and J.T. Sheperd, Editors. 1996, Published for the American Physiological Society by Oxford University Press: New York. p. 254-292.

104. Massion, J., *Movement, posture and equilibrium: interaction and coordination*. Progress in Neurobiology, 1992. **38**(1): p. 35-56.
105. Lee, W.A., C.F. Michaels, and Y.C. Pai, *The Organization of Torque and EMG Activity During Bilateral Handle Pulls by Standing Humans*. Experimental Brain Research, 1990. **82**: p. 304-314.
106. Lepers, R. and Y. Breniere, *The role of anticipatory postural adjustments and gravity in gait initiation*. Experimental Brain Research, 1995. **107**(1): p. 118-24.
107. Kaminski, T.R. and S. Simpkins, *The effects of stance configuration and target distance on reaching. I. Movement preparation*. Experimental Brain Research, 2001. **136**(4): p. 439-46.
108. Stapley, P.J., et al., *Does the coordination between posture and movement during human whole-body reaching ensure center of mass stabilization?* Experimental Brain Research, 1999. **129**(1): p. 134-46.
109. Thilmann, A.F., et al., *Different mechanisms underlie the long-latency stretch reflex response of active human muscle at different joints*. Journal of Physiology, 1991. **444**: p. 631-43.
110. Day, B.L., et al., *Changes in the response to magnetic and electrical stimulation of the motor cortex following muscle stretch in man*. Journal of Physiology, 1991. **433**: p. 41-57.
111. Matthews, P.B., *Interaction between short- and long-latency components of the human stretch reflex during sinusoidal stretching*. Journal of Physiology, 1993. **462**: p. 503-27.
112. Petersen, N., et al., *Evidence that a transcortical pathway contributes to stretch reflexes in the tibialis anterior muscle in man*. Journal of Physiology, 1998. **512**(Pt 1): p. 267-76.
113. Matthews, P.B., *Long-latency stretch reflexes of two intrinsic muscles of the human hand analysed by cooling the arm*. Journal of Physiology, 1989. **419**: p. 519-38.
114. Corden, D.M., et al., *Long-latency component of the stretch reflex in human muscle is not mediated by intramuscular stretch receptors*. Journal of Neurophysiology, 2000. **84**(1): p. 184-8.

115. Kearney, R.E. and C.W.Y. Chan, *Contrasts between the reflex responses of tibialis anterior and triceps surae to sudden ankle rotation in normal human subjects*. *Electroencephalography and Clinical Neurophysiology*, 1982. **54**: p. 301-310.
116. Grey, M.J., et al., *Ankle extensor proprioceptors contribute to the enhancement of the soleus EMG during the stance phase of human walking*. *Canadian Journal of Physiology & Pharmacology*, 2004. **82**(8-9): p. 610-6.
117. Sinkjaer, T., et al., *Soleus long-latency stretch reflexes during walking in healthy and spastic humans*. *Clinical Neurophysiology*, 1999. **110**(5): p. 951-959.
118. Weiss, P.L., R.E. Kearney, and I.W. Hunter, *Position dependence of stretch reflex dynamics at the human ankle*. *Experimental Brain Research*, 1986. **63**: p. 49-59.
119. Matthews, P., *Observations on the automatic compensation of reflex gain on varying the pre-existing level of motor discharge in man*. *Journal of Physiology*, 1986. **374**: p. 73-90.
120. Marsden, C., M. PA, and H. Morton, *Servo action in the human thumb*. *Journal of Physiology*, 1976. **257**: p. 1-44.
121. Gottlieb, G. and G. Agarwal, *Response to sudden torques about ankle in man: Myotatic reflex*. *Journal of Neurophysiology*, 1979. **42**: p. 91-106.
122. Toft, E., et al., *Mechanical and electromyographic responses to stretch of the human ankle extensors*. *Journal of Neurophysiology*, 1991. **65**: p. 1402-1410.
123. Hoffer, J. and S. Andreassen, *Regulation of soleus muscle stiffness in premammillary cats: intrinsic and reflex components*. *Journal of Neurophysiology*, 1981. **45**: p. 267-285.
124. Sinkjaer, T., J. Andersen, B. and B. Larsen, *Soleus stretch reflex modulation during gait in humans*. *Journal of Neurophysiology*, 1996. **76**(2): p. 1112-1120.
125. Kearney, R.E., M. Lortie, and R.B. Stein, *Modulation of stretch reflexes during imposed walking movements of the human ankle*. *Journal of Neurophysiology*, 1999. **81**(6): p. 2893-902.
126. Woollacott, M.H., M. Bonnet, and K. Yabe, *Preparatory process for anticipatory postural adjustments: modulation of leg muscles reflex pathways during preparation for arm movements in standing man*. *Experimental Brain Research*, 1984. **55**(2): p. 263-71.

127. El-Sakkary, B., *Modulation of Stretch Reflex Excitability with Postural Sway in the Frontal Plane*, in *Biomedical Engineering*. 2007, McGill University: Montreal.
128. Wagner, D.R. *REKLAB manual (McGill Faculty of Medicine- Biomedical Engineering Department)*. 27 May, 2008 [cited; Available from: <http://www.bmed.mcgill.ca/Reklab/manual/>].
129. Straube, A., et al., *Dependence of visual stabilization of postural sway on the cortical magnification factor of restricted visual fields*. *Experimental Brain Research*, 1994. **99**(3): p. 501-6.
130. Sinkjaer, T., *Muscle, reflex and central components in the control of the ankle joint in healthy and spastic man*. *Acta Neurologica Scandinavica*, 1997. **Supplementum** (170): p. 1-28.
131. Dietz, V., M. Discher, and M. Trippel, *Task-dependent modulation of short- and long-latency electromyographic responses in upper limb muscles*. *Electroencephalography & Clinical Neurophysiology*, 1994. **93**(1): p. 49-56.
132. Akazawa, K., Milner T.E., and R.B. Stein *Modulation of reflex EMG and stiffness in response to stretch of human finger muscle*. *Journal of Neurophysiology*, 1983. **49**: p. 16-27.
133. Macpherson, J.M., et al., *Bilateral vestibular loss in cats leads to active destabilization of balance during pitch and roll rotations of the support surface*. *Journal of Neurophysiology*, 2007. **97**(6): p. 4357-67.
134. Katz, R., Meunier, S., and Pierrot-Deseilligny, E., *Changes in presynaptic inhibition of Ia fibers in man while standing*. *Brain*, 1988. **111**: p. 417-437.
135. Koceja, D.M., M.H. Trimble, and D.R. Earles, *Inhibition of the soleus H-reflex in standing man*. *Brain Research*, 1993. **629**(1): p. 155-8.
136. Stewart, B.A. and J.D. Brooke, *Interaction of reciprocally induced inhibition and premotor facilitation of soleus H reflexes in humans*. *Electroencephalography & Clinical Neurophysiology*, 1993. **89**(1): p. 41-4.
137. Capaday, C., *The effects of baclofen on the stretch reflex parameters of the cat*. *Experimental Brain Research*, 1995. **104**(2): p. 287-96.

Appendix

A. Digital Signal Routing Enclosure

The setup was initially designed so that multiple targets could be illuminated, so as to cue the subject to make different kinds of voluntary movements (e.g. arm raises to different target distances versus an arm raise). For this purpose, we built a routing enclosure that could use just two digital output lines on the controller to illuminate up to four different light targets. The enclosure also had a number of other features to process the digital signals between the frame and controller respectively.

A circuit diagram was designed using computer software (*ExpressPCB*) and physically implemented by soldering the necessary components onto a PCB, which was enclosed in a plastic enclosure. The major integrated circuits (IC's) on the printed circuit board were the following:

1. 3-8 line decoder (74LS138): This chip was used to maximize the potential number of potential LED targets while minimizing the required number of digital outputs. Note that the experiment was originally setup to provide a mechanism of selectively illuminating up to 3 different targets by using two digital outputs from the D I/O, the idea being that different kinds of movements could be studied (only one was used in the experiment). The decoder received 3 TTL inputs and used a truth table to set the appropriate output to a TTL high level. By holding the third input at TTL low, and altering the first two input, 4 desired outputs could be achieved: LED 1 on, LED2 on, LED3 on, all LED's off.
2. Octal buffer and Line Driver (74LS240): The liner driver was used as an intermediary between the decoder and the LED's to ensure that sufficient current would be provided to drive the targets. Since, the driver incorporated a NOT gate with some hysteresis, two inputs were used for every desired output so as not to flip the logic (refer to circuit diagram- figure 3) of the input signal.
3. Schmitt Trigger (74LS14): The Schmitt Trigger is a comparator circuit that incorporates positive feedback. When the input to the trigger was higher than a chosen threshold, the output was high and similarly when the input was below another chosen threshold, the output was low. However, when the input value was between

the two thresholds, the output retained its current value. This made the system more resistant to noise, such that fluctuations about a threshold level would not cause transitions in output logic. The signals from the target switch on the frame and the “ready” trigger switch on the subject’s thigh were routed into two digital input ports on the D I/O through this IC. It also routed a digital output line on the I/O to the piezoelectric buzzer on the frame.

The circuit diagram for the printed circuit board and frame components is shown in Figure A.1.

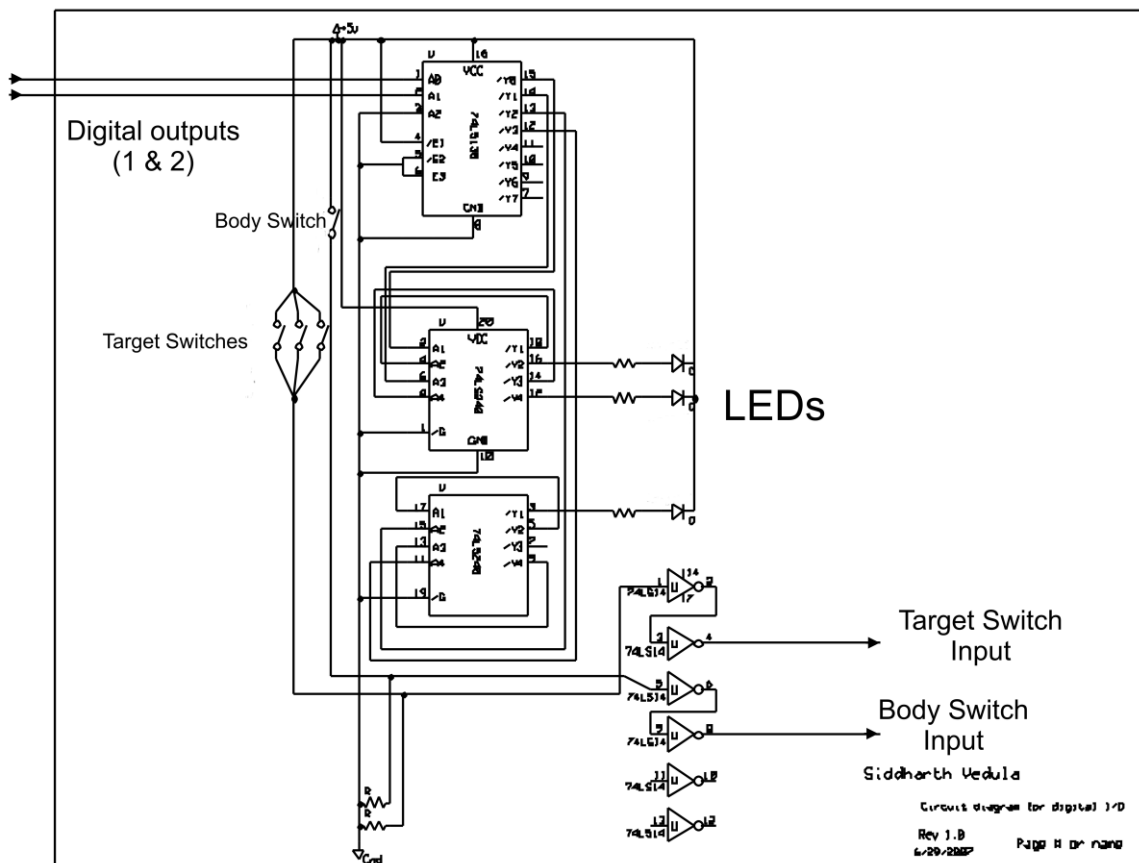


Figure A.1. Circuit diagram of the PCB used to interface frame components to the real-time controller and data acquisition system.

B. Subject Consent Form

System identification of intrinsic and reflex contributions to the control of posture and movement. CIHR Grant: FRN-81280

Experiment: Reflex changes during anticipatory postural adjustments preceding voluntary arm movements in standing humans

Subject Information & Consent Form

- These experiments are designed to study the neuromuscular mechanisms involved in controlling the ankle during the execution of tasks that destabilize posture. The experimental procedure involves:
 - The execution of 350-400 voluntary arm raises by a subject, when cued by a visual signal.
 - Measurement of the electrical activity of the ankle and deltoid muscles using surface electrodes applied with a standard technique.
 - A small displacement of the right foot about its axis of rotation by a rotary actuator.
 - A comfortable padded splint cast attached to the right forearm to measure arm position.
- Individual experiments will last for no longer than 3 hours. Subjects are to be given regular rest periods in 5 min intervals. During rest periods, the subject will be asked to sit down in a chair and relax.
- The forces applied to the foot will be no larger than those encountered during normal running or jumping.
- Subjects may withdraw from the experiment at any time and will suffer no personal consequences as result.

I, _____, voluntarily consent to participate in the research project entitled "Reflex changes during anticipatory postural adjustments preceding voluntary arm movements in standing humans" conducted by Mr. Siddharth Vedula (514-398-4400 ext. 00425) and Dr. Robert E. Kearney (514-398-6736) of the Department of Biomedical Engineering, McGill University.

I understand that the information obtained from this research may be published. However, my right to privacy will be retained and my involvement with the project will be kept confidential.

The procedures as set out in the accompanying information sheet have been explained to me and I understand what is expected of me and the benefits and risks involved.

My participation in the project is voluntary.

I acknowledge that I have the right to question any part of the procedure and that I can withdraw at any time without this being held against me.

Signed by Subject: _____ Date: _____

Signed by Investigator: _____ Date: _____

Name of Witness: _____

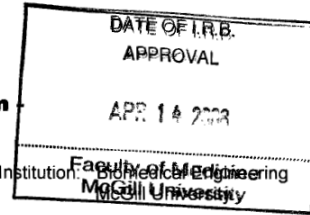
Signed by Witness: _____ Date: _____

C. Ethics Approval Form



Institutional Review Board

- Continuing Review Form -



Principal Investigator: Robert Kearney

Department/Institution: Faculty of Medicine
McGill University

IRB Review Number A04-MC9-97

Study Number (if any):

Review Interval: Annual

Title of Research Proposal:

CIHR: System identification of intrinsic and reflex contributions to the control of posture and movement,

FQRNT: Strategies biomimetiques pour le controle du mouvement en robotique et en rehabilitation'

INTERIM REPORT (PLEASE CHECK OR SPECIFY)

Current Status of Study : Active Study On Hold Closed to Enrolment
Interim Analysis Final Analysis Study Not Activated **

**If the study has not become active at McGill, please enclose correspondence to explain or provide explanation:

McGill hospital(s) where study is being conducted and has received acceptance of local Research Ethics Board(s) (if applicable):

Douglas: JGH: MUHC/MCH (Mtl Children's): MUHC/MCI (Mtl Chest Ins.): MUHC/MGH:
MUHC/MNH-MNI: MUHC/RVH: Shriners Hospital SMH: Other:

McGill hospital(s) where study is being conducted and has NOT received acceptance of local Research Ethics Board(s) (if applicable):
N/A

In the case of a clinical trial, has the sponsor registered the study in the WHO Clinical Trials Registry www.isrctn.com? Yes No
If study sponsorship or financial support has changed, please provide correspondence to explain; enclosed:

Total number of subjects to be enrolled in the study: 10/YEAR Number of subjects to be enrolled at McGill sites: 10/YEAR
10

Number of subjects enrolled by McGill PI to date: 50 Number of subjects enrolled by McGill PI since the last review: 10

Have any of these subjects withdrawn from the study, and if yes, how many? Yes No

Has the study been revised since the last review? Yes No

Has the consent form been revised since the last review? Yes No Date of current consent form 1-APRIL-008

Have the study and consent form revisions been submitted and approved by the IRB? Yes No

Are there any new data since the last review that could influence a subject's willingness to provide continuing consent?: No

Have there been any Serious Adverse Experiences (SAEs)? Yes No

Have all Serious Adverse Experiences (SAEs) and Safety Reports relevant to the study been reported to the IRB?: Yes No

SIGNATURES:

Principal Investigator:

Date: 4 April 2008

IRB Chair:

Date: April 14, 2008